

Recent Hot Topics of Tropical Cyclones and the Promotion of Tropical Cyclone Size Asymmetry Index

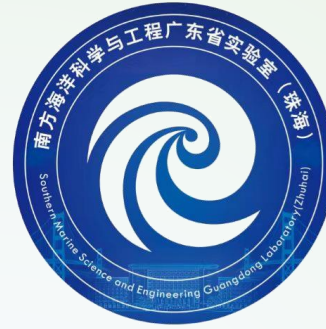
Kelvin T. F. CHAN

陈庭辉

School of Atmospheric Sciences, Sun Yat-sen University

Recent Hot Topics of Tropical Cyclones

- Translation Speed
- Landfall Decay



Are Global Tropical Cyclones Moving Slower in a Warming Climate?

Kelvin T. F. CHAN^{1,2}

¹School of Atmospheric Sciences, Sun Yat-sen University, and Southern Marine Science and Engineering Guangdong Laboratory (Zhuhai), Zhuhai, China

²Guangdong Province Key Laboratory for Climate Change and Natural Disaster Studies, Sun Yat-sen University, Zhuhai, China

Background

LETTER

<https://doi.org/10.1038/s41586-018-0158-3>

A global slowdown of tropical-cyclone translation speed

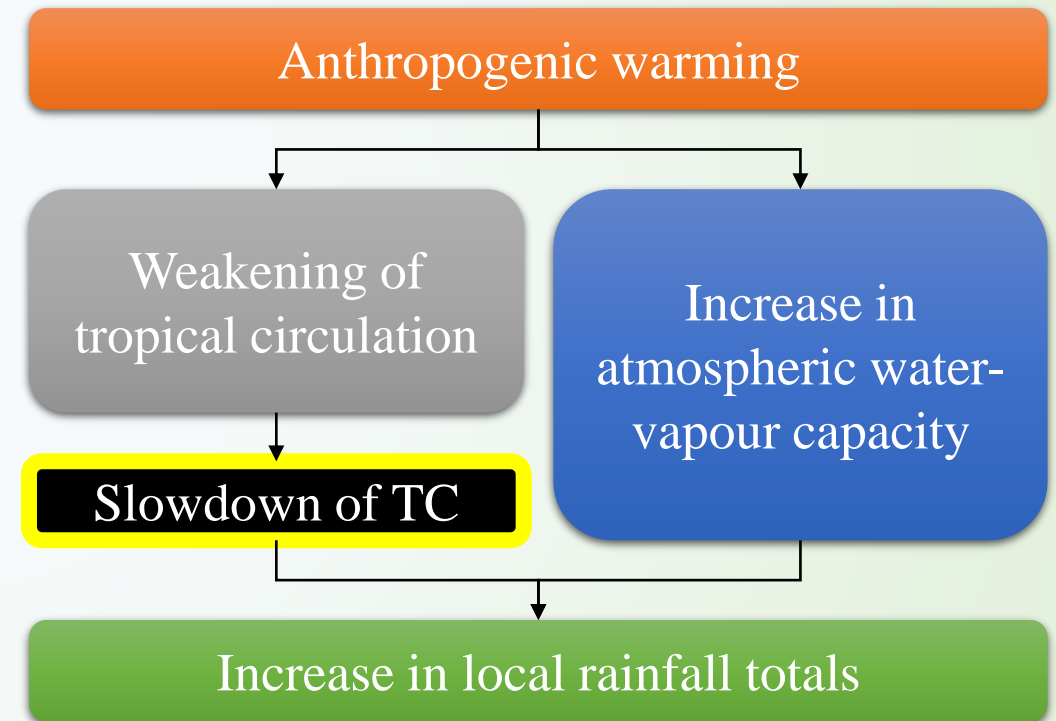
James P. Kossin^{1*}

As the Earth's atmosphere warms, the atmospheric circulation changes. These changes vary by region and time of year, but there is evidence that anthropogenic warming causes a general weakening of summertime tropical circulation^{1–8}. Because tropical cyclones are carried along within their ambient environmental wind, there is a plausible a priori expectation that the translation speed of tropical cyclones has slowed with warming. In addition to circulation changes, anthropogenic warming causes increases in atmospheric water-vapour capacity, which are generally expected to increase precipitation rates⁹. Rain rates near the centres of tropical cyclones are also expected to increase with increasing global temperatures^{10–12}. The amount of tropical-cyclone-related rainfall that any given local area will experience is proportional to the rain rates and inversely proportional to the translation speeds of tropical cyclones. Here I show that tropical-cyclone translation speed has decreased globally by 10 per cent over the period 1949–2016, which is very likely to have compounded, and possibly dominated, any increases in local rainfall totals that may have occurred as a result of increased tropical-cyclone rain rates. The magnitude of the slowdown varies substantially by region

is proportional to the rate of rain produced in a tropical cyclone and inversely proportional to its translation speed; that is, a proportional unit of decrease in translation speed would have about the same effect on local rainfall totals as the same proportional unit of increase in rain rate.

Anthropogenic warming, both past and projected, is expected to affect the strength and patterns of global atmospheric circulation^{1–8}. Tropical cyclones are generally carried along within these circulation patterns so their past translation speeds may be indicative of past circulation changes. In particular, warming is linked to a weakening of tropical summertime circulation and there is a plausible a priori expectation that tropical-cyclone translation speed may be decreasing. In addition to changing circulation, anthropogenic warming is expected to increase lower-tropospheric water-vapour capacity by about 7% per degree (Celsius) of warming, as per the Clausius–Clapeyron relationship². Expectations of increased mean precipitation under global warming are well documented, but not as straightforward to quantify^{9,18}. Increases in global precipitation are constrained by the atmospheric energy budget to about 1%–2% per degree of warming^{19,20}; those in regional precipitation are further controlled by variability in moisture

Kossin 2018, *Nature* (Out of print)





Calculations were Deficient.

Kossin 2018,
Nature (Out
of print)

Corrections

CORRECTIONS & AMENDMENTS

CORRECTION

<https://doi.org/10.1038/s41586-018-0585-1>

Author Correction: A global slowdown of tropical-cyclone translation speed

James P. Kossin

Correction to: Nature <https://doi.org/10.1038/s41586-018-0158-3>, published online 6 June 2018.

In this Letter, there are two errors in the methodology. These corrections revise regional values; they do not affect the conclusions and none of the global numbers (trend and statistics) change.

In the first error, data were inadvertently omitted just prior to and subsequent to reporting times that were asynoptic (that is, when data were not provided on the synoptic times of 00, 06, 12 and 18 hours UTC). These data have now been included.

In the second error, the 'non-main' track types (unusual tracks identified as 'merge', 'split' or 'other' by the IBTrACS algorithm (see ref. 32 of the original Letter) in the data were not adequately screened. Such screening is important when counting storms to obtain annual storm frequency (see ref. 32 of the original Letter) but less so for calculating metrics such as translation speed; however, a correction is nevertheless warranted here. The non-main track types can represent physical cases where two storms formed near each other or cases of vortex merger, but they can also be spurious. To remove the spurious cases while retaining the physical cases, I have now set a duration threshold of a minimum of 3 days because it is unlikely that a spurious track would exceed 2–3 days.

The revised numbers, after inclusion of the data that were inadvertently removed and additional screening for track type by setting a conservative track duration threshold of 3 days, are tabulated

in Figs. 6 and 7, along with the original numbers from Extended Data Tables 1 and 2 for comparison. Globally, as noted above, the translation speed trend, percentage change and 95% confidence interval do not change. The slowing trend in the Northern Hemisphere increases slightly and the trend in the Southern Hemisphere becomes statistically significant. That is, the correction strengthens the trends on a hemispheric scale in each hemisphere. The statement that slowing is observed in every basin except the Northern Indian Ocean remains true.

On finer regional scales, the correction has a number of varying effects. For example, the slowing trend in the western North Pacific is reduced from 20% to 16% in the basin as a whole and from 30% to 21% over land in that region, but both trends remain highly significant. The slowing trends in the global latitude bands north of 25° N are reduced and are no longer significant with 95% confidence, whereas the slowing trends from 0–15° N and 15–25° N both increase and the latter trend becomes statistically significant. Slowing over land in the Atlantic region is reduced from 20% to 16% and the confidence level of the trend drops below 95% (but remains above 90%). Slowing over land in the Australia region increases from 18% to 22%. The speed-up over land in the Northern Indian Ocean region increases from 26% to 29% and becomes significant. All of these changes have been made to the text of the original Letter.

All relevant original figures and tables (Figs. 1–3 and Extended Data Figs. 1 and 2 and Extended Data Tables 1 and 2) have been corrected and are shown below alongside the original figures for comparison and transparency (see Figs. 1–7 of this Amendment). All corrections provided here have been peer-reviewed. I thank K. T. F. Chan of the Guangdong Province Key Laboratory for Climate Change and Natural Disaster Studies, School of Atmospheric Sciences, Sun Yat-sen University, China, for pointing out the methodology errors in the original paper. The original Letter has been corrected online.

Error #1: Data that are asynoptic are omitted.

Error #2: Data that are spurious are not screened.

Kossin 2018, *Nature*

Author Correction

LETTER

Corrected: Author Correction

<https://doi.org/10.1038/s41586-018-0158-3>

A global slowdown of tropical-cyclone translation speed

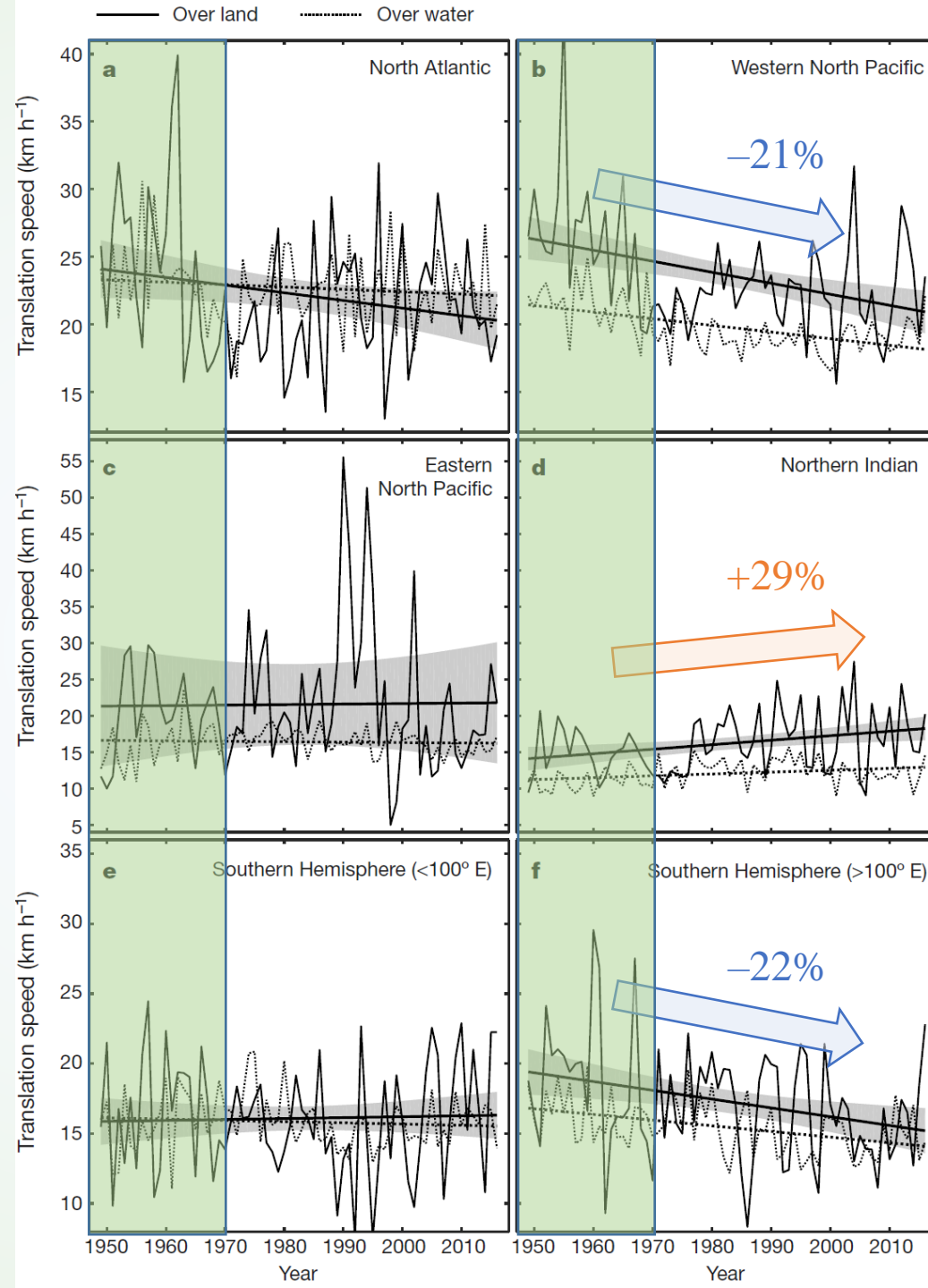
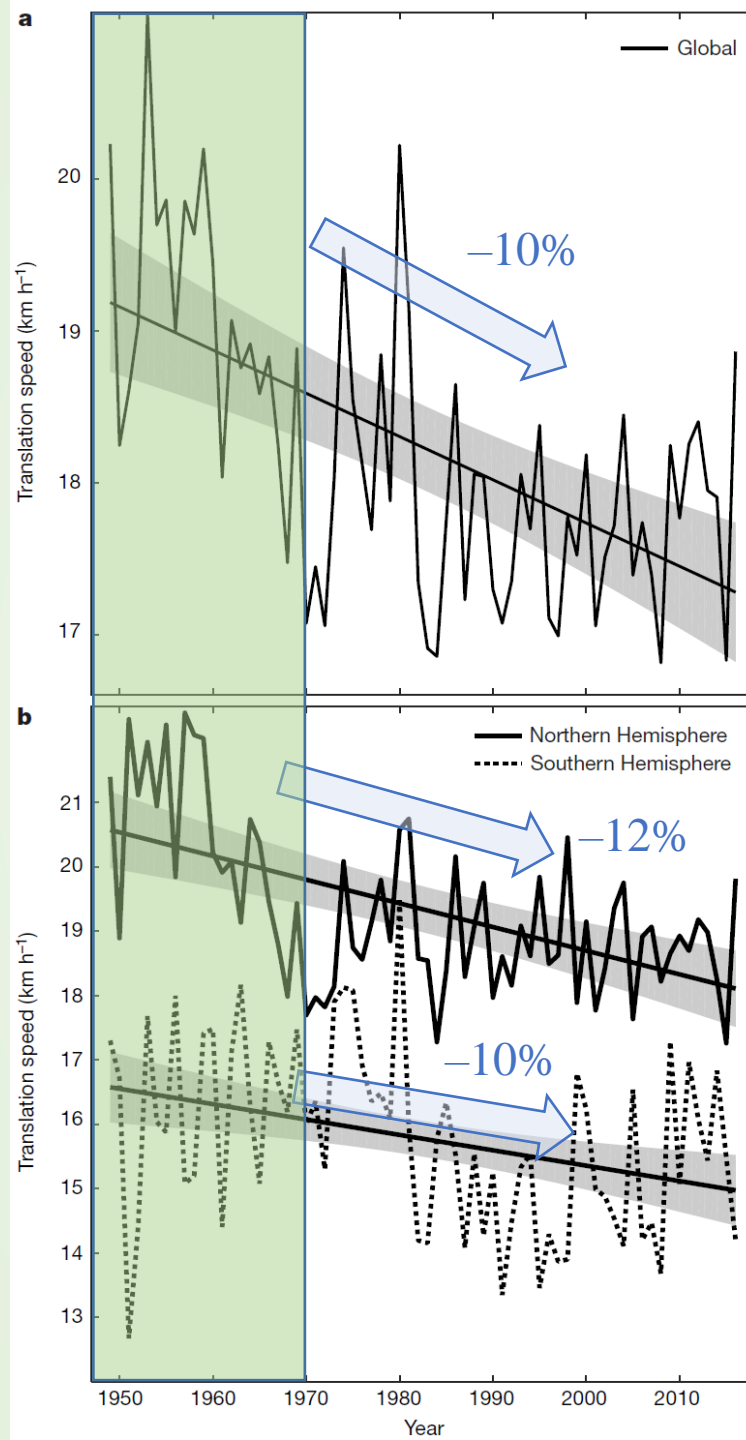
James P. Kossin^{1*}

As the Earth's atmosphere warms, the atmospheric circulation changes. These changes vary by region and time of year, but there is evidence that anthropogenic warming causes a general weakening of summertime tropical circulation^{1–8}. Because tropical cyclones are carried along within their ambient environmental wind, there is a plausible a priori expectation that the translation speed of tropical cyclones has slowed with warming. In addition to circulation changes, anthropogenic warming causes increases in atmospheric water-vapour capacity, which are generally expected to increase precipitation rates⁹. Rain rates near the centres of tropical cyclones are also expected to increase with increasing global temperatures^{10–12}. The amount of tropical-cyclone-related rainfall that any given local area will experience is proportional to the rain rates and inversely proportional to the translation speeds of tropical cyclones. Here I show that tropical-cyclone translation speed has decreased globally by 10 per cent over the period 1949–2016, which is very likely to have compounded, and possibly dominated, any increases in local rainfall totals that may have occurred as a result of increased tropical-cyclone rain rates. The magnitude of the slowdown varies substantially by region and by latitude, but is generally consistent with expected changes

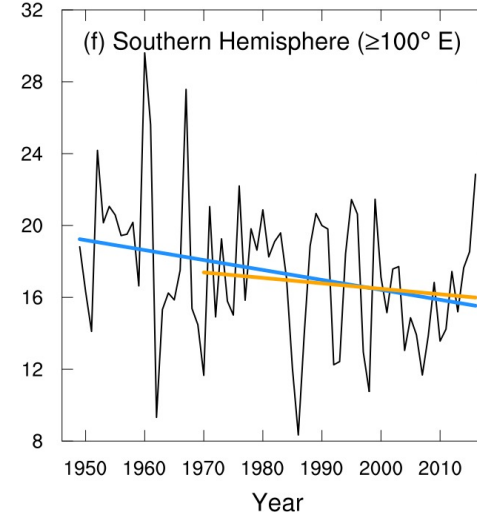
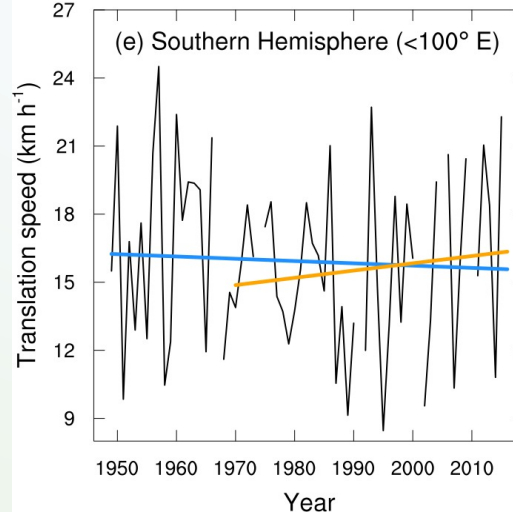
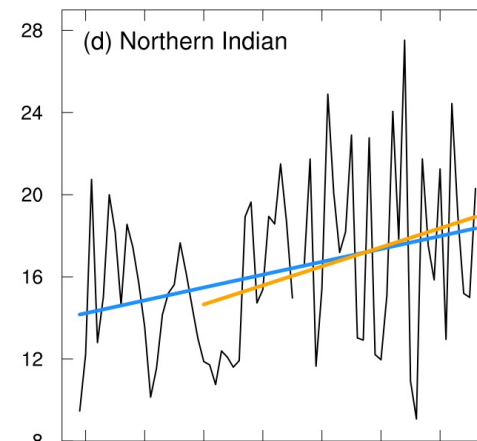
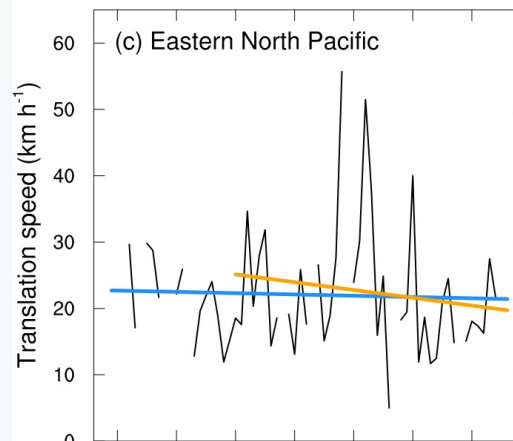
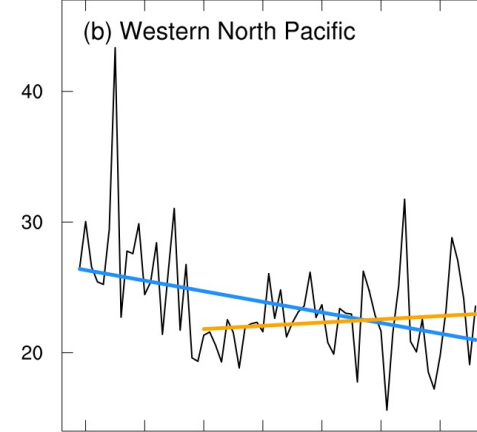
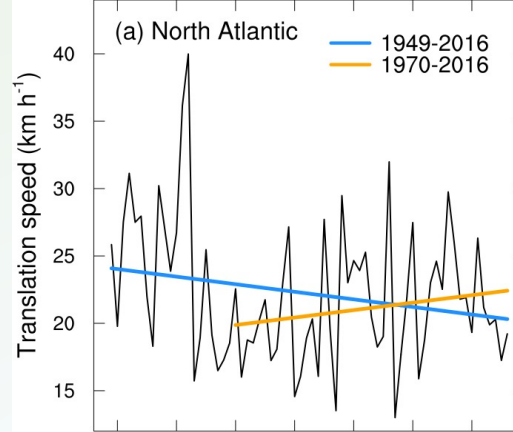
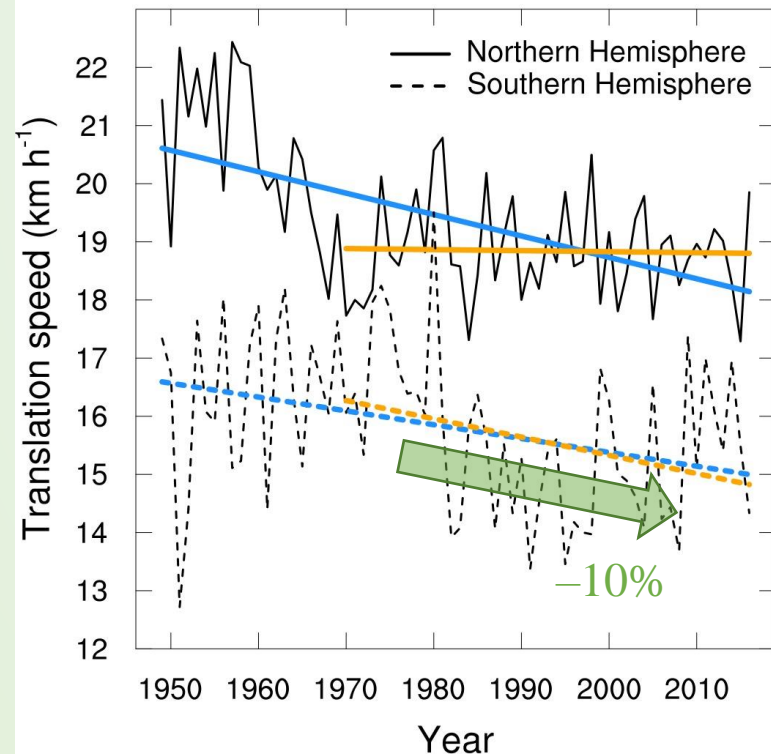
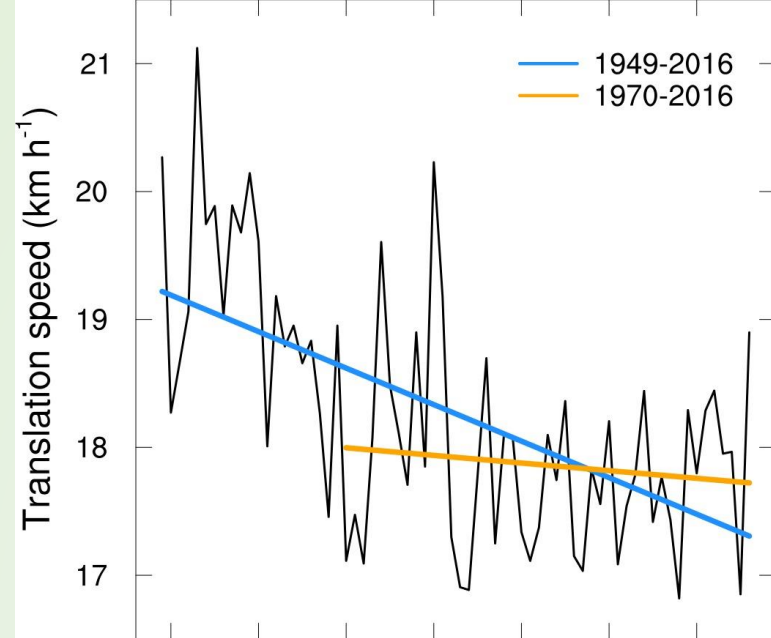
is proportional to the rate of rain produced in a tropical cyclone and inversely proportional to its translation speed; that is, a proportional unit of decrease in translation speed would have about the same effect on local rainfall totals as the same proportional unit of increase in rain rate.

Anthropogenic warming, both past and projected, is expected to affect the strength and patterns of global atmospheric circulation^{1–8}. Tropical cyclones are generally carried along within these circulation patterns so their past translation speeds may be indicative of past circulation changes. In particular, warming is linked to a weakening of tropical summertime circulation and there is a plausible a priori expectation that tropical-cyclone translation speed may be decreasing. In addition to changing circulation, anthropogenic warming is expected to increase lower-tropospheric water-vapour capacity by about 7% per degree (Celsius) of warming, as per the Clausius–Clapeyron relationship². Expectations of increased mean precipitation under global warming are well documented, but not as straightforward to quantify^{9,18}. Increases in global precipitation are constrained by the atmospheric energy budget to about 1%–2% per degree of warming^{19,20}; those in regional precipitation are further controlled by variability in moisture convergence driven by variability in regional circulation. Precipitation

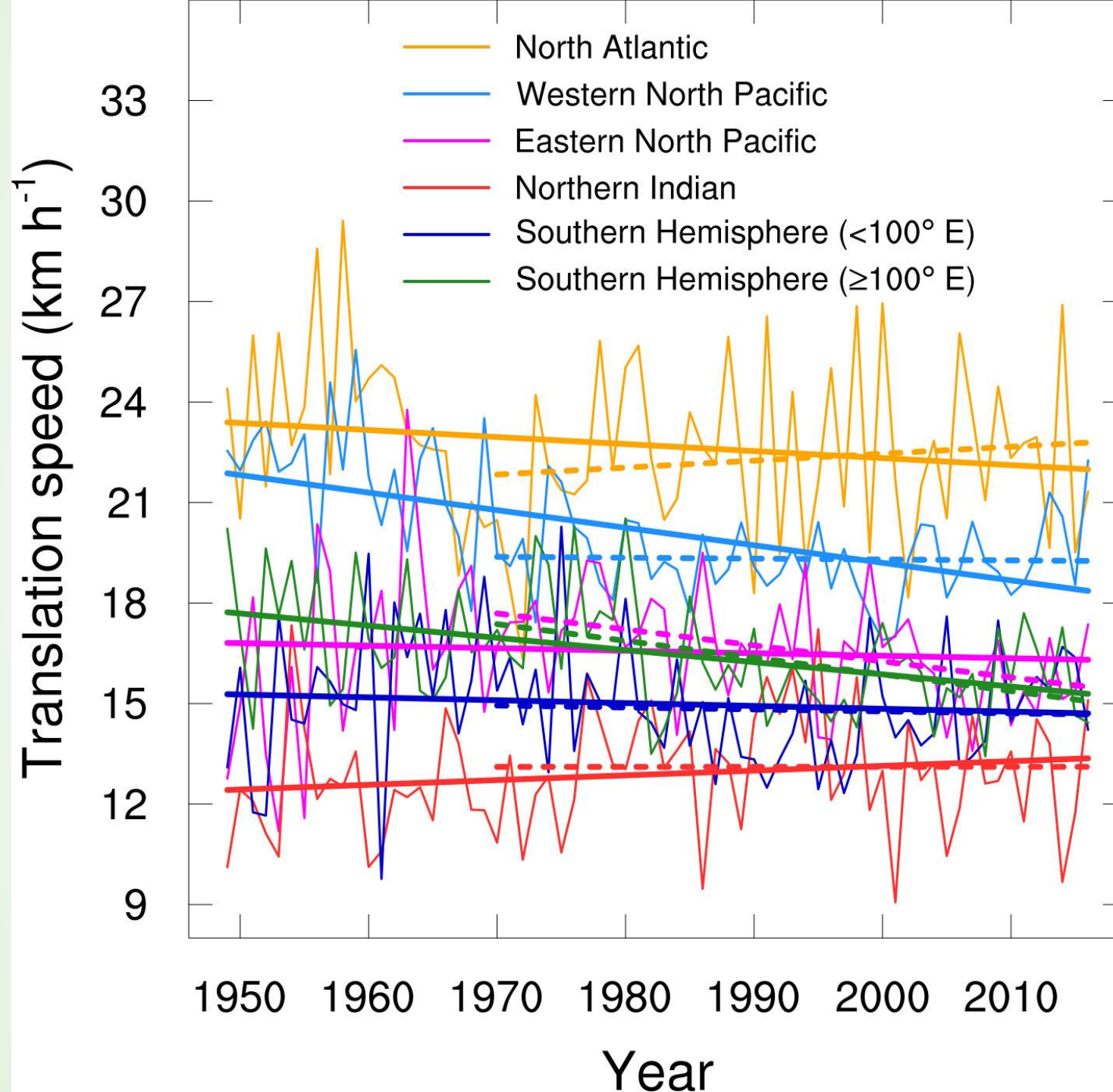
Kossin 2018, *Nature*



Kossin 2018,
Nature



Chan 2019,
*Environmental
Research Letters*



Chan 2019,
*Environmental
Research Letters*

Period	1949–2016	1970–2016
Globe	−0.03 [−10]	−0.01 [−2]
NH	−0.04 [−12]	−0.00 [−0]
SH	−0.02 [−10]	−0.03 [−10]
NA	−0.02 [−6]	+0.02 [+4]
WNP	−0.05 [−16]	−0.00 [−0]
ENP	−0.01 [−3]	−0.05 [−13]
NI	+0.01 [+8]	+0.00 [+0]
SH (<100° E)	−0.01 [−4]	−0.01 [−2]
SH (≥100° E)	−0.04 [−14]	−0.05 [−14]
>35° N	−0.06 [−11]	+0.07 [+9]
25–35° N	−0.02 [−8]	+0.00 [+1]
15–25° N	−0.01 [−6]	−0.02 [−5]
0–15° N	−0.01 [−3]	−0.02 [−4]
0–30 ° S	−0.02 [−9]	−0.03 [−8]
>30 ° S	+0.09 [+21]	−0.07 [−10]
Globe (water)	−0.03 [−11]	−0.01 [−3]
Globe (land)	+0.01 [+2]	+0.05 [+13]
NA (land)	−0.06 [−16]	+0.06 [+13]
WNP (land)	−0.08 [−21]	+0.02 [+5]
ENP (land)	−0.02 [−5]	−0.05 [−10]
NI (land)	+0.06 [+30]	+0.09 [+30]
SH (<100° E, land)	−0.01 [−4]	+0.03 [+10]
SH (≥100° E, land)	−0.06 [−20]	−0.03 [−8]

Table 1. Trends of tropical-cyclone translation speed over the periods 1949–2016 and 1970–2016 by region. Trends are in unit of $\text{km h}^{-1} \text{yr}^{-1}$ and values in squared brackets are percentage changes during corresponding periods. Significant trends, based on the two-sided 95% confidence interval, are shown in bold.

Data Caveats



NOAA NATIONAL CENTERS FOR ENVIRONMENTAL INFORMATION
NATIONAL OCEANIC AND ATMOSPHERIC ADMINISTRATION

NCDC > WDC-Meteorology > IBTrACS

International Best Track Archive for Climate Stewardship (IBTrACS)

Introduction
Status
Principles
Workshops
Previous versions
Feedback

IBTrACS News

IBTrACS Data Access

Browse IBTrACS

IBTrACS Climatology

Data Sources
Original data

IBTrACS Q&A
FAQ

Terms of Use

Bibliography

Contact Info

News
Jan 2016
All news about IBTrACS will be announced using the [news forum](#)

World Data Center for Meteorology, Asheville

Data access Parameters Formats & samples Shapefiles

IBTrACS-All data

Version: v03r10

Check out the [changes from v03r09 to v03r10](#).

Announcement

This is the last release of IBTrACS version 3. The next release (Sept. 2018) will be in the new IBTrACS version 4 format. [This page](#) provides more information.

IBTrACS News

Please [join the news forum](#) to be notified of: new releases, data set errors and other important information about IBTrACS.

Feedback

We welcome feedback on IBTrACS through our [feedback form](#). You can also provide information on how you use IBTrACS which helps us justify continued updates, support and improvements.

Caveats

The following caveats should be considered prior to using IBTrACS:

- **BUGS** - Dataset errors will be noted on the [status page](#).
- Due to the disparity between storm positions prior to 1970, some tracks during that period may not be properly merged.
- Due to the disparities in time between sources, some dates and times were changed in one source to match another. However, it is not clear which source had the correct time or date. From the original 16,539 storm tracks, only 255 required time adjustments.

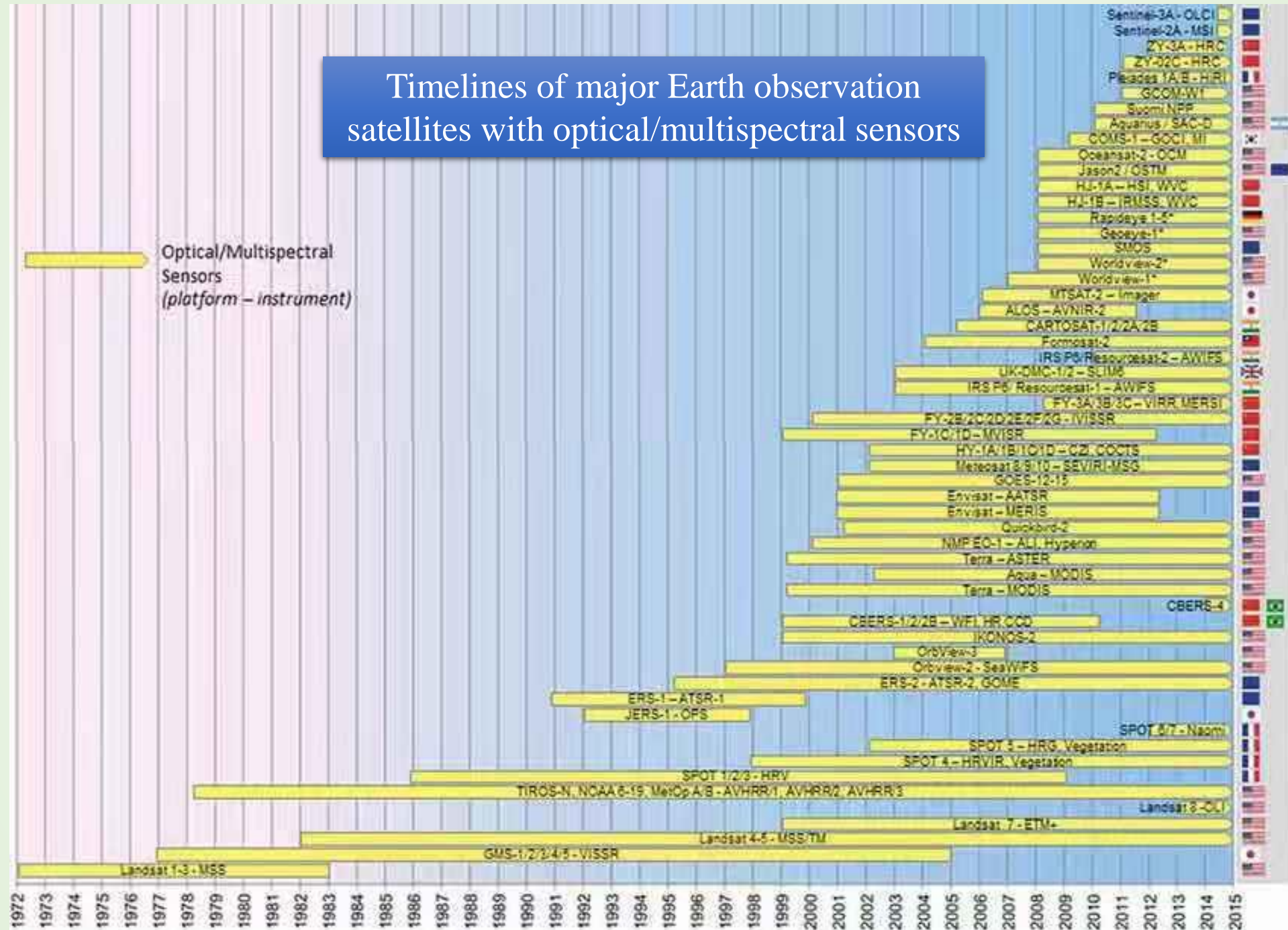
NCDC Data set identification

- IBTrACS has been assigned NCDC data set identification (DSI) 9637
- [ISO 19115-2 Metadata is also available](#)

IBTrACS:

“Due to the disparities between storm positions prior to 1970, some tracks during that period may not be properly merged.”

Timelines of major Earth observation satellites with optical/multispectral sensors



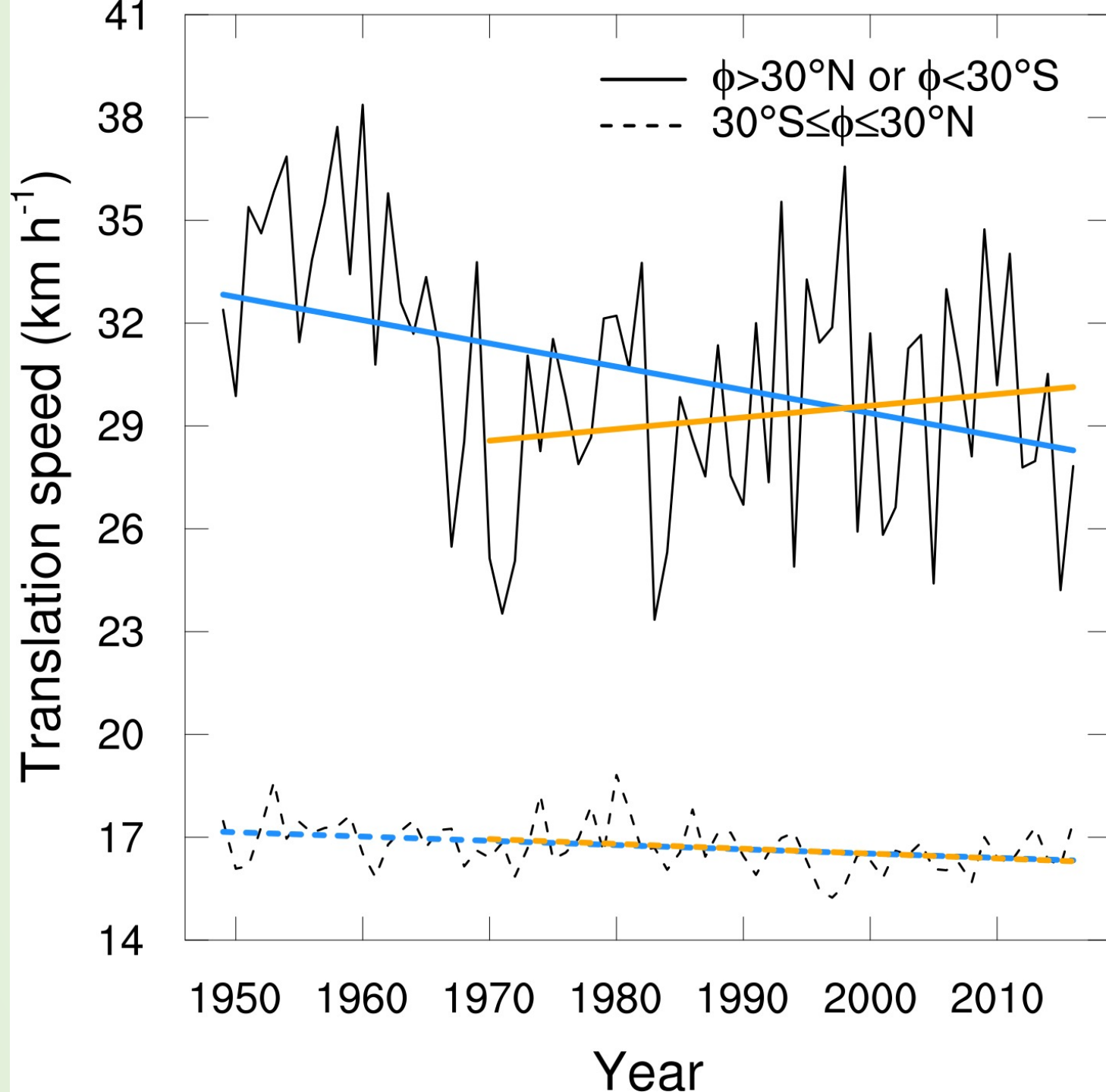
	Period		Change (%)
	1949–1969 (Pre-satellite era)	1970–2016 (Satellite era)	
Globe	1898	2594	+37
Globe (water)	1668	2391	+43
Globe (land)	230	203	–12
NH	1273	1818	+43
NH (water)	1111	1670	+50
NH (land)	162	148	–9
SH	625	777	+24
SH (water)	557	722	+30
SH (land)	68	55	–20
NA	343	379	+10
NA (water)	299	335	+12
NA (land)	44	44	+0
WNP	617	866	+40
WNP (water)	563	795	+41
WNP (land)	54	71	+31
ENP	151	447	+196
ENP (water)	146	440	+201
ENP (land)	4	7	+75
NI	163	126	–23
NI (water)	102	99	–3
NI (land)	60	27	–55
SH (<100° E)	289	386	+34
SH (<100° E, water)	271	371	+37
SH (<100° E, land)	18	15	–17
SH (≥100° E)	336	391	+16
SH (≥100° E, water)	286	351	+23
SH (≥100° E, land)	50	40	–20

Table 2. Annual-mean numbers and percentage changes of tropical-cyclone position records by period and region. Significant changes, based on the one-sided 95% confidence interval, are shown in bold.

Increase in records is far beyond the natural or external climate variabilities.

Records in pre-satellite era is likely incomplete, hence, they cannot well represent the reality.

		<30° S	20–30° S	10–20° S	0–10° S	0–10° N	10–20° N	20–30° N	>30° N
NH	1949–1969					70	552	433	218
	1970–2016					156	959	471	232
	Change (%)					+123	+74	+9	+6
SH	1949–1969	31	176	382	36				
	1970–2016	22	170	514	70				
	Change (%)	–29	–3	+35	+94				
NA	1949–1969					2	88	123	130
	1970–2016					2	117	121	139
	Change (%)					+0	+33	–2	+7
WNP	1949–1969					50	282	200	84
	1970–2016					122	419	239	86
	Change (%)					+144	+49	+20	+2
ENP	1949–1969					0*	102	45	4
	1970–2016					10	345	86	7
	Change (%)					—	+238	+91	+75
NI	1949–1969					19	80	64	0*
	1970–2016					22	78	25	0
	Change (%)					+16	–3	–61	—
SH (<100° E)	1949–1969	8	77	177	27				
	1970–2016	10	84	243	50				
	Change (%)	+25	+9	+37	+85				
SH (≥100° E)	1949–1969	22	100	205	9				
	1970–2016	12	87	272	20				
	Change (%)	–45	–13	+33	+122				



Slowdown trend in 1949–2016:
1. High values in pre-satellite era (1949–1969) at high latitudes
2. More low-latitude records in satellite era (1970s onward)

Insignificant trend in 1970–2016

Chan 2019,
*Environmental
Research Letters*

Modelling Study

Dynamical Downscaling Projections of Twenty-First-Century Atlantic Hurricane Activity: CMIP3 and CMIP5 Model-Based Scenarios

THOMAS R. KNUTSON,* JOSEPH J. SIRUTIS,* GABRIEL A. VECCHI,* STEPHEN GARNER,* MING ZHAO,*
HYEONG-SEOG KIM,⁺ MORRIS BENDER,* ROBERT E. TULEYA,[#] ISAAC M. HELD,*
AND GABRIELE VILLARINI[@]

^{*} NOAA/Geophysical Fluid Dynamics Laboratory, Princeton, New Jersey

⁺ Program in Atmospheric and Oceanic Sciences, Princeton University, Princeton, New Jersey

[#] Center for Coastal Physical Oceanography, Old Dominion University, Norfolk, Virginia

[@] IHR-Hydroscience and Engineering, The University of Iowa, Iowa City, Iowa

(Manuscript received 27 July 2012, in final form 8 February 2013)

ABSTRACT

Twenty-first-century projections of Atlantic climate change are downscaled to explore the robustness of potential changes in hurricane activity. Multimodel ensembles using the phase 3 of the Coupled Model Intercomparison Project (CMIP3)/Special Report on Emissions Scenarios A1B (SRES A1B; late-twenty-first century) and phase 5 of the Coupled Model Intercomparison Project (CMIP5)/representative concentration pathway 4.5 (RCP4.5; early- and late-twenty-first century) scenarios are examined. Ten individual CMIP3 models are downscaled to assess the spread of results among the CMIP3 (but not the CMIP5) models. Downscaling simulations are compared for 18-km grid regional and 50-km grid global models. Storm cases from the regional model are further downscaled into the Geophysical Fluid Dynamics Laboratory (GFDL) hurricane model (9-km inner grid spacing, with ocean coupling) to simulate intense hurricanes at a finer resolution.

A significant reduction in tropical storm frequency is projected for the CMIP3 (−27%), CMIP5-early (−20%) and CMIP5-late (−23%) ensembles and for 5 of the 10 individual CMIP3 models. Lifetime maximum hurricane intensity increases significantly in the high-resolution experiments—by 4%–6% for CMIP3 and CMIP5 ensembles. A significant increase (+87%) in the frequency of very intense (categories 4 and 5) hurricanes (winds $\geq 59 \text{ m s}^{-1}$) is projected using CMIP3, but smaller, only marginally significant increases are projected (+45% and +39%) for the CMIP5-early and CMIP5-late scenarios. Hurricane rainfall rates increase robustly for the CMIP3 and CMIP5 scenarios. For the late-twenty-first century, this increase amounts to +20% to +30% in the model hurricane's inner core, with a smaller increase (~10%) for averaging radii of 200 km or larger. The fractional increase in precipitation at large radii (200–400 km) approximates that expected from environmental water vapor content scaling, while increases for the inner core exceed this level.

We have computed storm propagation speed statistics from our storm samples (labeled trans speed in Tables 3 and 4). The results for the CMIP3 and CMIP5 ensembles indicate no significant changes, and only 2 of the 10 individual CMIP3 model projections show a significant change (increase). In short, there is not a clear consistent signal in the storm propagation speed projections.

Relevant Concerns

MATTERS ARISING

<https://doi.org/10.1038/s41586-019-1222-3>

Climate change and tropical cyclone trend

Il-Ju Moon^{1*}, Sung-Hun Kim^{1*} & Johnny C. L. Chan²

ARISING FROM J. P. Kossin *Nature* <https://www.nature.com/articles/s41586-018-0158-3>

Understanding the response of tropical cyclones to a changing climate has become a topic of great interest and research. Kossin¹ showed that tropical-cyclone translation speed (TCS) has decreased globally by 10% over the period 1949–2016 and stated that this is consistent with the expected changes in atmospheric circulation forced by anthropogenic warming. However, we question the robustness of his conclusions¹ for the following reasons: (1) TCSs generally increase with the latitude of the tropical cyclones and are therefore very sensitive to the bias of tropical-cyclone detection with respect to latitude; and (2) in the pre-satellite era (1949–1965), there is a high possibility that systematic biases in the detection of tropical cyclones exist in the best-track data, which could produce spurious trends in TCS. Therefore, the slowdown of TCS stated¹ may not be a real climate signal or it may be exaggerated.

approach the fact missed tions o
And speeds era. For 30 annua 35 kno icantly 129% i climate 8% in

Moon et al. 2019, *Nature*

MATTERS ARISING

Uncertainties in tropical-cyclone translation speed

John R. Lanzante^{1*}

ARISING FROM J. P. Kossin *Nature* <https://www.nature.com/articles/s41586-018-0158-3> (2018)

In the scientific literature there have been suggestions that anthropogenic climate change (ACC) may lead to slower movement of tropical cyclones, potentially resulting in more intense precipitation in their path. Motivated by this, a recent innovative study¹ suggested that over about the past 70 years there has been a considerable monotonic slowdown in translational speed in many regions of the world. Here I raise doubt as to the veracity of that finding, because the long-term changes appear to be due primarily to a few abrupt, step-like changes, both natural and artificial, in the early part of the record. This greatly reduces the likelihood that the apparent slowdown is driven primarily by anthropogenic causes.

Time series for the six basins used by Kossin¹ (NA, North Atlantic; EP, Eastern Pacific; WP, Western Pacific; NI, Northern Indian; SP, Southern Pacific; and SI, Southern Indian), constructed in a similar fashion (see Supplementary Methods) are given in Fig. 1, along with those for three aggregate regions (GL, Global; NH, Northern Hemisphere; SH, Southern Hemisphere). In addition, Fig. 1 displays the steps formed by the change-points and the relative likelihoods (see Extended Data Table 2).

Although the character of the TCS time series in Fig. 1 varies between regions, the results of the BIC analyses are consistent in that the FS model is selected as most likely in all cases except for in the WP in

Multidecadal Variability of Tropical Cyclone Translation Speed over the Western North Pacific

YI-PENG GUO¹,^a ZHE-MIN TAN¹,^a AND XU CHEN^a

^a Key Laboratory of Mesoscale Severe Weather, Ministry of Education, and School of Atmospheric Sciences, Nanjing University, Nanjing, China

(Manuscript received 3 October 2022, in final form 4 April 2023, accepted 2 May 2023)

ABSTRACT: Tropical cyclone (TC) translation speed (TCS) over the western North Pacific (WNP) has experienced a long-term decreasing trend. To date, however, little is known about the multidecadal variability of TCS and its possible influence on this trend. This study investigated the multidecadal variability of the WNP TCS and the underlying physical mechanisms. Results show that the WNP TCS presents robust multidecadal variability during the past seven decades, which is dominated by the TCS over the extratropics. Further analysis shows that the Atlantic multidecadal oscillation (AMO) is responsible for the TCS multidecadal variability. AMO positive (negative) phases lead to favorable (unfavorable) large-scale environmental conditions for maintaining TCs over the extratropics, which results in longer (shorter) residence time for TCs having been accelerated by the midlatitude westerlies, thus, leading to higher (lower) TCS. The TCS phase shift strongly offsets its slowdown trend, leading to the inconsistent trends during past decades. This inconsistency may also relate to the influence of extratropical transitioned cyclones without being totally excluded. These cyclones may be inhomogeneously recorded due to the absence of satellite observation before the 1980s. Our results indicate that internal variation such as AMO may dominate TCS low-frequency variations over the past several decades. Previous studies have attributed the inconsistent trends of TCS during different subperiods to data inhomogeneity. This study shows that AMO can modulate the TCS trends in different subperiods with phase shift, thus providing new evidence for the recent controversial TCS slowdown.

Guo et al. 2023,
Journal of Climate

Lanzante 2019, *Nature*

Conclusions

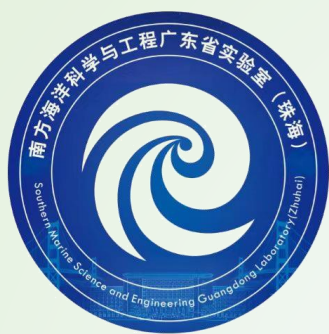
- No rigorous and significant observational and modelling evidences show that global tropical cyclones are moving slower in a warming climate.
- The local tropical-cyclone-related rainfall totals over land are more likely to decrease. The potential increase in local rainfall totals over land by the tropical cyclones in the future climate suggested by Kossin (2018a) is suspicious.
- The data artefacts introduced by the changes in measurement practices, particularly the introduction of satellite remote sensing capabilities since the 1970s, are likely the main source of heterogeneities leading to such disagreement.
- Thousands of cares must be taken when dealing with the tropical-cyclone best-track data in the pre-satellite era.

References

- Knutson, T. R. et al. (2013) Dynamical downscaling projections of twenty-first-century Atlantic hurricane activity: CMIP3 and CMIP5 model-based scenarios. *Journal of Climate*, 26, 6591–6617.
- Kossin, J. P. (2018) A global slowdown of tropical-cyclone translation speed. *Nature*, 558, 104–107.
- Kossin, J. P. (2018) Author correction: A global slowdown of tropical-cyclone translation speed. *Nature*, 564, E11–E16.
- Lanzante, J. R. (2019) Uncertainties in tropical-cyclone translation speed. *Nature*, 570, E6–E15.
- Moon, I.-J., Kim, S.-H., & Chan, J. C. L. (2019) Climate change and tropical cyclone trend. *Nature*, 570, E3–E5.
- Chan, K. T. F. (2019) Are global tropical cyclones moving slower in a warming climate? *Environmental Research Letters*, 10, 104015.
- Guo, Y.-P. et al. (2023) Multidecadal variability of tropical cyclone translation speed over the western North Pacific. *Journal of Climate*, 36, 5793–5807.

Recent Hot Topics of Tropical Cyclones

- Translation Speed
- Landfall Decay



Uncertainties in Tropical Cyclone Landfall Decay

Kelvin T. F. CHAN^{1,2,3}, Johnny C. L. CHAN^{4,5,6}, Kailin ZHANG¹, and Yue WU¹

¹School of Atmospheric Sciences, Sun Yat-sen University, and Southern Marine Science and Engineering Guangdong Laboratory (Zhuhai), Zhuhai, China

²Guangdong Province Key Laboratory for Climate Change and Natural Disaster Studies, Sun Yat-sen University, Zhuhai, China

³Key Laboratory of Tropical Atmosphere-Ocean System (Sun Yat-sen University), Ministry of Education, Zhuhai, China

⁴Guy Carpenter Asia-Pacific Climate Impact Centre, School of Energy and Environment, City University of Hong Kong, Hong Kong, China

⁵Shanghai Typhoon Institute, China Meteorological Administration, Shanghai, China

⁶Asia-Pacific Typhoon Collaborative Research Center, Shanghai, China

Background

Li and Chakraborty 2020, *Nature*

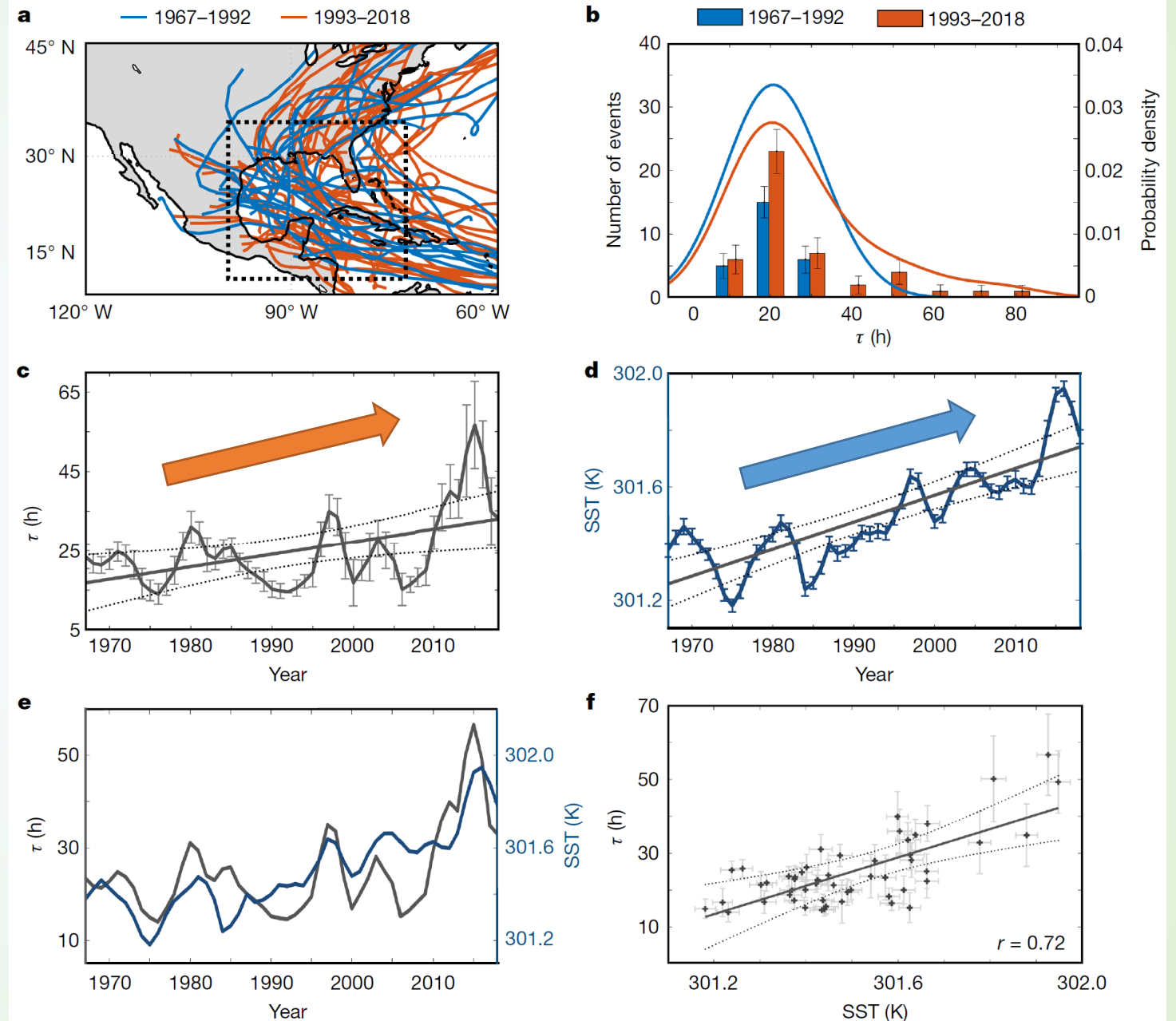
$$V(t) = V(t_1)e^{-\frac{t-t_1}{\tau}}$$

Decay timescale τ

Slower decay of landfalling
hurricanes in 1967–2018

$\tau \propto \text{SST}_s$ (June–November)

Slower decay of landfalling
hurricanes in a warming world



Background

Li and Chakraborty 2020, *Nature*

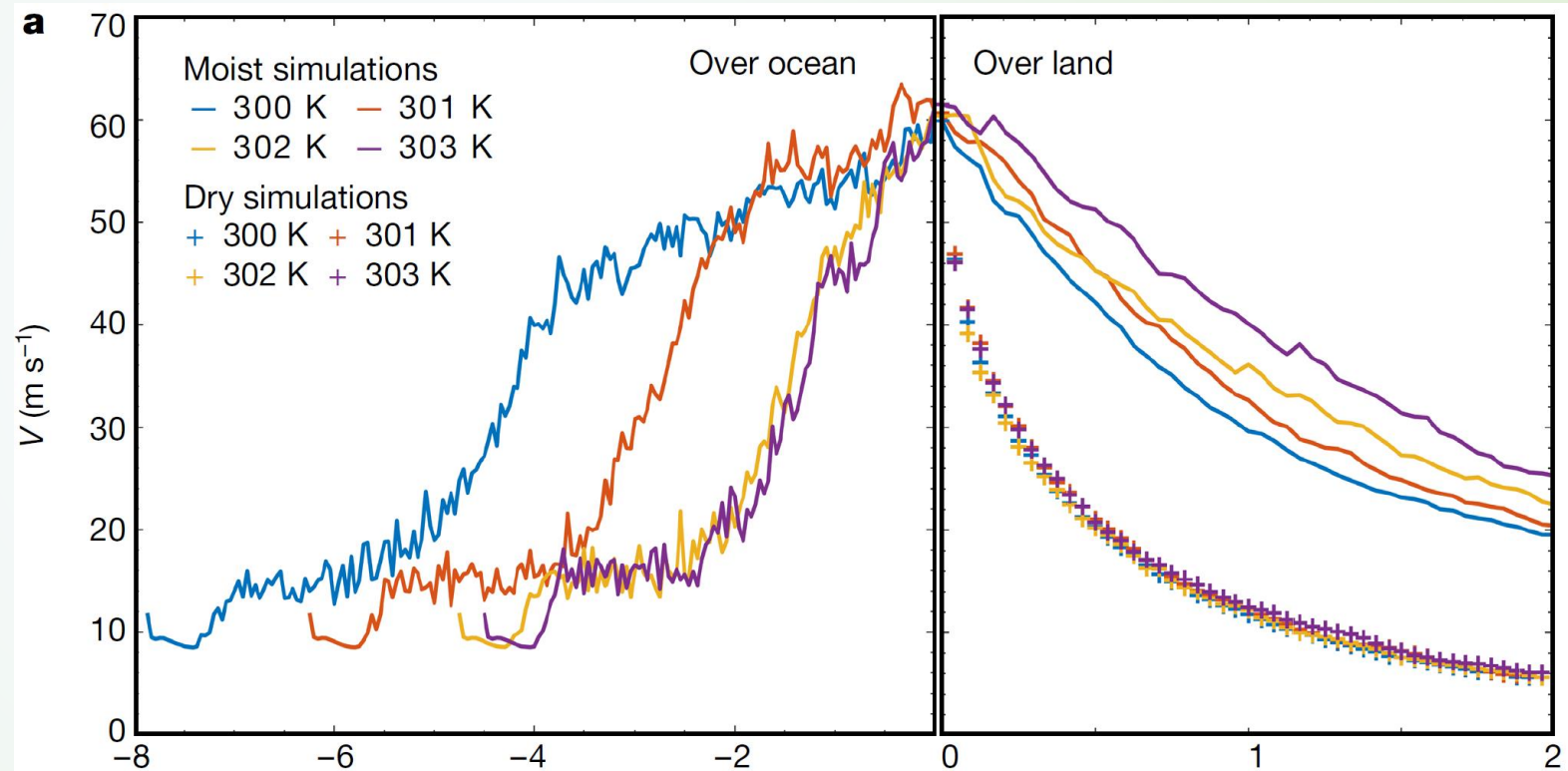
Dry simulations:

- Not sensitive to SST
- Decay rapidly after landfall

Moist simulations:

- Sensitive to SST
- Warmer SST, slower decay

Role of moisture is important.



Higher SST



More Moisture



Slower Decay

Matters Arising

Chan et al. 2022, *Nature*

[based on raw data without smoothing]

Sampling

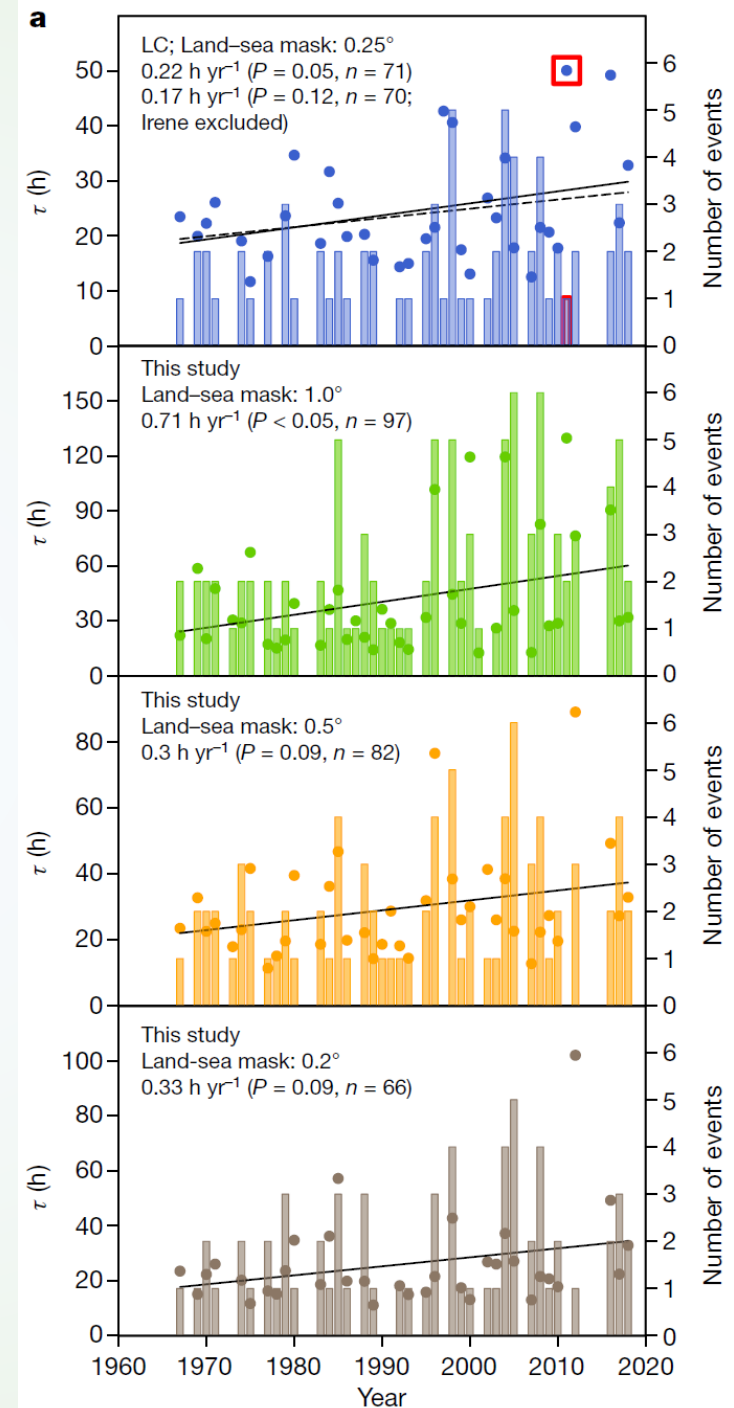
- Sample size large enough?
- Landfall or not-landfall?

Method

- Double 3-year smoothing?
- Large-area 6-month SST average?

Significance

- Attributed to the warming SST?



Matters Arising

Chan et al. 2022, *Nature*

[based on raw data without smoothing]

Sampling

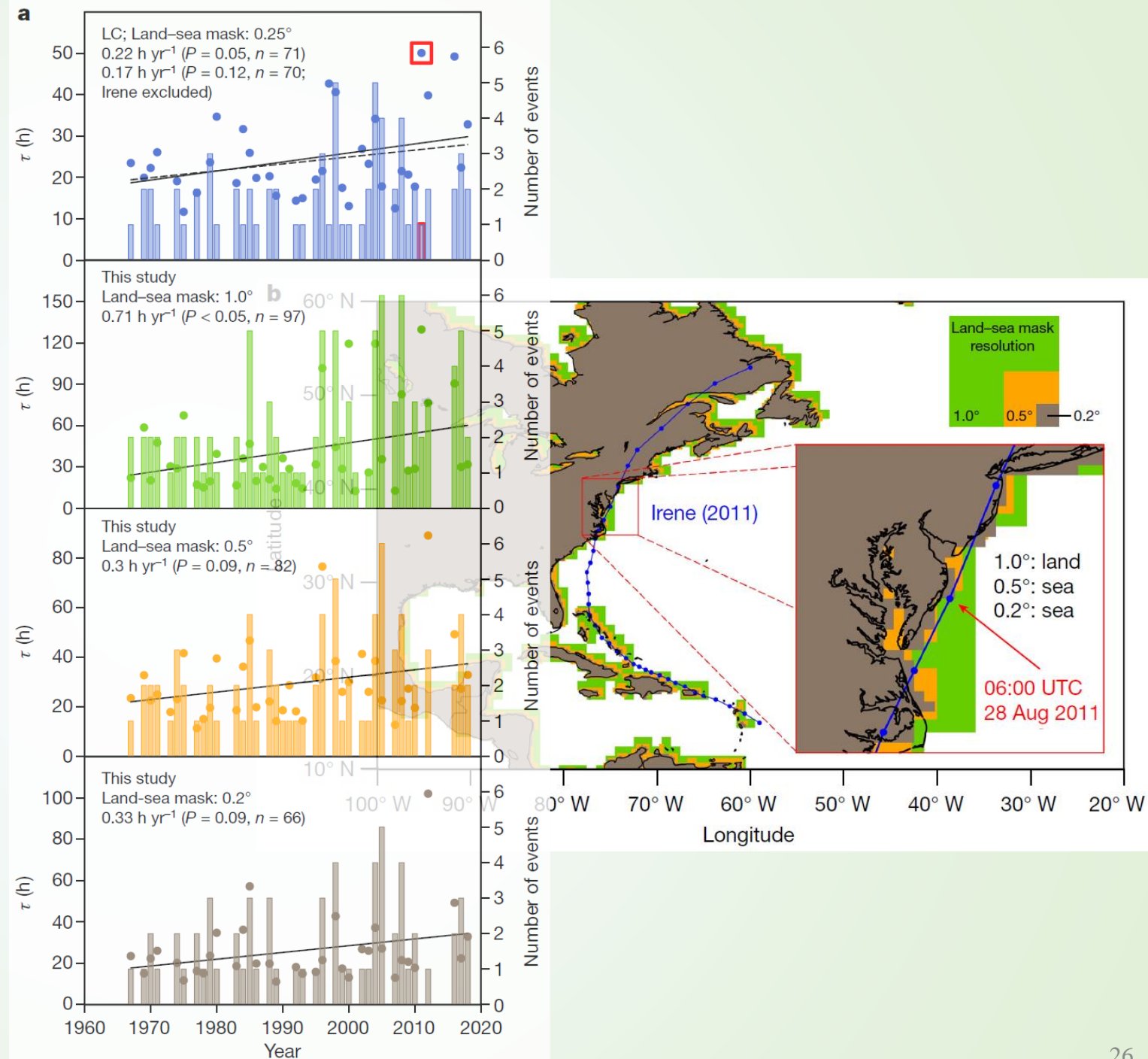
- Sample size large enough?
- Landfall or not-landfall?

Method

- Double 3-year smoothing?
- Large-area 6-month SST average?

Significance

- Attributed to the warming SST?



Matters Arising

Chan et al. 2022, *Nature*

[based on raw data without smoothing]

Sampling

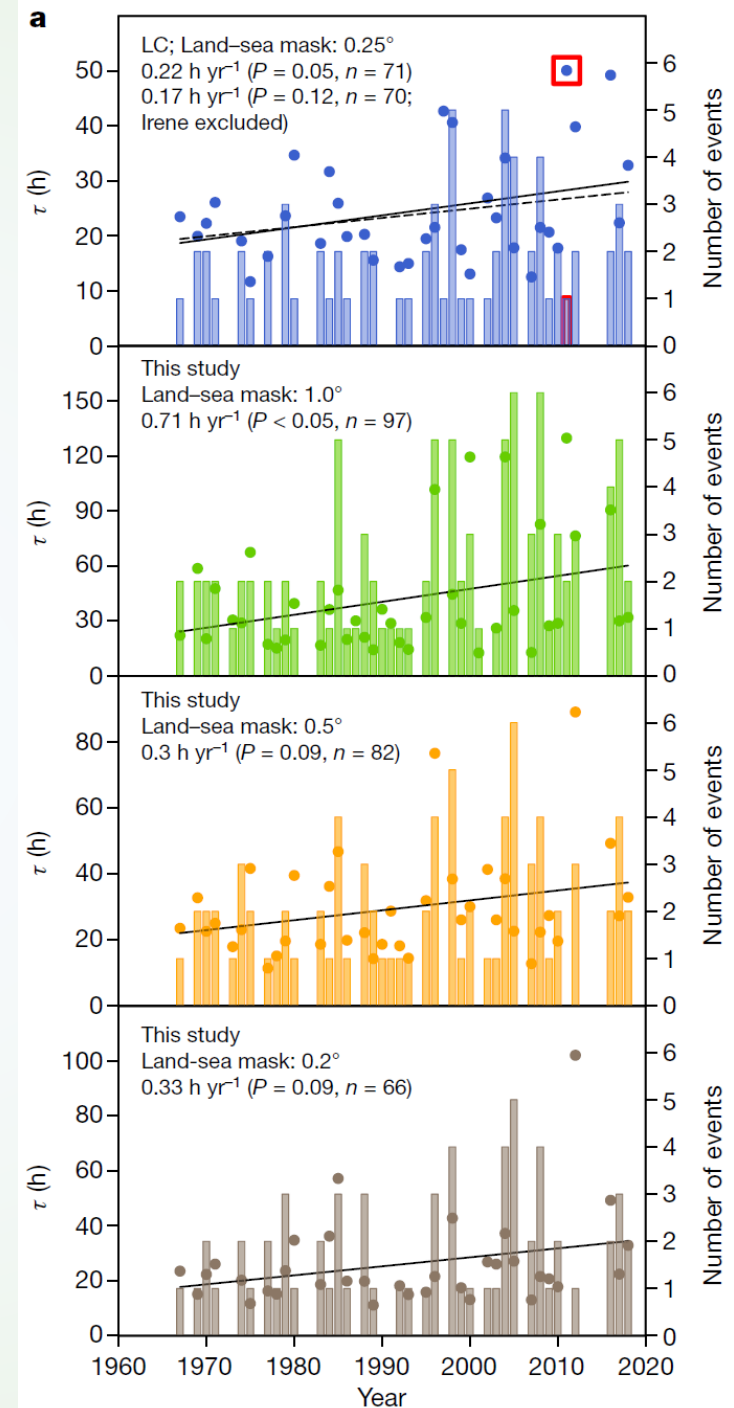
- Sample size large enough?
- Landfall or not-landfall?

Method

- Double 3-year smoothing?
- Large-area 6-month SST average?

Significance

- Attributed to the warming SST?



Matters Arising

Chan et al. 2022, *Nature*

[based on raw data without smoothing]

Sampling

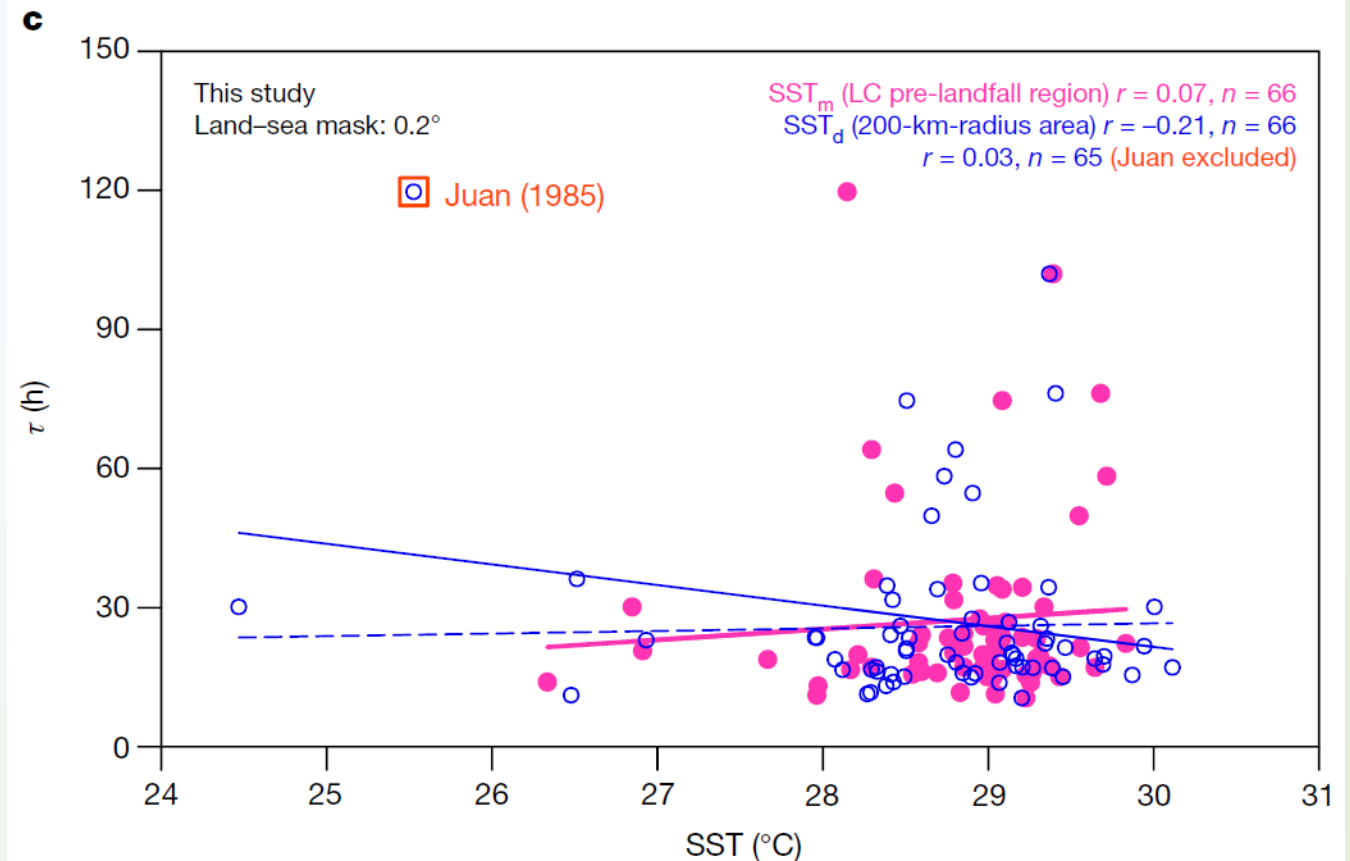
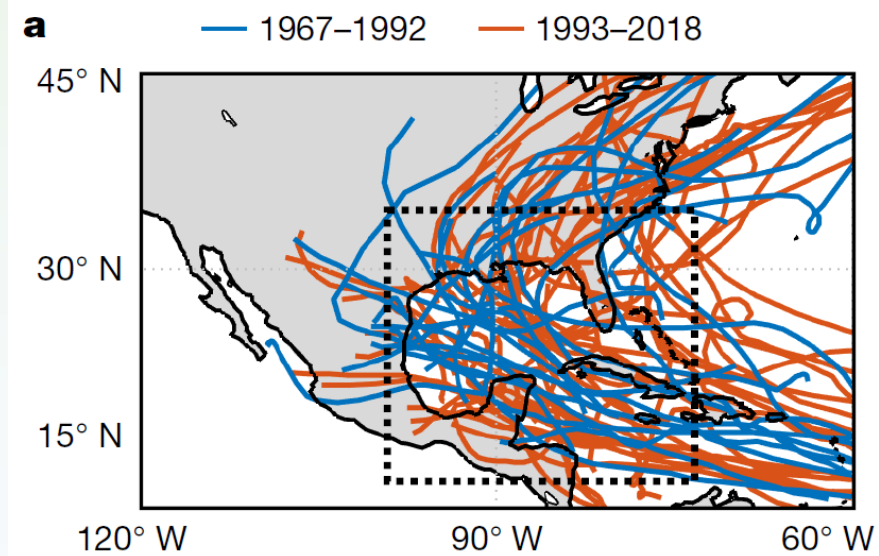
- Sample size large enough?
- Landfall or not-landfall?

Method

- Double 3-year smoothing?
- Large-area 6-month SST average?

Significance

- Attributed to the warming SST?



Matters Arising

Chan et al. 2022, *Nature*

[based on raw data without smoothing]

Sampling

- Sample size large enough?
- Landfall or not-landfall?

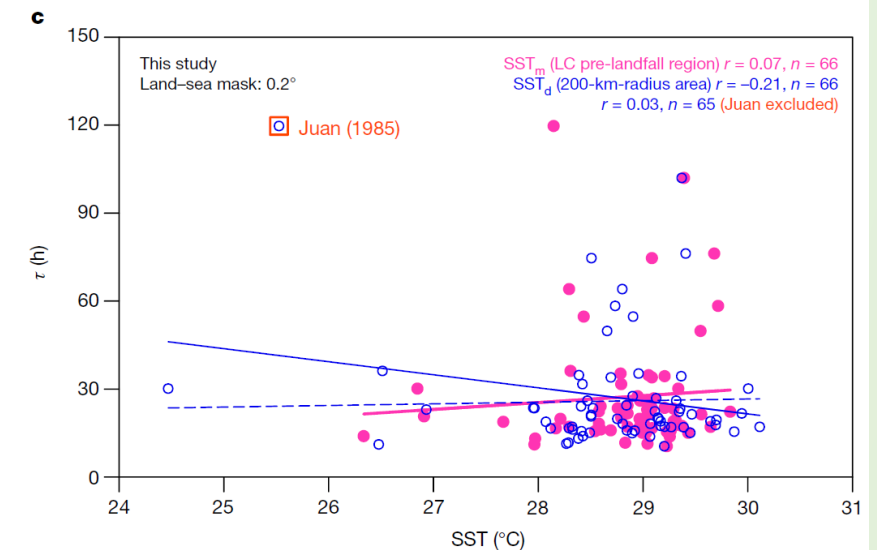
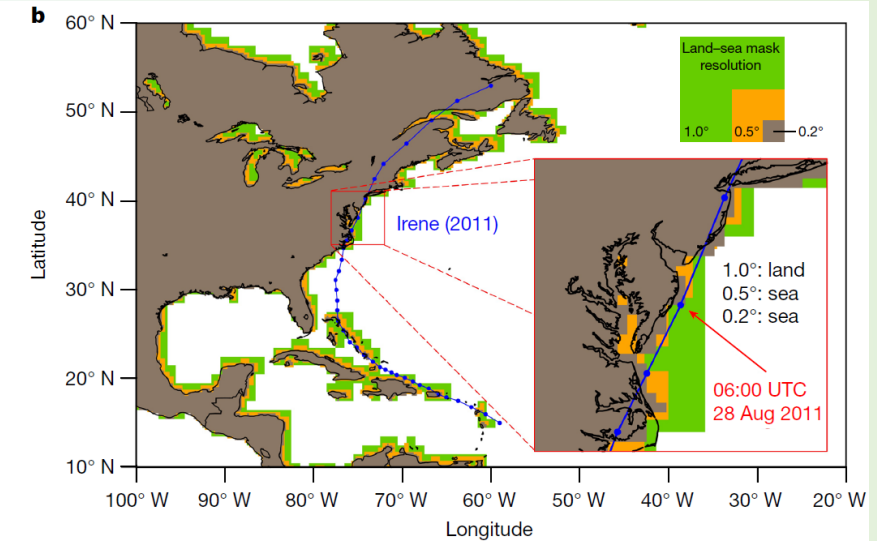
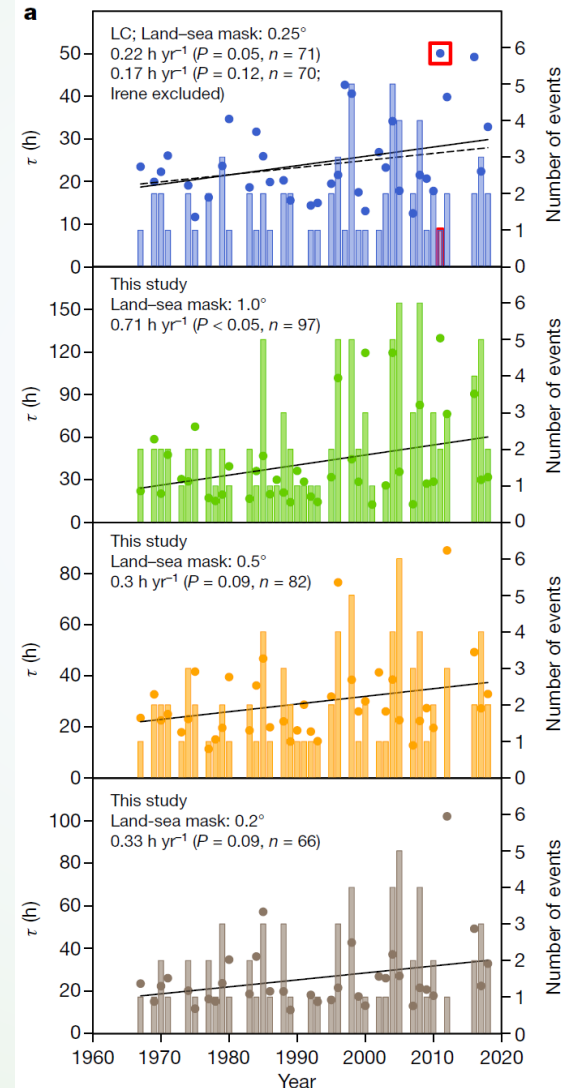
Method

- Double 3-year smoothing?
- Large-area 6-month SST average?

Significance

- Attributed to the warming SST?

τ is increasing but not significant and likely not primarily related to the warming SST.



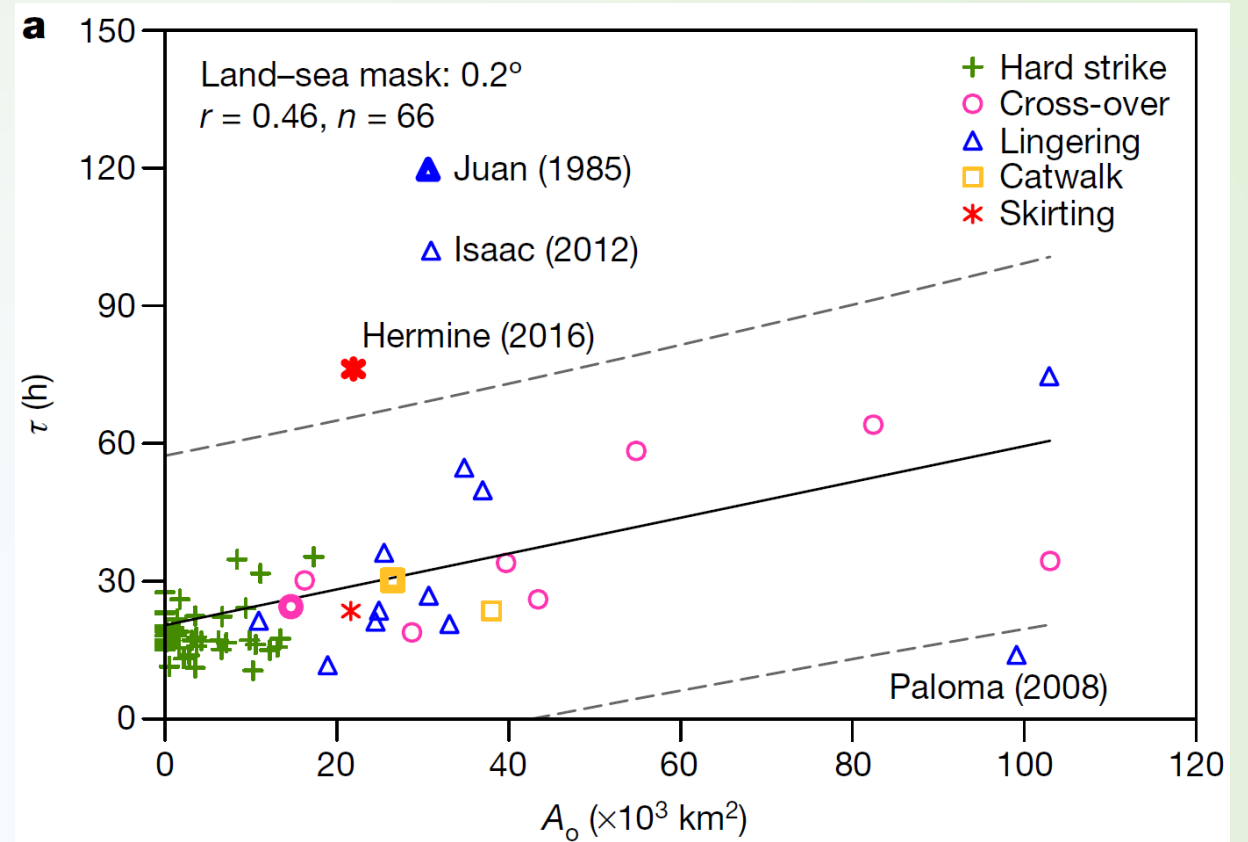
Matters Arising

Chan et al. 2022, *Nature*

[based on raw data without smoothing]

radius ≤ 200 km

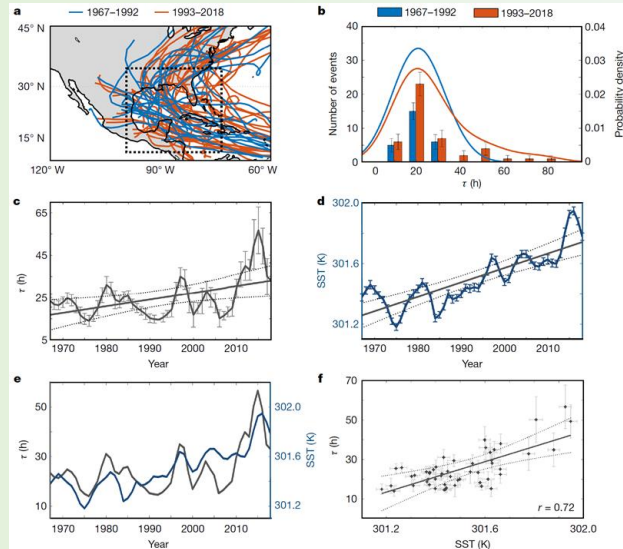
Effective area of moisture supply
from ocean A_o



Larger the A_o , the less the land-surface friction and less energy dissipated, and, thus, the longer the τ .

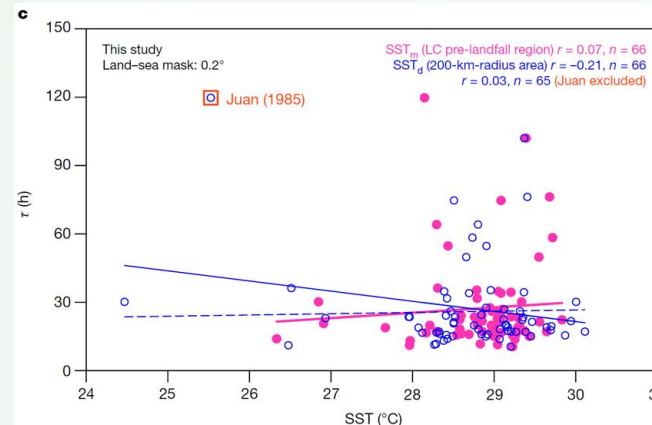
A larger A_o implies more sea surface enthalpy flux so that more thermal energy is available for kinetic energy conversion, and the decay would slow down as a result.

Matters Arising



Li and Chakraborty (2020, *Nature*)

SST_s (June–November; pre-landfall big area)



Chan et al (2022, *Nature*)

SST_m (contemporaneous month; pre-landfall big area)

SST_d (daily; 200-km-radius area)

$$\tau = 9.17A_o' + 1.68SST_s' + C \quad r = 0.69$$

$(P < 10^{-3}) \quad (P = 0.47)$

$$\tau = 10.35A_o' + 3.86SST_m' + C \quad r = 0.71$$

$(P < 10^{-3}) \quad (P = 0.10)$

$$\tau = 9.13A_o' - 3.34SST_d' + C \quad r = 0.70$$

$(P < 10^{-3}) \quad (P = 0.14)$

A_o is the primary

SST_m and SST_d are more contributory than SST_s

Matters Arising

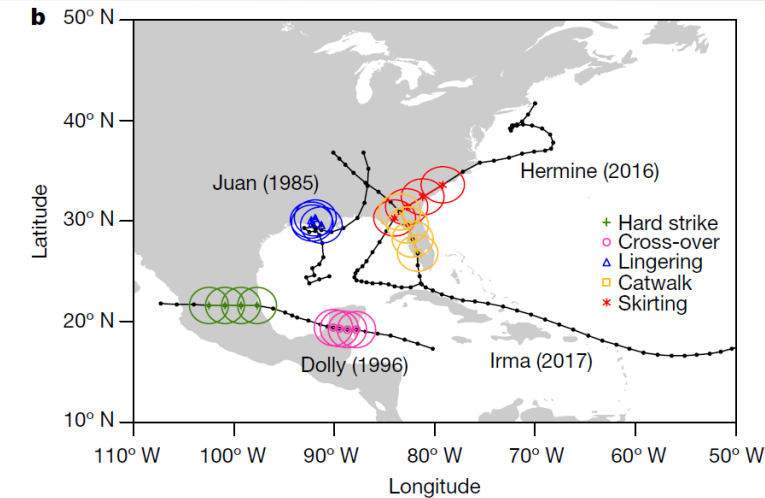
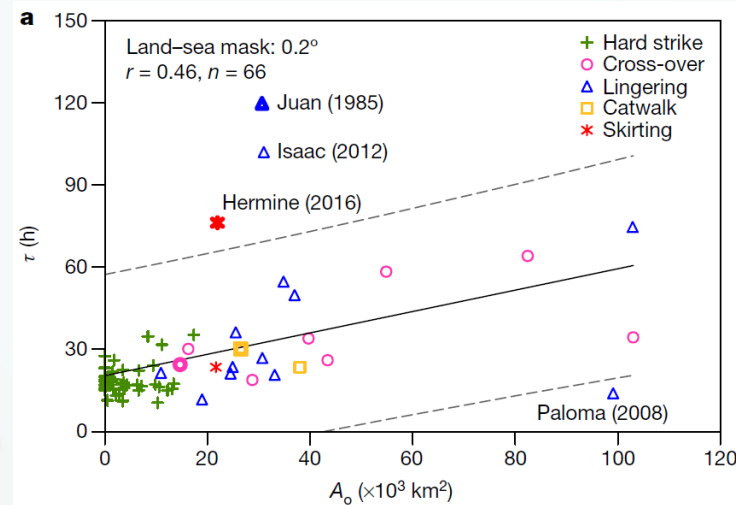
Chan et al. 2022, *Nature*

[based on raw data without smoothing]

radius ≤ 200 km

Effective area of moisture supply
from ocean A_O

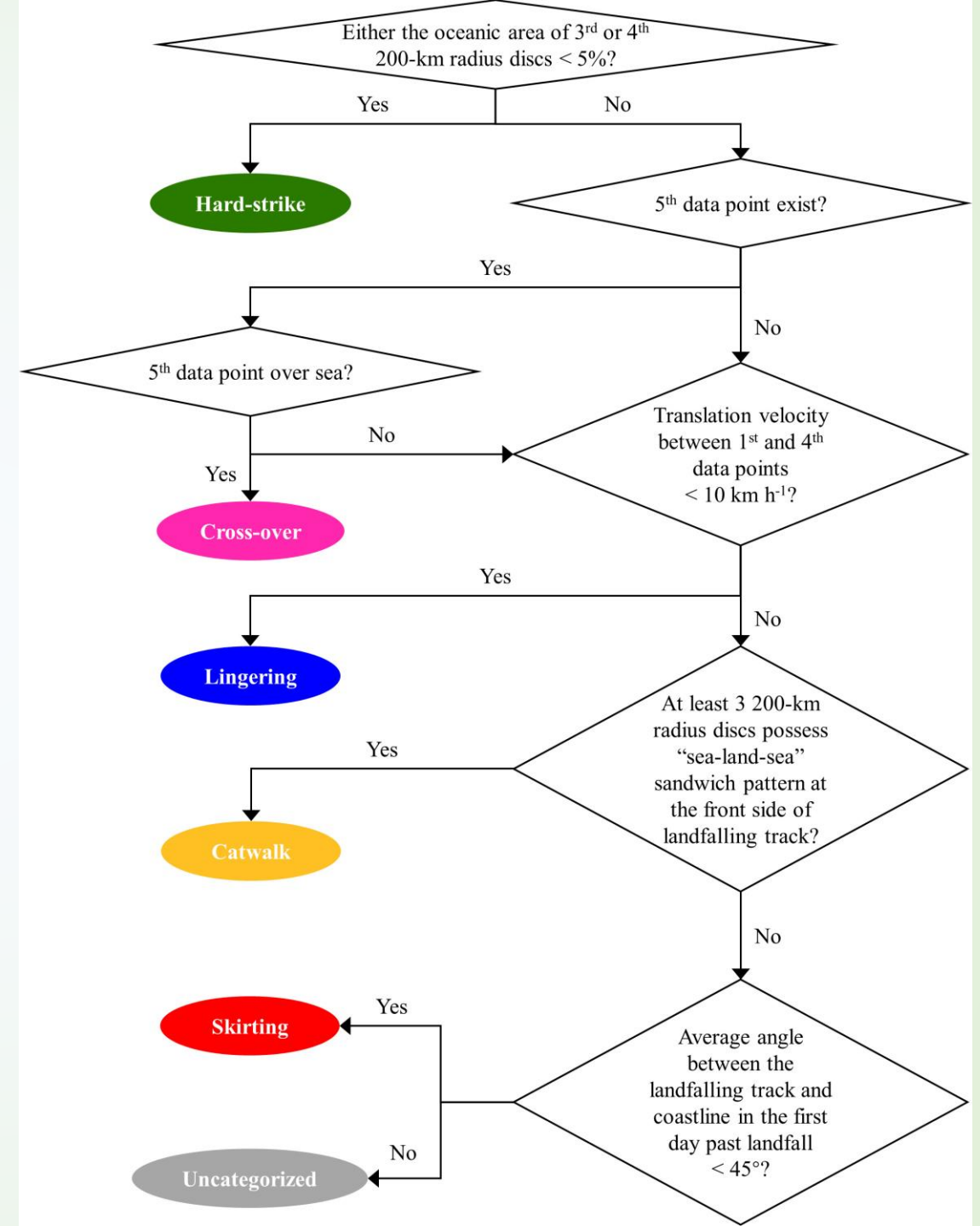
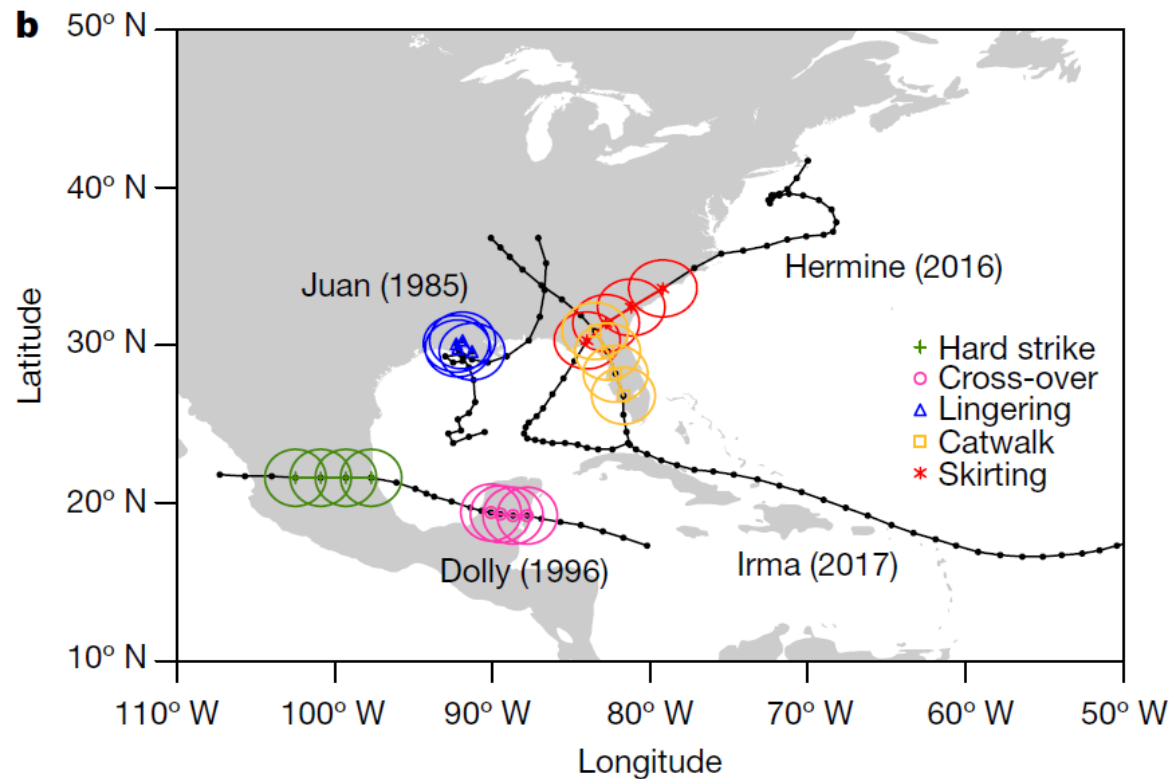
Landfalling Track Modes



Matters Arising

Chan et al. 2022, *Nature*

[based on raw data without smoothing]



Matters Arising

Chan et al. 2022, *Nature*

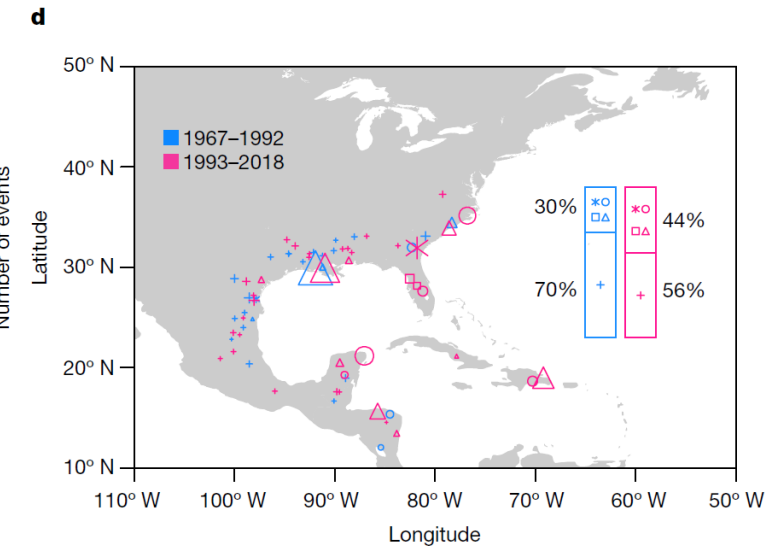
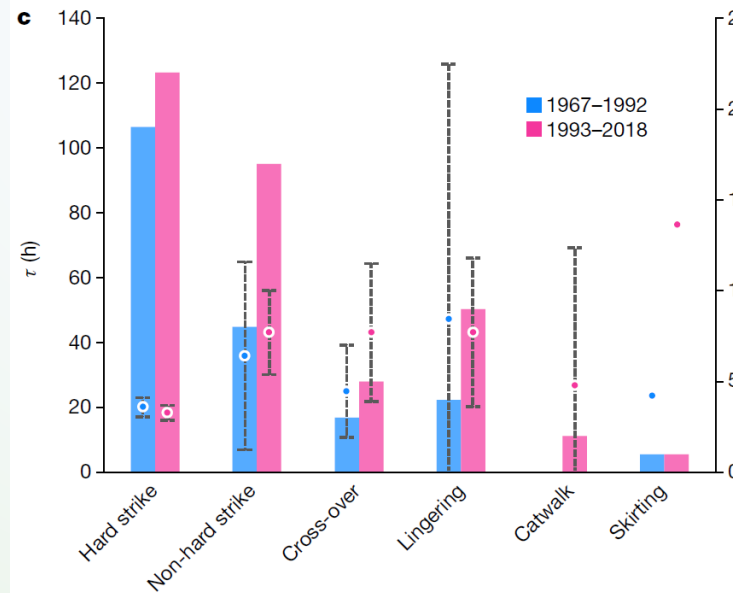
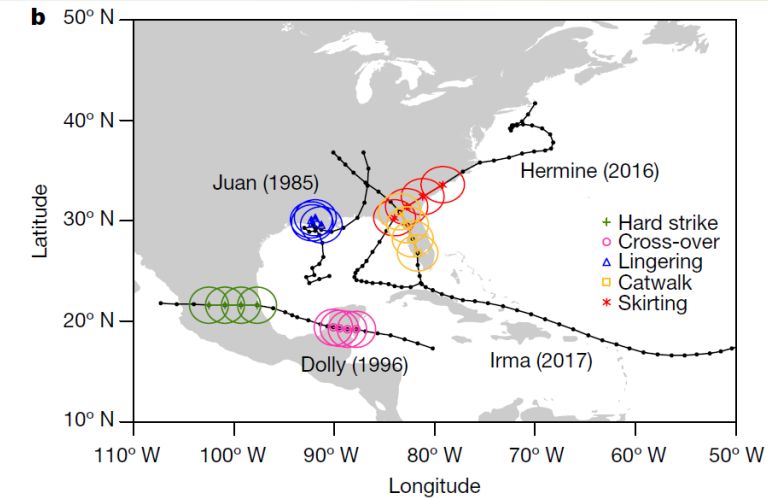
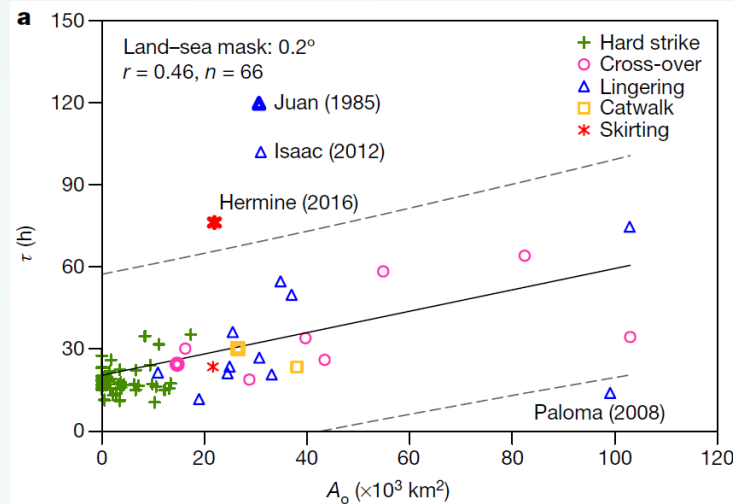
[based on raw data without smoothing]

radius ≤ 200 km

Effective area of moisture supply
from ocean A_O

Landfalling Track Modes

Proportion of non-hard strike TCs
is getting higher.



Questions



Chan et al. 2022, *npj Climate and Atmospheric Science*

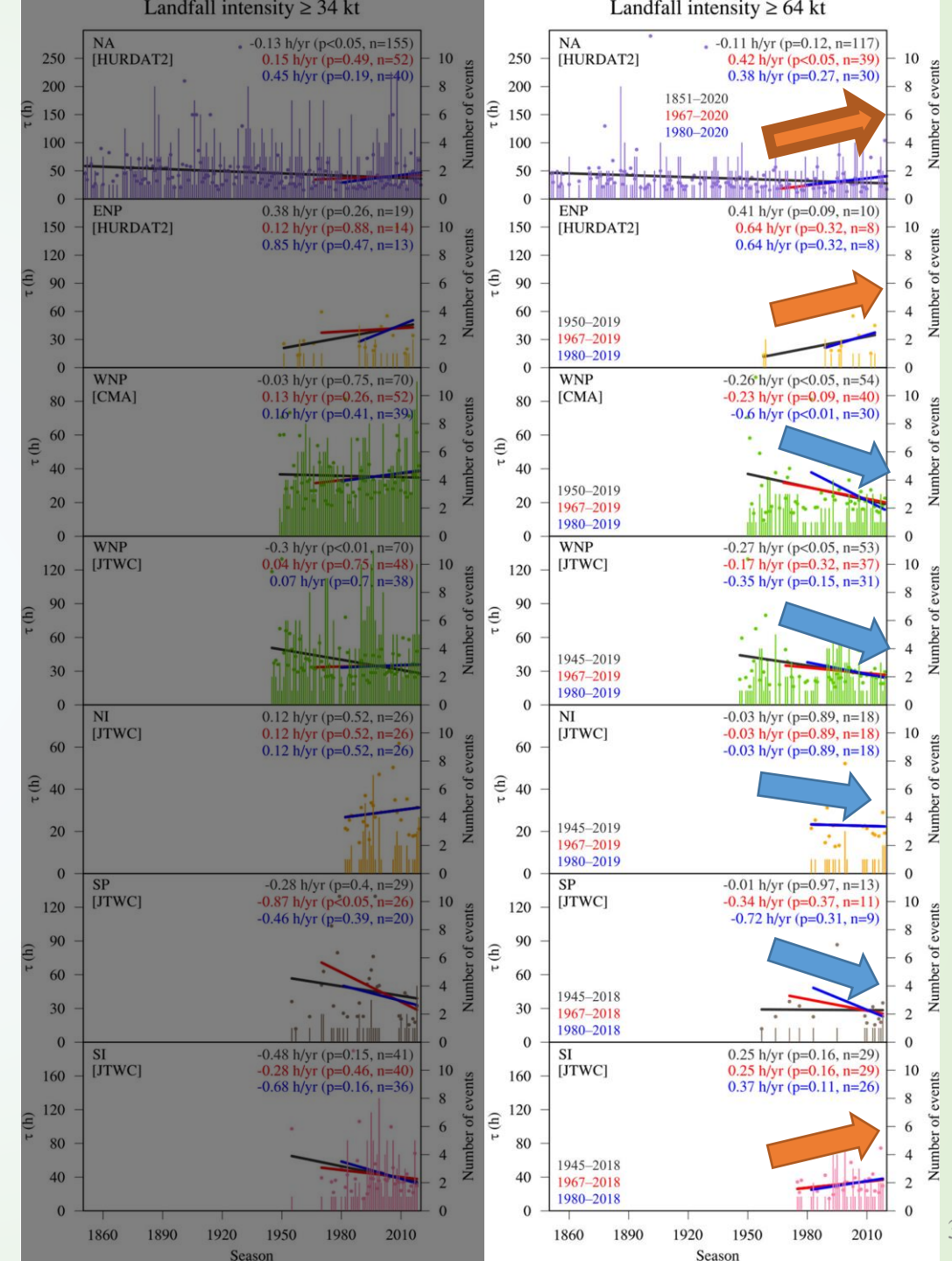


Basin-Dependent

Given the same study period

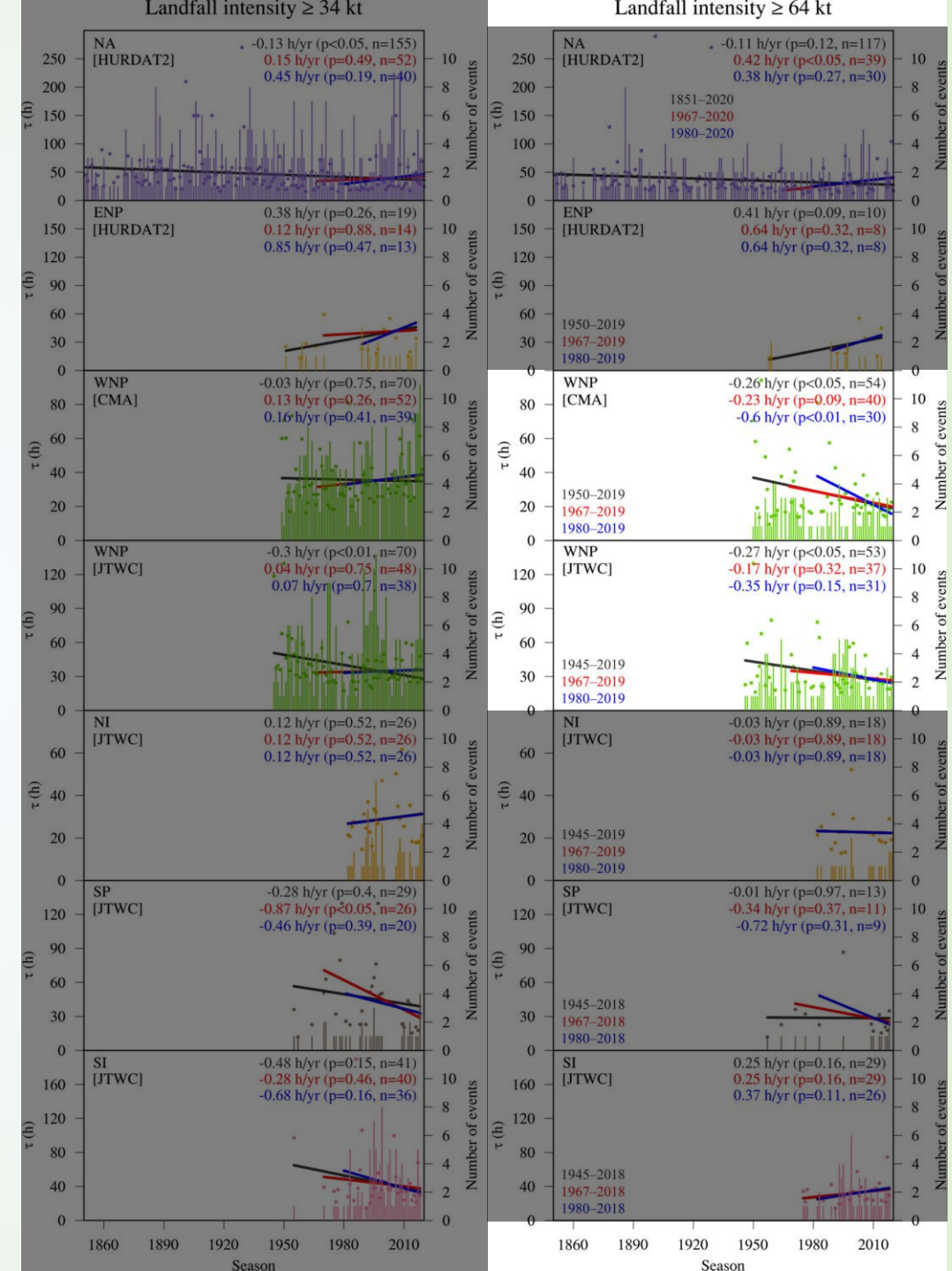
- some trends are increasing while some are decreasing
- some trends are statistically significant whereas some are not

Chan et al. 2022, *npj Climate and Atmospheric Science*



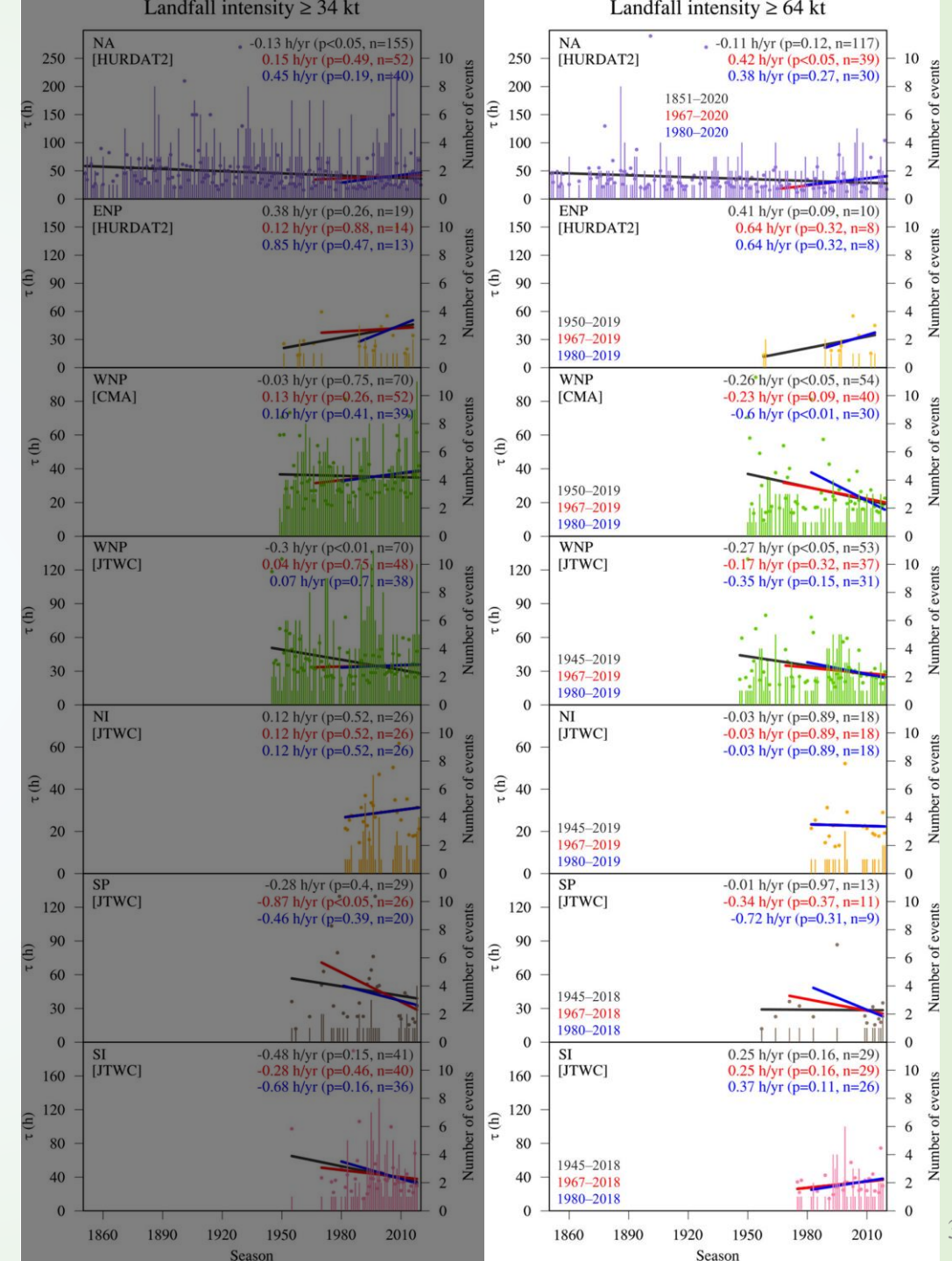
Data-Dependent

- Given the same study period, different sources of best-track data exhibit different trends even in the same basin.
- These inconsistencies are very likely due to the heterogeneities of operational procedures between the agencies, particularly the discrepancies in the estimation of TC intensity.



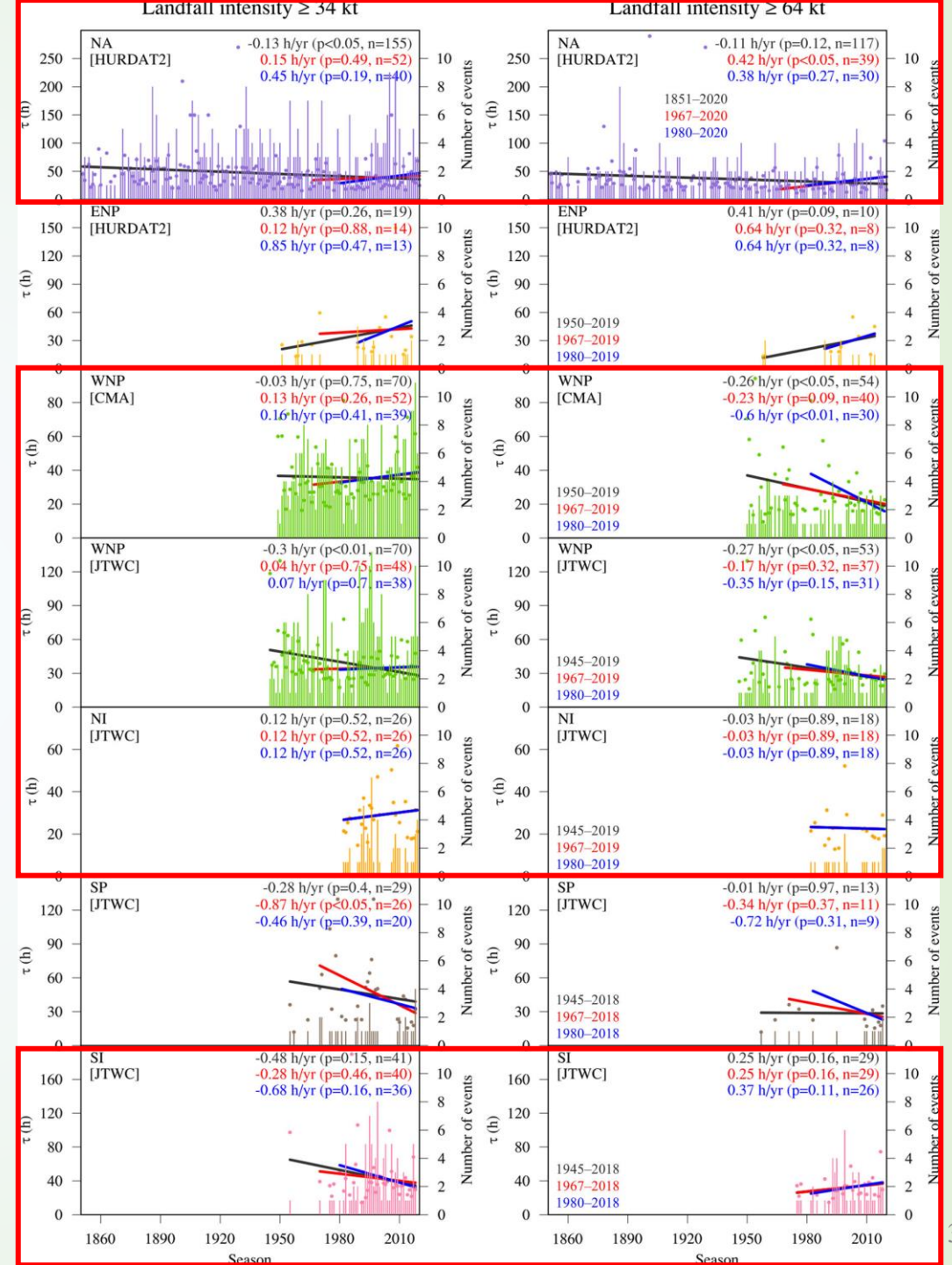
Study Period-Dependent

- Even within the same basin and from the same data source, the trends and their corresponding significances are not consistent with time.

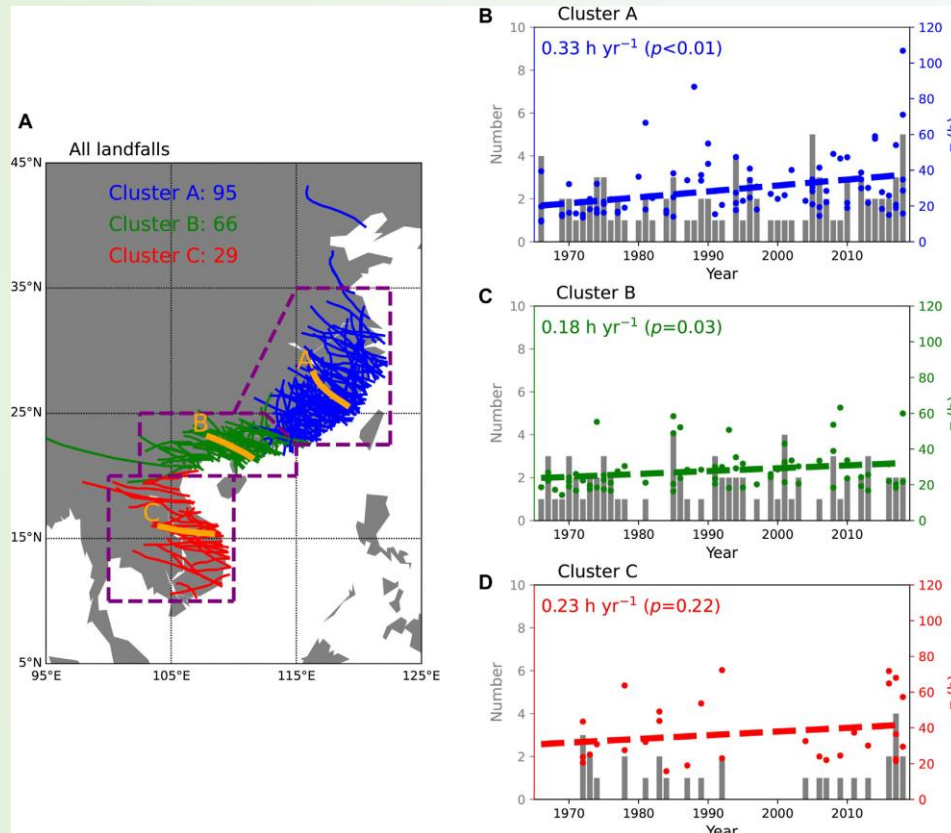


Landfall Intensity-Dependent

- Trends are sensitive to the landfall events conditioned by the thresholds of landfall intensity.



Land-sea Mask-Dependent

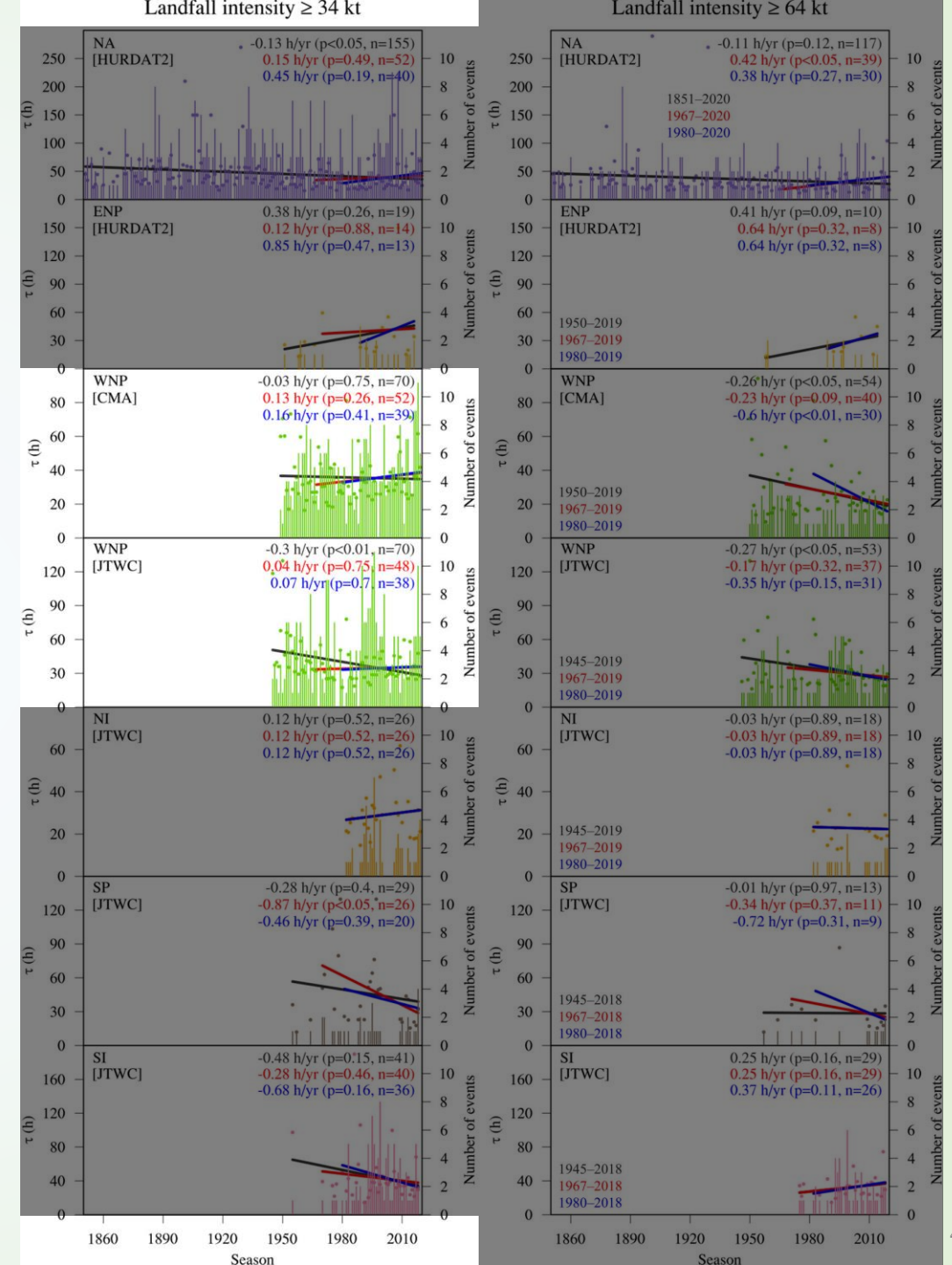


Song et al. 2022, *Frontiers in Earth Science*

JRA-55: $1.25^\circ \times 1.25^\circ$

ETOPO1: $0.1^\circ \times 0.1^\circ$

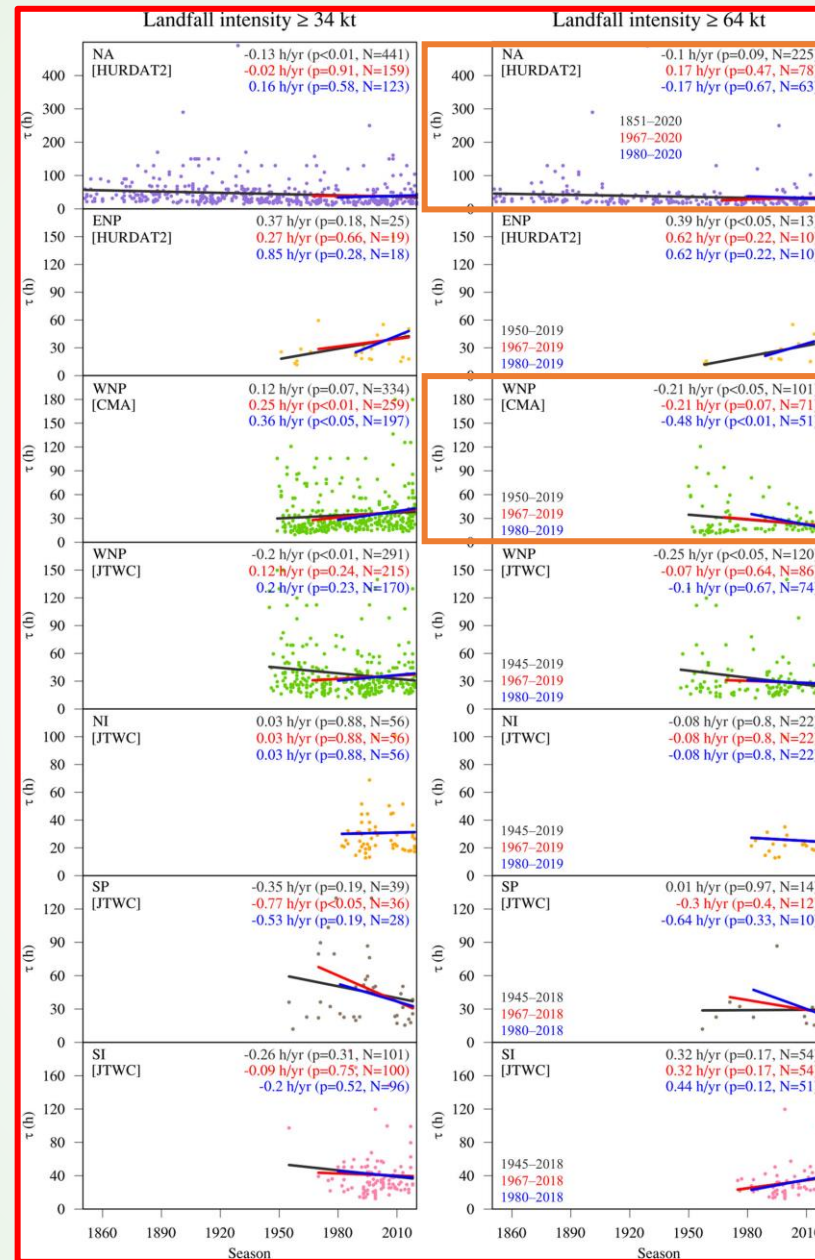
Chan et al. 2022, *npj Climate and Atmospheric Science*



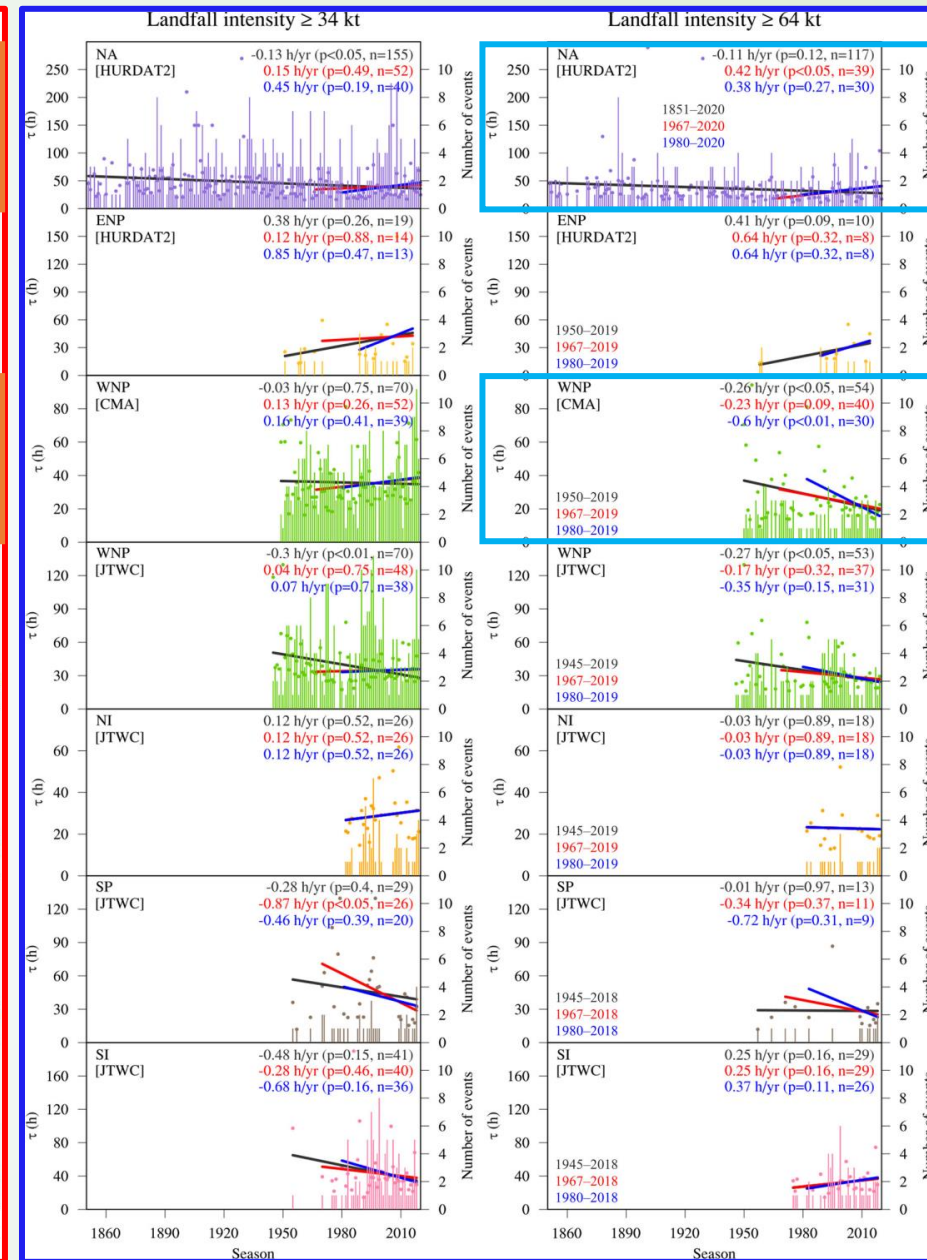
Statistical Technique-Dependent

- Trends deduced from the **season-level τ** and **event-level τ** are different.

Chan et al. 2022, *npj Climate and Atmospheric Science*

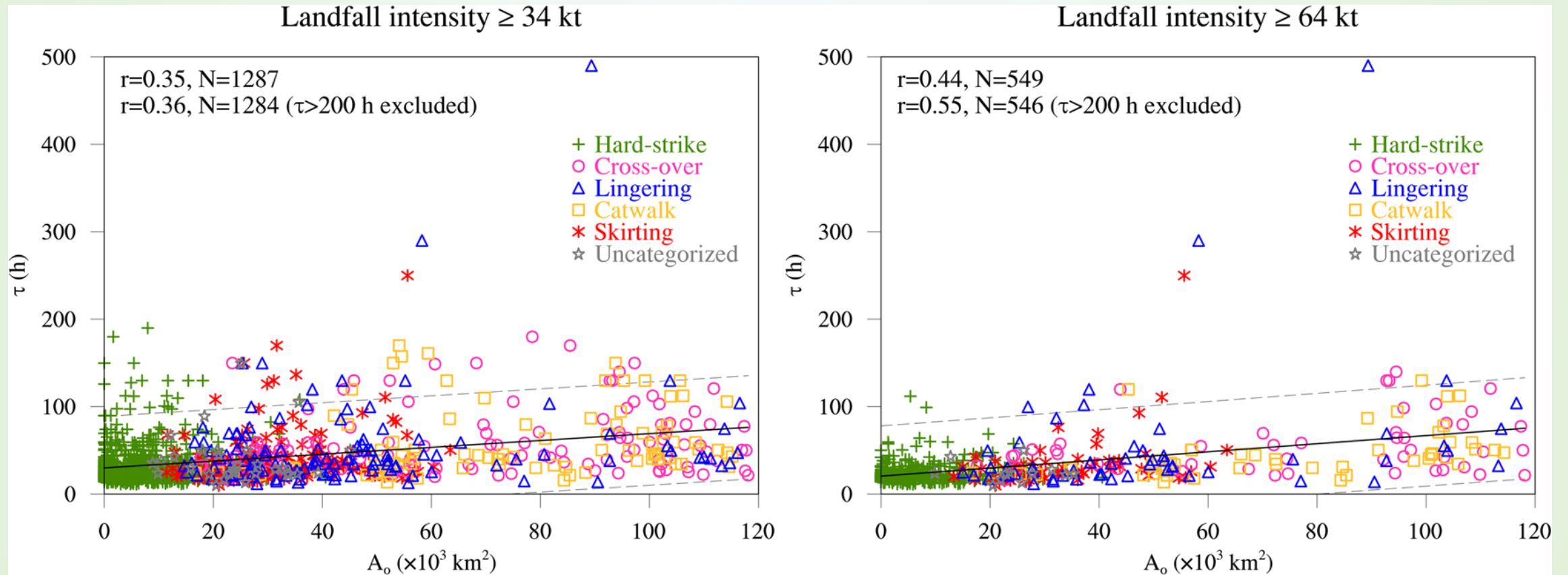


Event-level



Season-level

Landfalling Track Modes

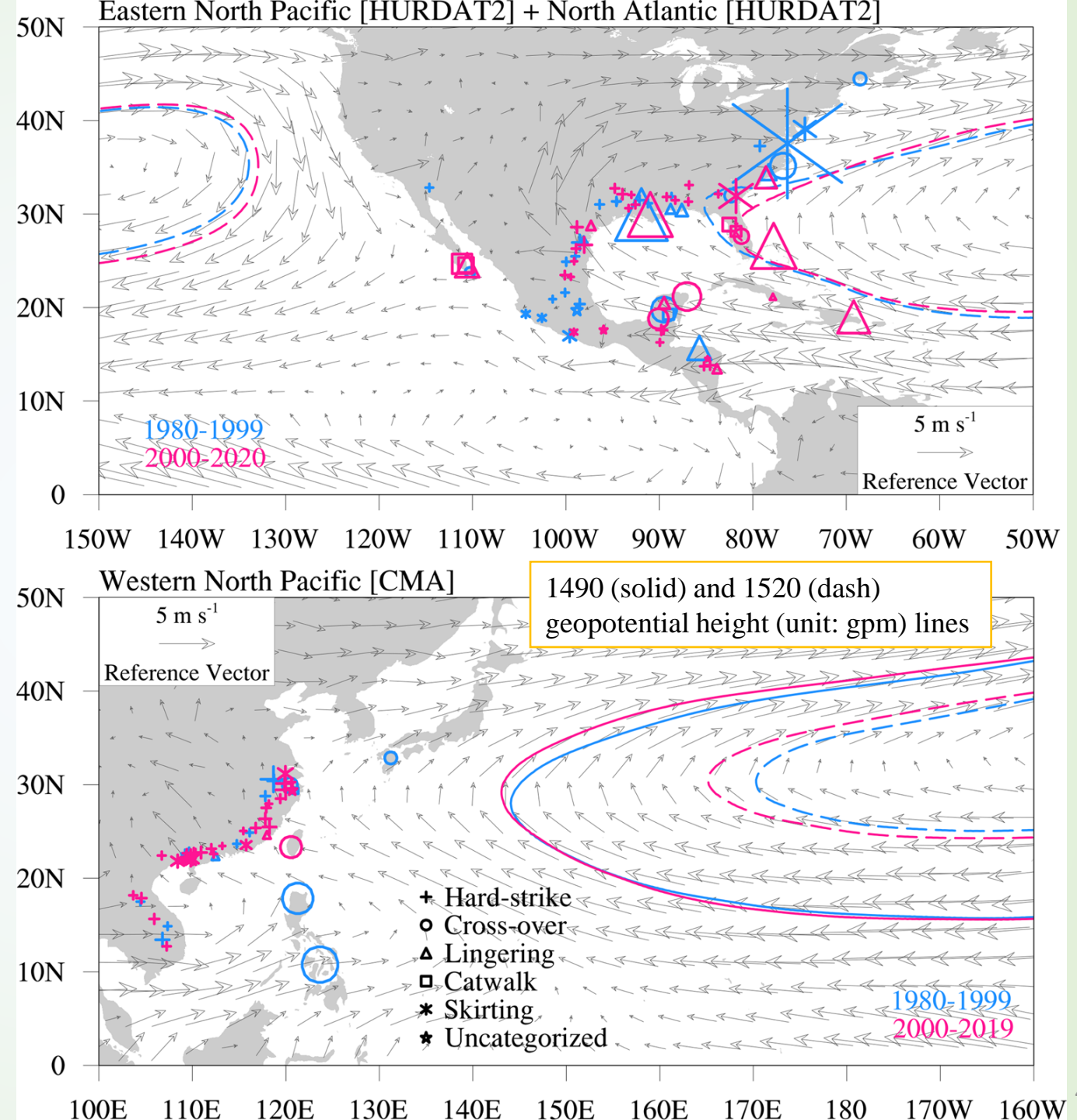


Chan et al. 2022, *npj Climate and Atmospheric Science*

$\tau \propto$ Effective area of moisture supply from ocean A_o

Subtropical High

- Subtropical high varies from time to time.
- Steering flow therefore varies correspondingly, so does the landfalling track modes.



Conclusions

- This global study further consolidates that the trends of TC landfall decay are **uncertain** and **insignificant**.
- Trends are **basin, data, study period, landfall intensity, land-sea mask,** and **statistical technique-dependent**.
- The decay highly depends on the **landfalling track modes** (likely results from the **subtropical high variability**) rather than the SST, with the **effective area of moisture supply from the ocean** playing a vital role.

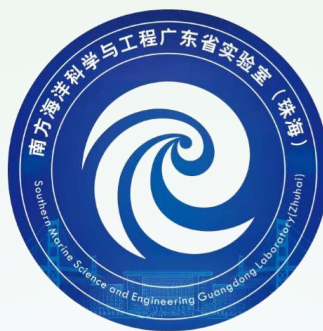
IMPORTANT: Do not take a part for the whole, there is no consensus yet.

References

- Li, L., & Chakraborty, P. (2020) Slower decay of landfalling hurricanes in a warming world. *Nature*, 587, 230–234.
- Li, L., & Chakraborty, P. (2021) Author Correction: Slower decay of landfalling hurricanes in a warming world. *Nature*, 593, E4–E11.
- Song, J., Klotzbach, P. J., Zhao, H. & Duan, Y. (2021) Slowdown in the decay of western North Pacific tropical cyclones making landfall on the Asian continent. *Frontiers in Earth Science*, 9, 749287.
- Chan, K. T. F., Zhang, K., Wu, Y., & Chan, J. C. L. (2022) Landfalling hurricane track modes and decay. *Nature*, 606, E7–E11.
- Chan, K. T. F., Chan, J. C. L., Zhang, K., & Wu, Y. (2022) Uncertainties in tropical cyclone landfall decay. *npj Climate and Atmospheric Science*, 5, 93.

Promotion of Tropical Cyclone Size Asymmetry Index

- Size Asymmetry
- Index



An ERA5 Global Climatology of Tropical Cyclone Size Asymmetry

Kailin ZHANG¹, and Kelvin T. F. CHAN^{1,2,3}

¹School of Atmospheric Sciences, Sun Yat-sen University, and Southern Marine Science and Engineering Guangdong Laboratory (Zhuhai), Zhuhai, China

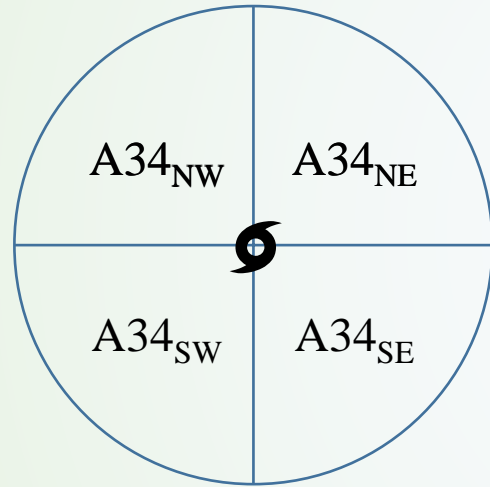
²Guangdong Province Key Laboratory for Climate Change and Natural Disaster Studies, Sun Yat-sen University, Zhuhai, China

³Key Laboratory of Tropical Atmosphere-Ocean System (Sun Yat-sen University), Ministry of Education, Zhuhai, China

TC Size Asymmetry

Size: Radius of 10-m gale force 34-kt wind (R34)

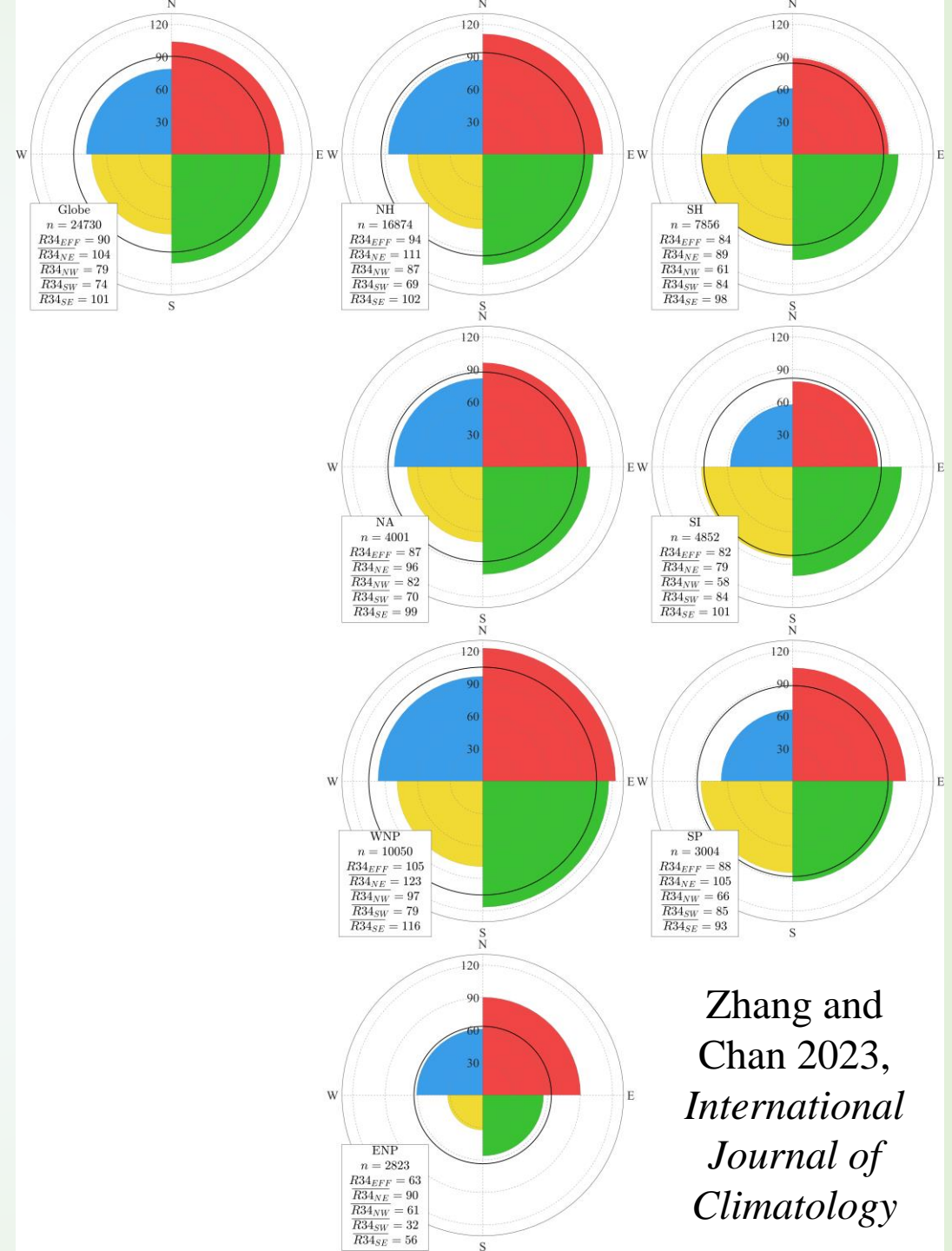
R34_{EFF}: Effective azimuthal-area-average radius of R34



$$A34_{EFF} = A34_{NE} + A34_{NW} + A34_{SW} + A34_{SE}$$

$$\pi R34_{EFF}^2 = \frac{\pi R34_{NE}^2}{4} + \frac{\pi R34_{NW}^2}{4} + \frac{\pi R34_{SW}^2}{4} + \frac{\pi R34_{SE}^2}{4}$$

$$R34_{EFF} = \frac{\sqrt{R34_{NE}^2 + R34_{NW}^2 + R34_{SW}^2 + R34_{SE}^2}}{2}$$



Zhang and
Chan 2023,
*International
Journal of
Climatology*

TC Size Asymmetry

Climatologically (1979–2019),

- Globe $R34_{EFF} = 90$ NM
- NH $R34_{EFF} = 94$ NM
- SH $R34_{EFF} = 84$ NM
- WNP $R34_{EFF} = 105$ NM (largest)
- ENP $R34_{EFF} = 63$ NM (smallest)

Globally,

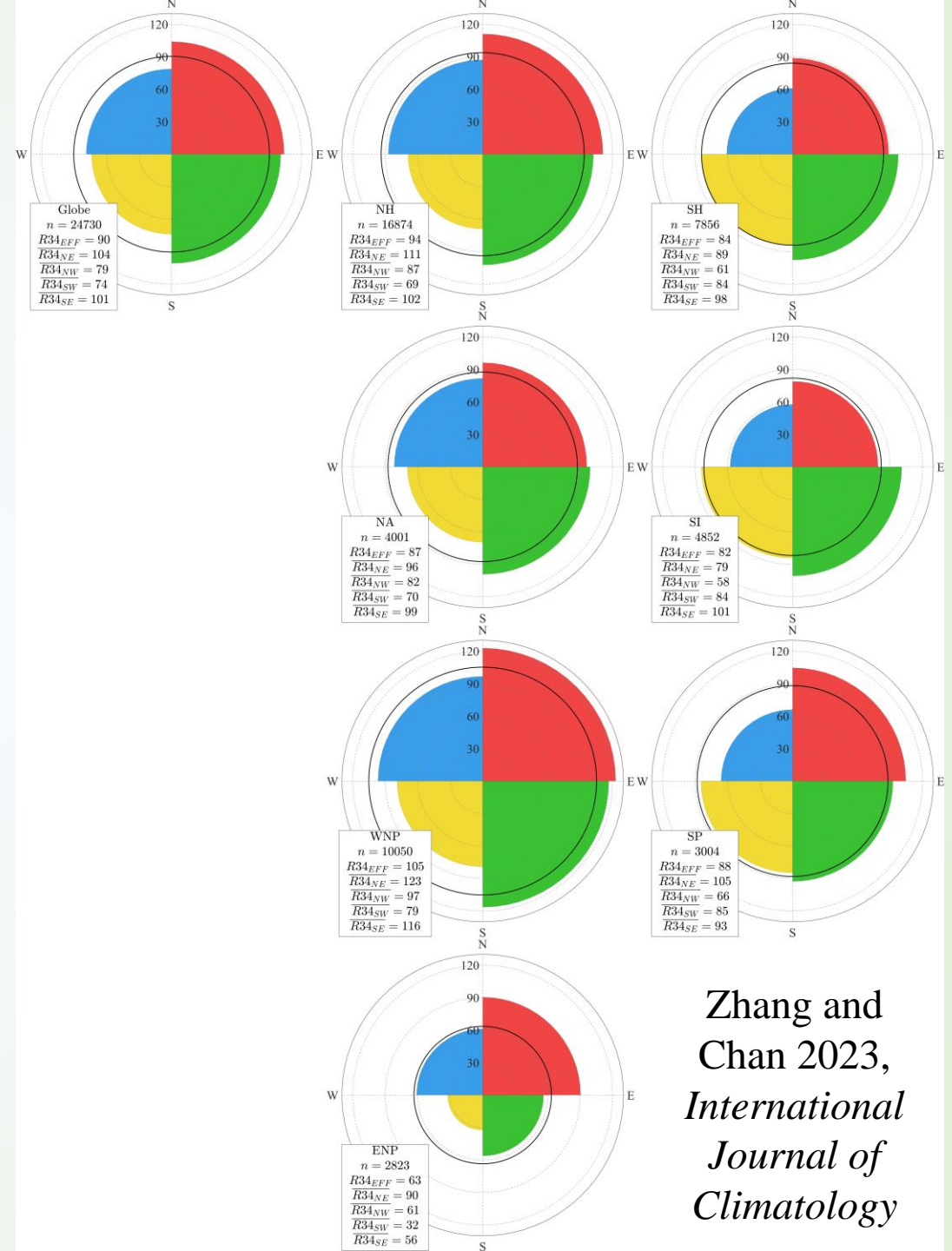
- West-small, east-large

In NH,

- $R34_{SW}$ is smallest

In SH,

- $R34_{NW}$ is smallest



Zhang and
Chan 2023,
*International
Journal of
Climatology*

Interannual Variations

Interannual variation

- Obvious

Trend

- No significant long-term trend is found in a warming world except the $R34_{NE}$, $R34_{SW}$, and $R34_{EFF}$ in SI (5.2 NM, 3.9 NM, and 3.6 NM per decade, respectively)

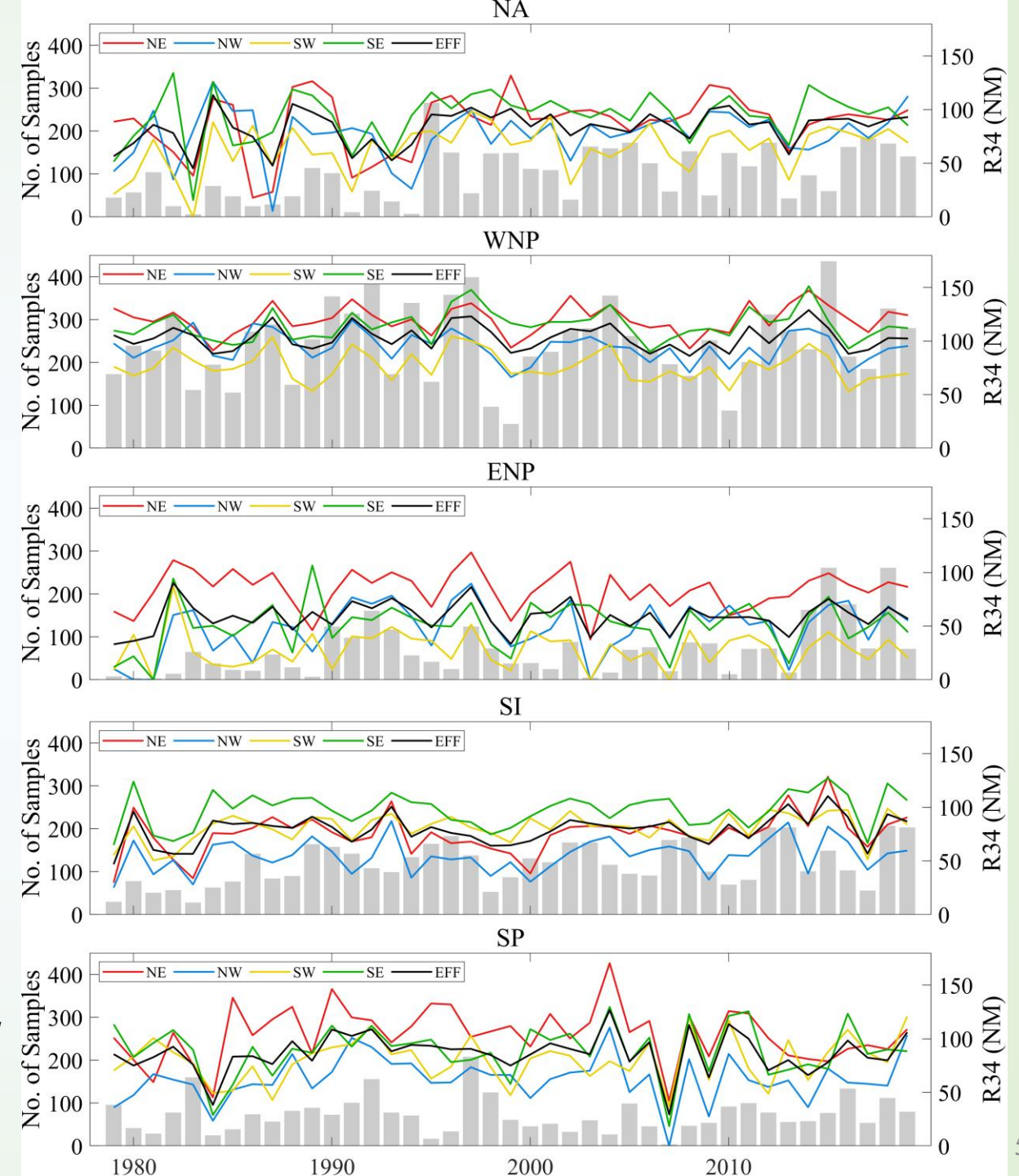
In NH,

- $R34_{SW}$ is smallest

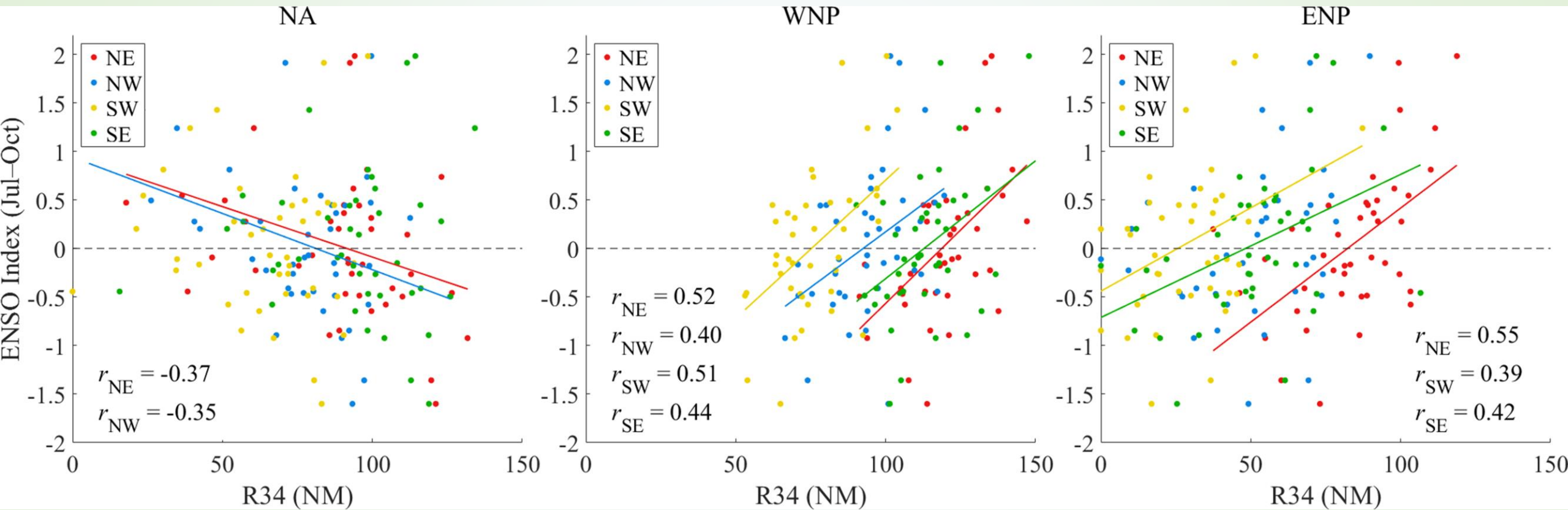
In SH,

- $R34_{NW}$ is smallest

Zhang and
Chan 2023,
*International
Journal of
Climatology*



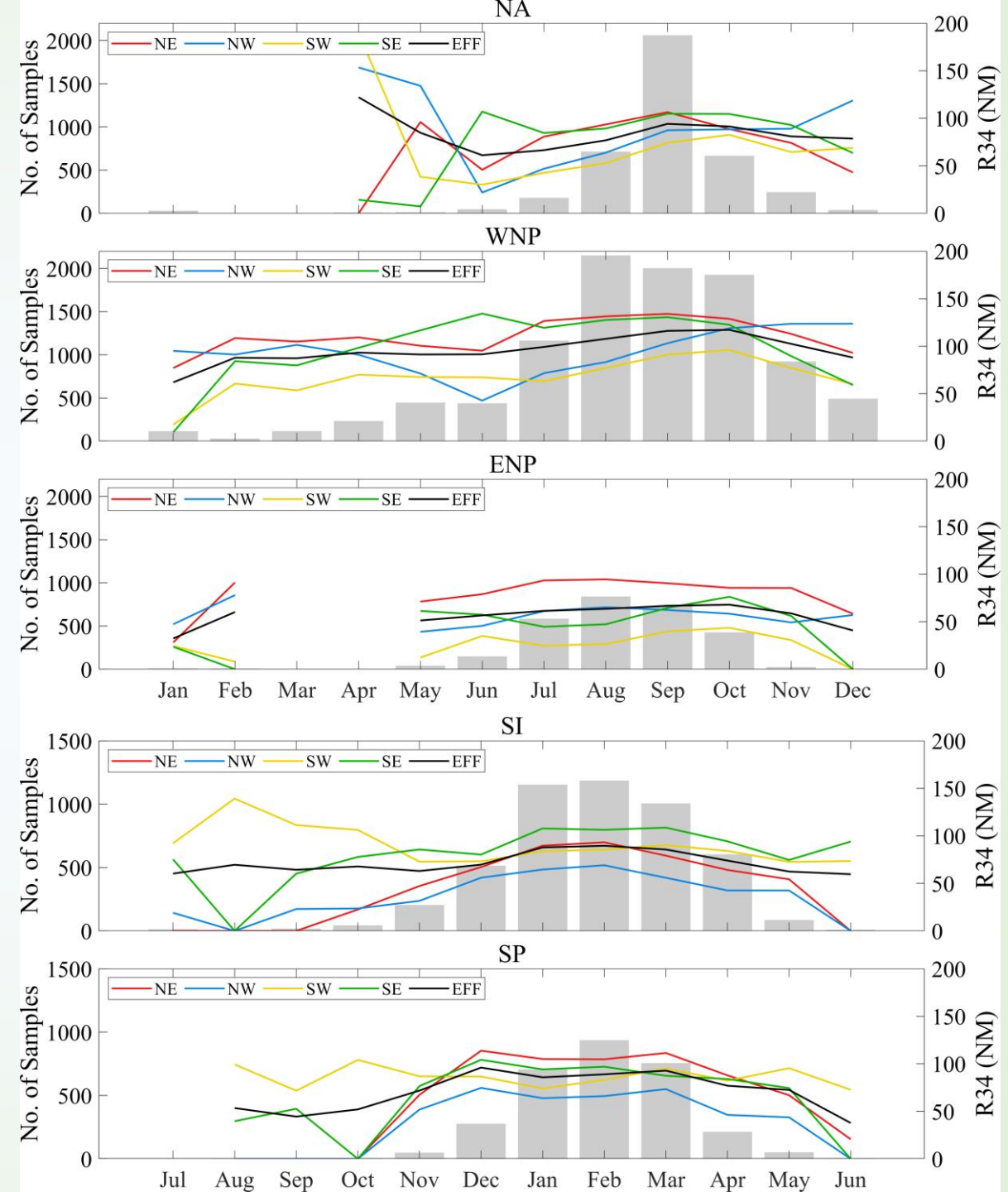
Interannual Variations



Zhang and Chan 2023, *International Journal of Climatology*

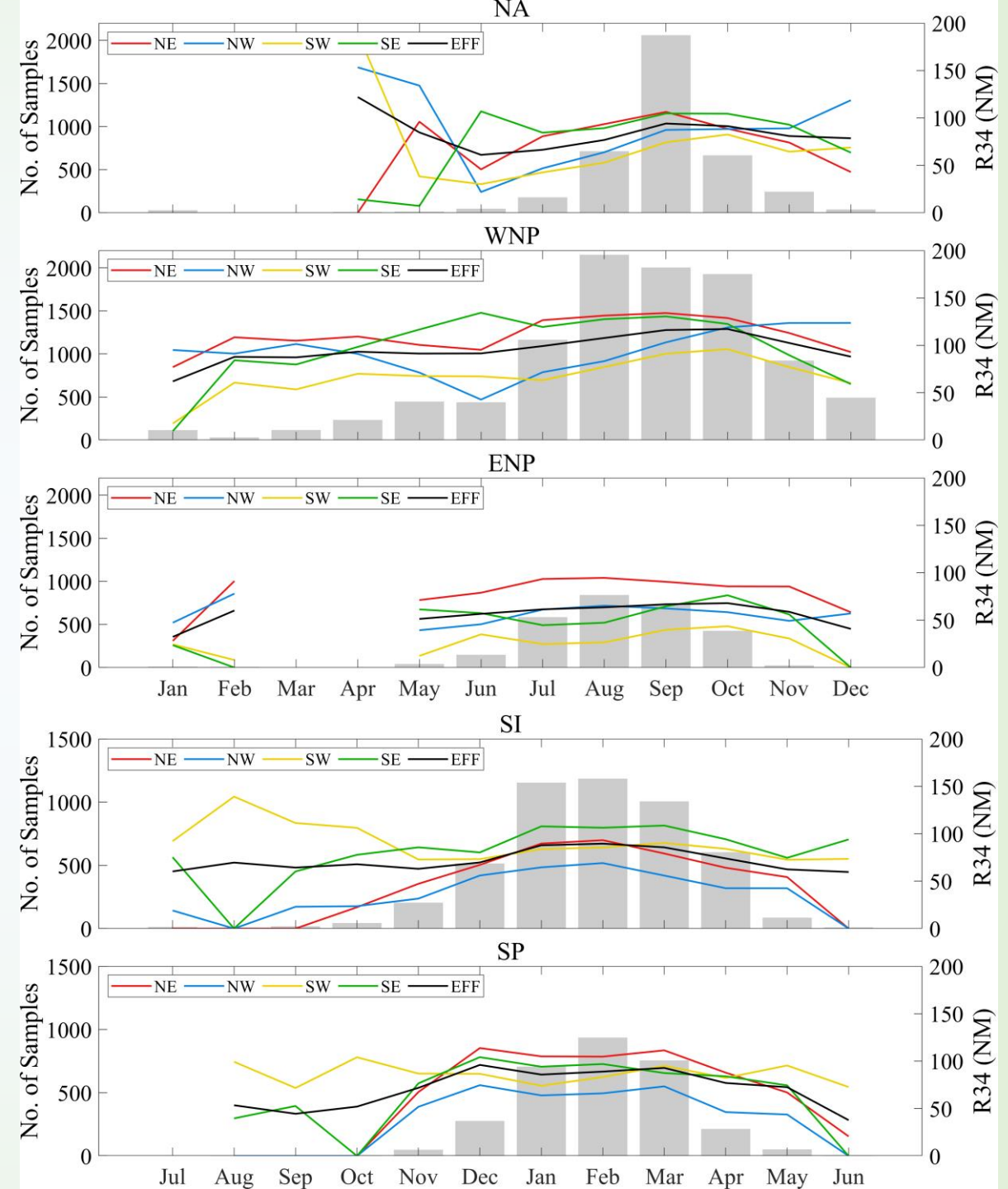
Monthly Variations

- In boreal early-to-mid summer (June, July, August, and September), the size of TC generally shows a west-small east-large asymmetric structure in NA and WNP.
- The $R34_{NE}$ becomes smaller and the $R34_{NW}$ becomes larger in late season (since September). Such asymmetry transits to south-small north-large in the WNP.
- It is noted that the $R34$ in all quadrants gradually increase from July to September in NA and WNP. This suggests that the size of TC is increasing during the main TC season.



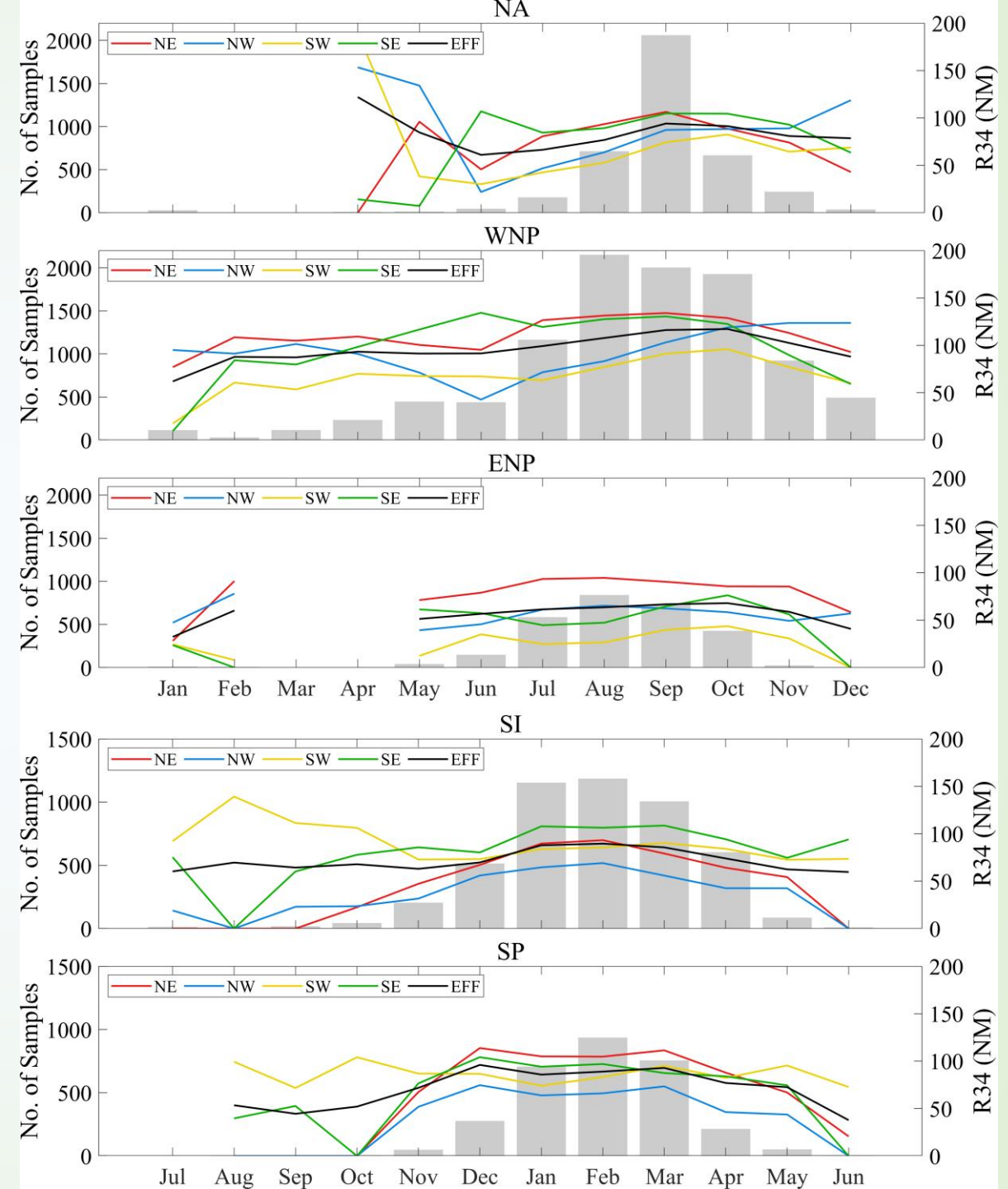
Monthly Variations

- The late-season TCs are typically larger than those in the early season.
- The increase in $R34_{NW}$ from June to December in the WNP is prominent. This suggests that there could be an existence of seasonal system (e.g., the build-up of the continental high) to the NW of TCs that contributes the expansion of $R34_{NW}$.
- In the ENP, the $R34_{SW}$ is the smallest, while the $R34_{NE}$ is the largest in general. The size in the southern flank shows a bimodal seasonal variation such that $R34_{SW}$ and $R34_{SE}$ are large in the early and late seasons, but small in peak summer.



Monthly Variations

- In SH, $R34_{NW}$ is the smallest throughout the entire TC season.
- In SI, the size increases gradually from early to peak season (November to proceeding March) and then decreases afterward. It is particularly apparent in the NE quadrant. The size in the SE quadrant is generally largest.
- In SP, the seasonal size variation is comparatively small among the basins. The size decreases slightly during the TC season (December to proceeding April). The $R34_{NE}$ is generally the largest.

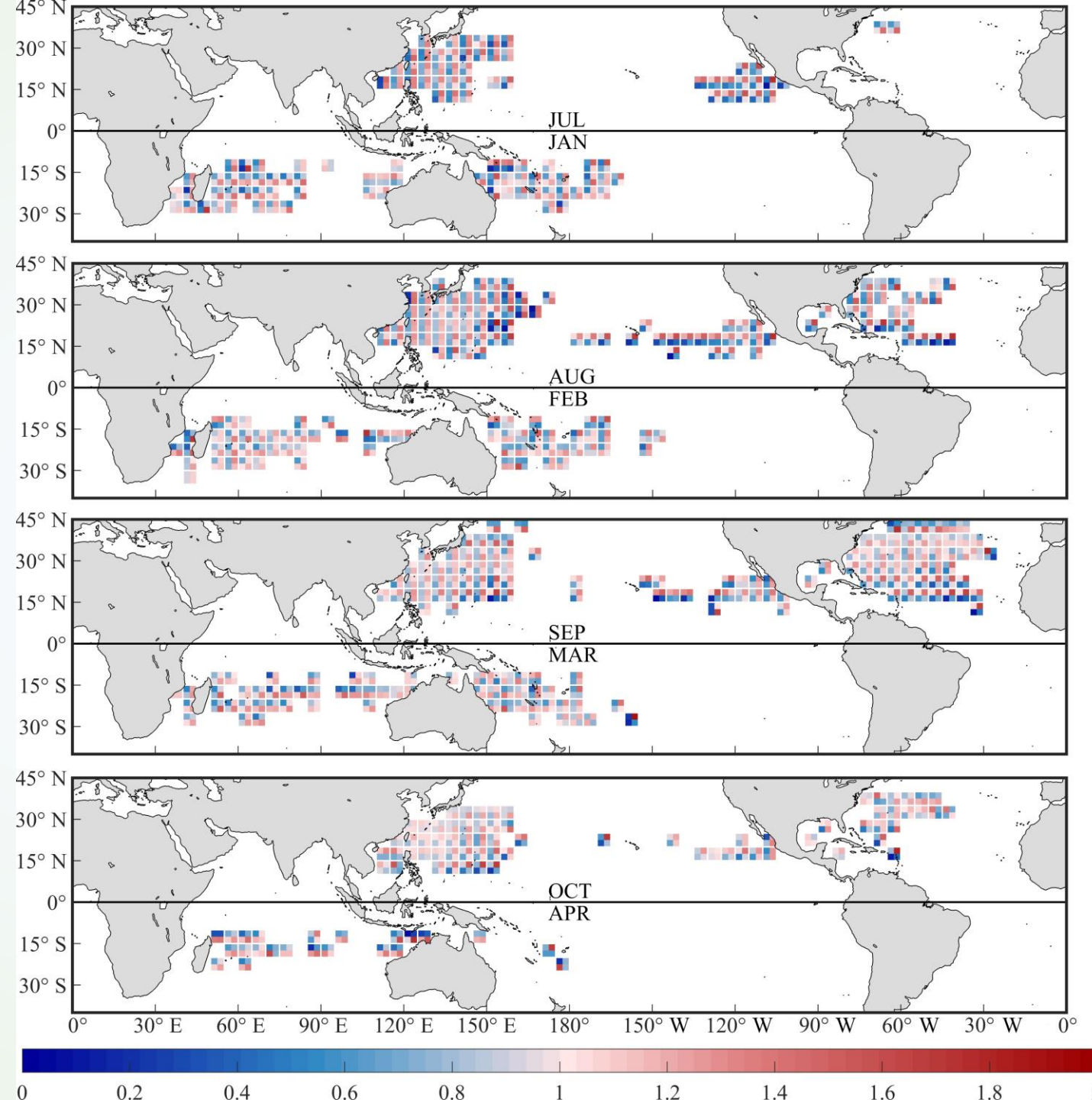


Spatiotemporal Distributions

In WNP,

- In July and August, the size asymmetry patterns are generally west-small east-large.
- In September, the $R34_{NW}$ is getting larger, especially in the west of 150° E.
- When it comes to the late season (October), the size asymmetry becomes more variable within the basin.

Zhang and Chan 2023, *International Journal of Climatology*

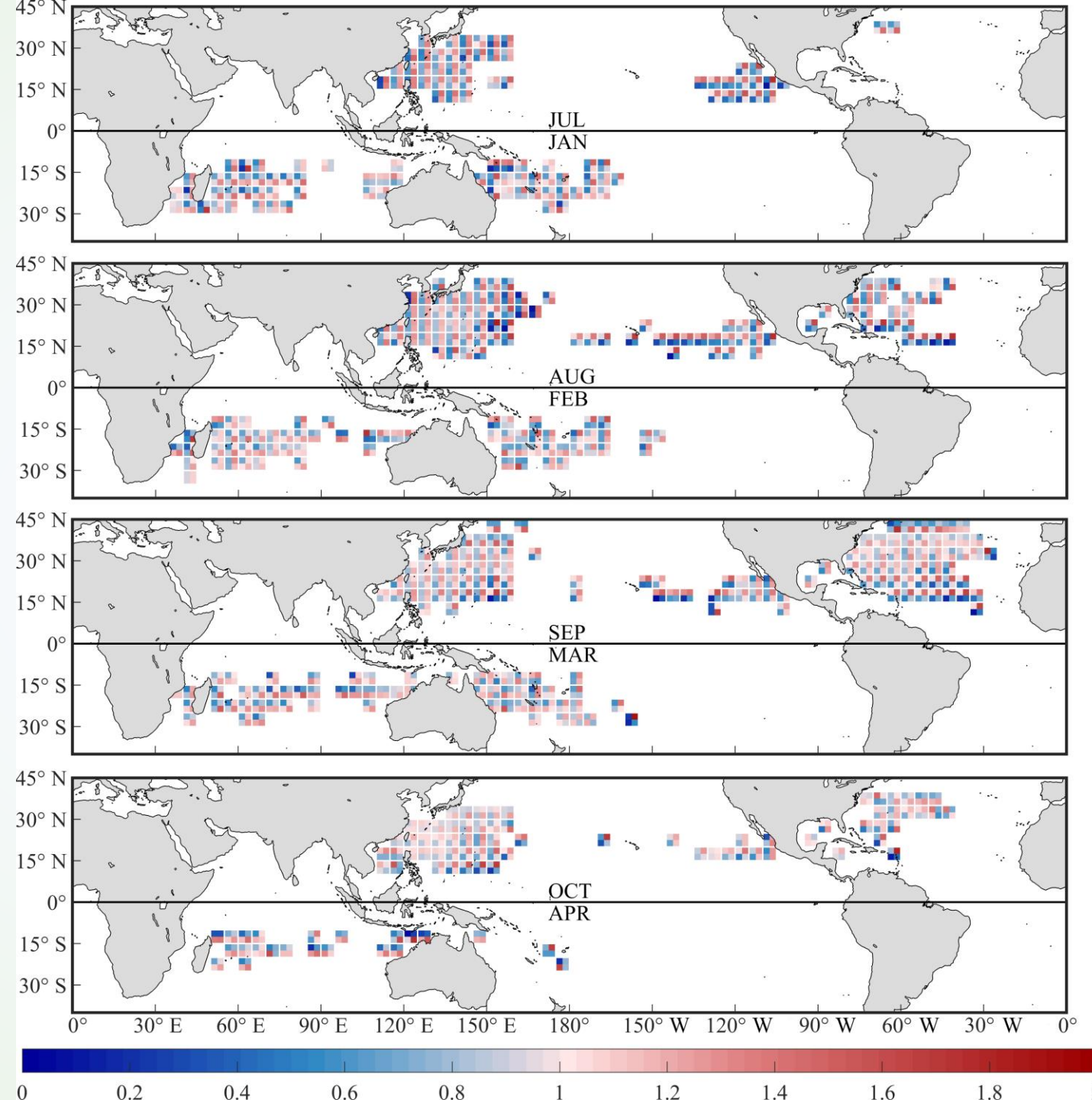


Spatiotemporal Distributions

In NA,

- In September, the size asymmetry pattern in the southern part of NA is generally south-small north-large.
- Meanwhile, it is inverse in the northern part of NA such that the size asymmetry pattern is north-small south-large in general.
- The transition appears at around 30° N, where is the latitude about the TC recurvature, such that the size asymmetry pattern is likely west-small east-large.

Zhang and Chan 2023, *International Journal of Climatology*



Conclusions

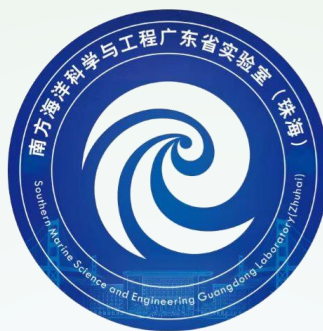
- A 41-year (1979–2019) ERA5 global climatology of TC size asymmetry is established.
- TC size asymmetry varies with space (hemispheric, basin, and intrabasin) and time (interannual, interseasonal, and intraseasonal).
- No apparent long-term trend is found, except in SI. This suggests that the relationship between the long-term variability of TC size and global warming needs further investigation.
- The ENSO could have influence on the interannual variations in the Northern Hemisphere.
- The season-variant systems (e.g., the continental high, subtropical high, monsoon, etc.) could contribute to the seasonal variations of TC size asymmetry.

Reference

- Zhang K., & Chan K. T. F. (2023) An ERA5 global climatology of tropical cyclone size asymmetry. *International Journal of Climatology*, 43, 950–963.

Promotion of Tropical Cyclone Size Asymmetry Index

- Size Asymmetry
- Index



Tropical Cyclone Size Asymmetry Index and Climatology

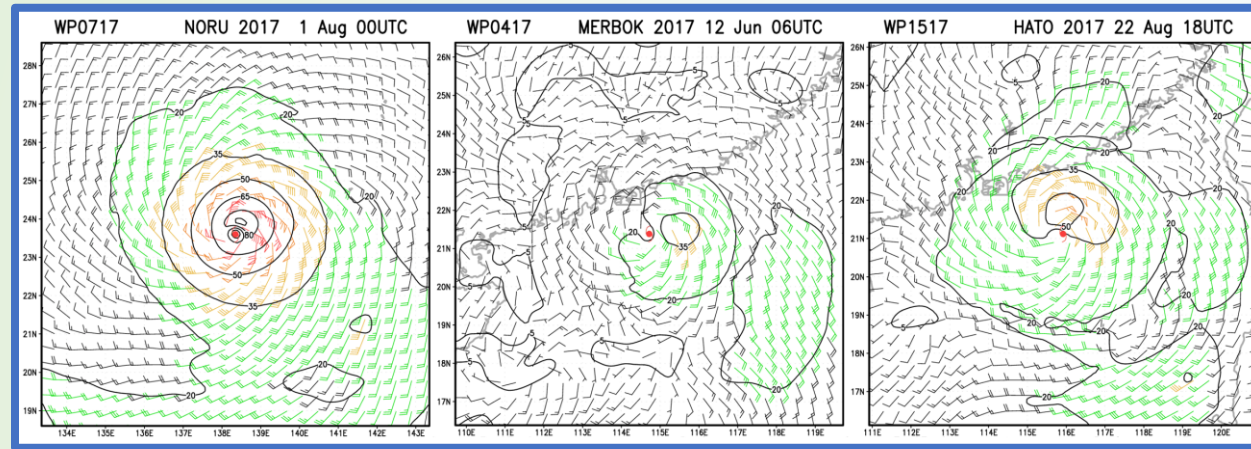
Kelvin T. F. CHAN^{1,2,3}, Kailin ZHANG¹, and Lifeng XU¹

¹School of Atmospheric Sciences, Sun Yat-sen University, and Southern Marine Science and Engineering Guangdong Laboratory (Zhuhai), Zhuhai, China

²Guangdong Province Key Laboratory for Climate Change and Natural Disaster Studies, Sun Yat-sen University, Zhuhai, China

³Key Laboratory of Tropical Atmosphere-Ocean System (Sun Yat-sen University), Ministry of Education, Zhuhai, China

Review of Size Asymmetry Index in Past



Weaknesses:

- Many undefined values (missing data: $R34_{MIN}$)
- Unphysical α range $[1, \infty)$

Weaknesses:

- We often have hard time to estimate V_{MAX} and $\overline{V_{Rmax}}$ (uncertainties in V_{MAX} and $\overline{V_{Rmax}}$)
- Unphysical α range $[0, \infty)$
- Not truly corresponds to size

Hong et al. 2020, *Atmospheric Science Letters*

$$\alpha = \frac{R34_{MAX}}{R34_{MIN}} \text{ or } \alpha = \frac{R34_{MIN}}{R34_{MAX}}$$

Olfateh et al. 2017, *Journal of Geophysical Research: Oceans*
Sun et al. 2019, *Remote Sensing*

$$\alpha = \frac{V_{MAX}}{\overline{V_{Rmax}}} - 1$$

Not generic and incomplete (merely measure the degree of asymmetry; pattern of asymmetry is missed)

Size Asymmetry Index (SAI)

Chan et al. 2023, *Climate Dynamics*

Generic: applicable to most situations

α and $R34_{\text{EFF}}$ always exists once any $R34_{\text{NE}}$, $R34_{\text{NW}}$, $R34_{\text{SW}}$, and $R34_{\text{SE}}$ is well-defined/estimated.

$$SAI = \underbrace{[\alpha]}_{\text{Degree}} \underbrace{[TOQ]}_{\text{Pattern}}$$

α ranges $[0, 1]$

$\alpha = 0$: absolutely symmetric

$\alpha \leq \alpha_c$: quasi-symmetric

$\alpha_c < \alpha < 1$: asymmetric

$\alpha = 1$: absolutely asymmetric

$\alpha \in [0, 1]$

$\alpha_c = 0.13$

$$\alpha = \frac{R34_{\text{MAX}}}{R34_{\text{EFF}}} - 1$$

$$R34_{\text{MAX}} = \max(R34_{\text{NE}}, R34_{\text{NW}}, R34_{\text{SW}}, R34_{\text{SE}})$$

$$R34_{\text{EFF}} = \sqrt{\frac{R34_{\text{NE}}^2 + R34_{\text{NW}}^2 + R34_{\text{SW}}^2 + R34_{\text{SE}}^2}{4}}$$

$$\alpha_c = \frac{\max\left(\frac{R34_{\text{NE,NH}} + R34_{\text{NE,SH}}}{2}, \frac{R34_{\text{NW,NH}} + R34_{\text{NW,SH}}}{2}, \frac{R34_{\text{SW,NH}} + R34_{\text{SW,SH}}}{2}, \frac{R34_{\text{SE,NH}} + R34_{\text{SE,SH}}}{2}\right)}{\sqrt{\frac{\left(\frac{R34_{\text{NE,NH}} + R34_{\text{NE,SH}}}{2}\right)^2 + \left(\frac{R34_{\text{NW,NH}} + R34_{\text{NW,SH}}}{2}\right)^2 + \left(\frac{R34_{\text{SW,NH}} + R34_{\text{SW,SH}}}{2}\right)^2 + \left(\frac{R34_{\text{SE,NH}} + R34_{\text{SE,SH}}}{2}\right)^2}{4}}} - 1$$

Size Asymmetry Index (SAI)

Chan et al. 2023, *Climate Dynamics*

Degree and Pattern are synthetically considered.

$$SAI = \underbrace{[\alpha]}_{\text{Degree}} \underbrace{[TOQ]}_{\text{Pattern}}$$

Quadrant in black: $R34 > R34_{\text{EFF}}$

Degree α	$\leq \alpha_C$	$> \alpha_C$													
Type T															
Orientation O															
Quadrant of the maximum size of interest Q															


















































Constitutions of SAI

$$SAI = \underbrace{[\alpha]}_{\text{Degree}} \underbrace{[TOQ]}_{\text{Pattern}}$$

α	T	O	Q	SAI Code form	SAI Symbolic form
0.11	O	O	O	0.11OOO	0.11⊙
0.56	H	d	4	0.56Hd4	0.56⊕
0.18	X	b	4	0.18Xb4	0.18⊗
0.37	C	d	2	0.37Cd2	0.37⊖
1.00	L	a	1	1.00La1	1.00⊙

Generic, complete, and intuitive

Chan et al. 2023, *Climate Dynamics*

Degree	Pattern						
α	Type T	Orientation O	Quadrant of the maximum size of interest Q				
			1	2	3	4	
$\leq \alpha_c$							
$> \alpha_c$							
							
							
							
							
							
							
							
							
							
							
							
							
							

Overall Statistics

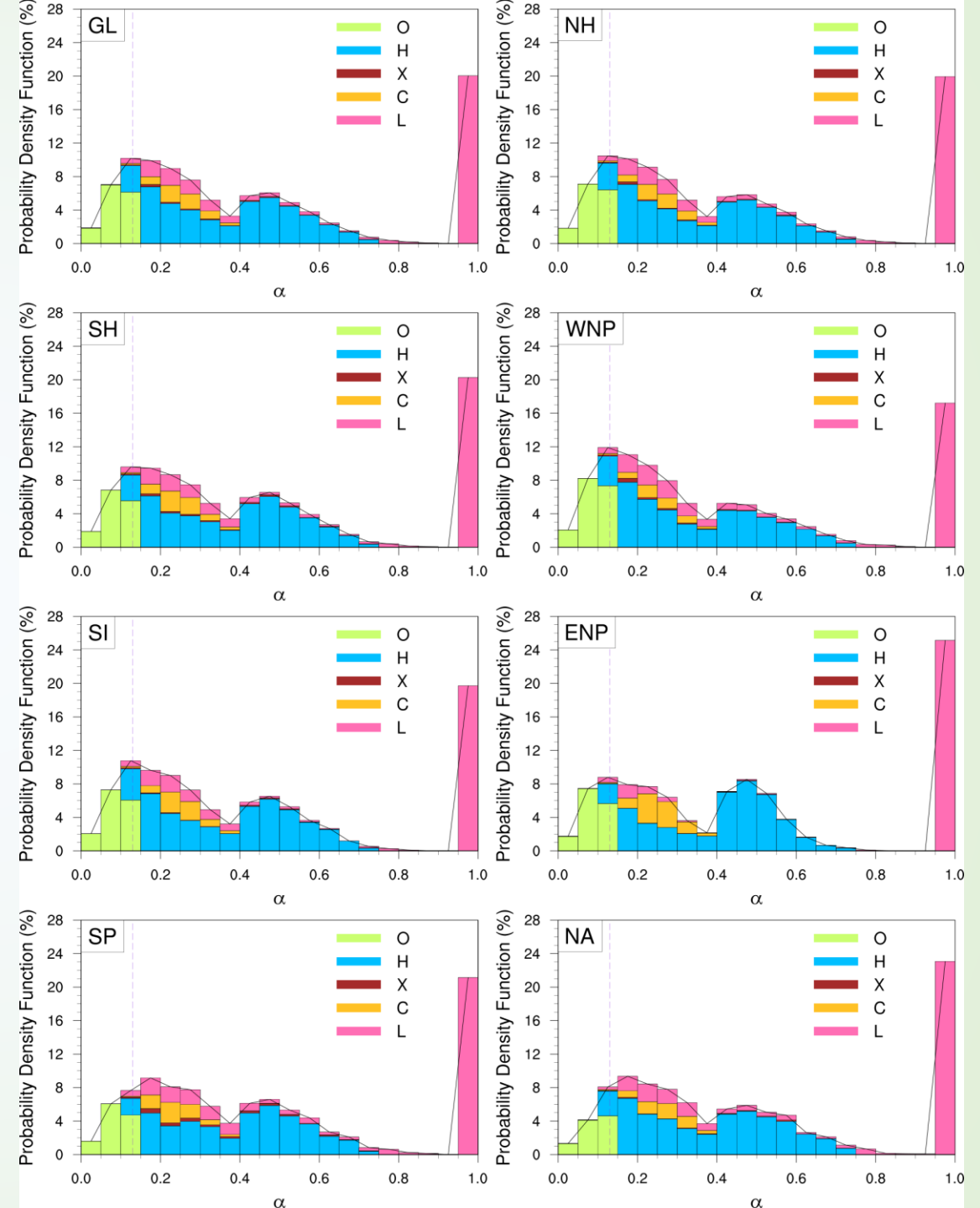
- α
 - 1st: NA (0.49)
 - 2nd: ENP (0.48)
 - 3rd: SP (0.47)
 - 4th: SI (0.44)
 - 5th: WNP (0.41)
- T
 - 1st: Type H
 - 2nd: Type L
 - 3rd: Type O
- Q
 - 1: WNP, ENP, NA, and SP
 - 4: SI

First
Second
Third

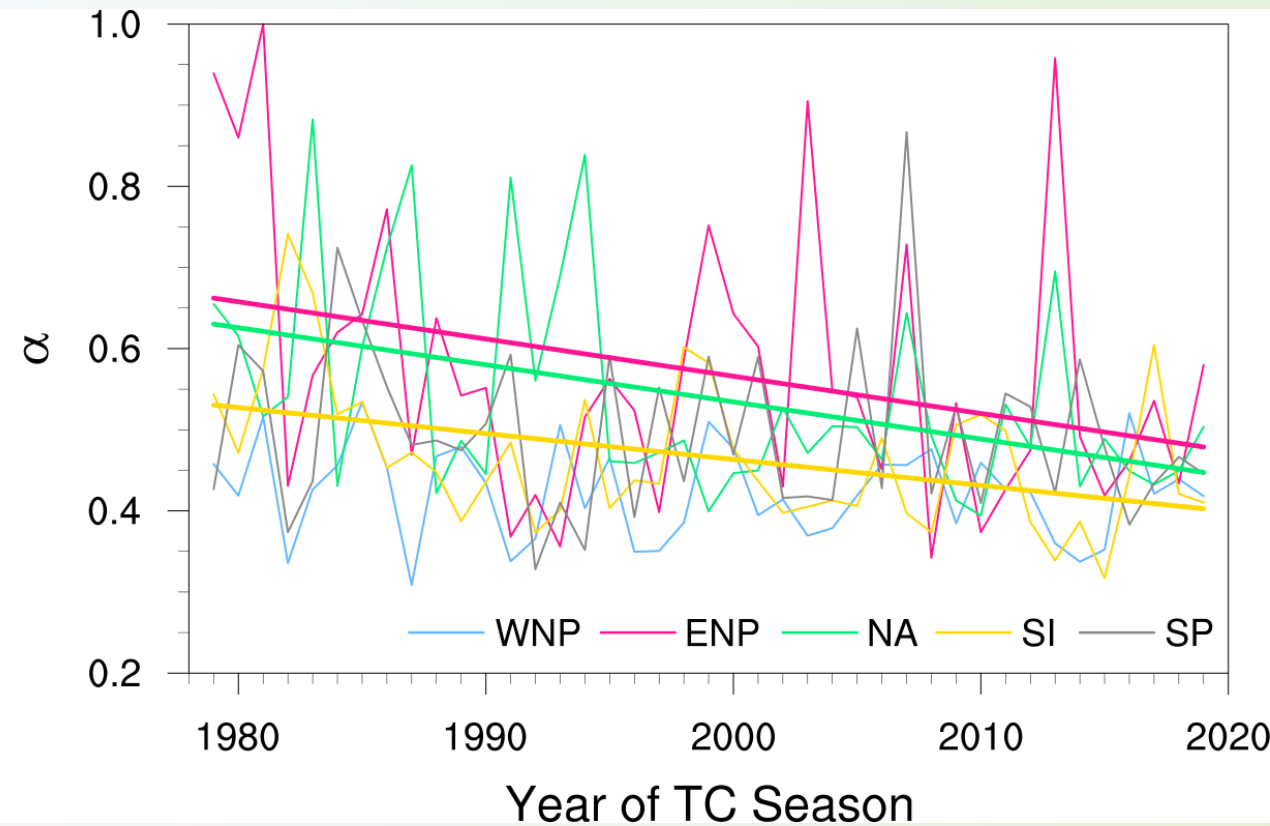
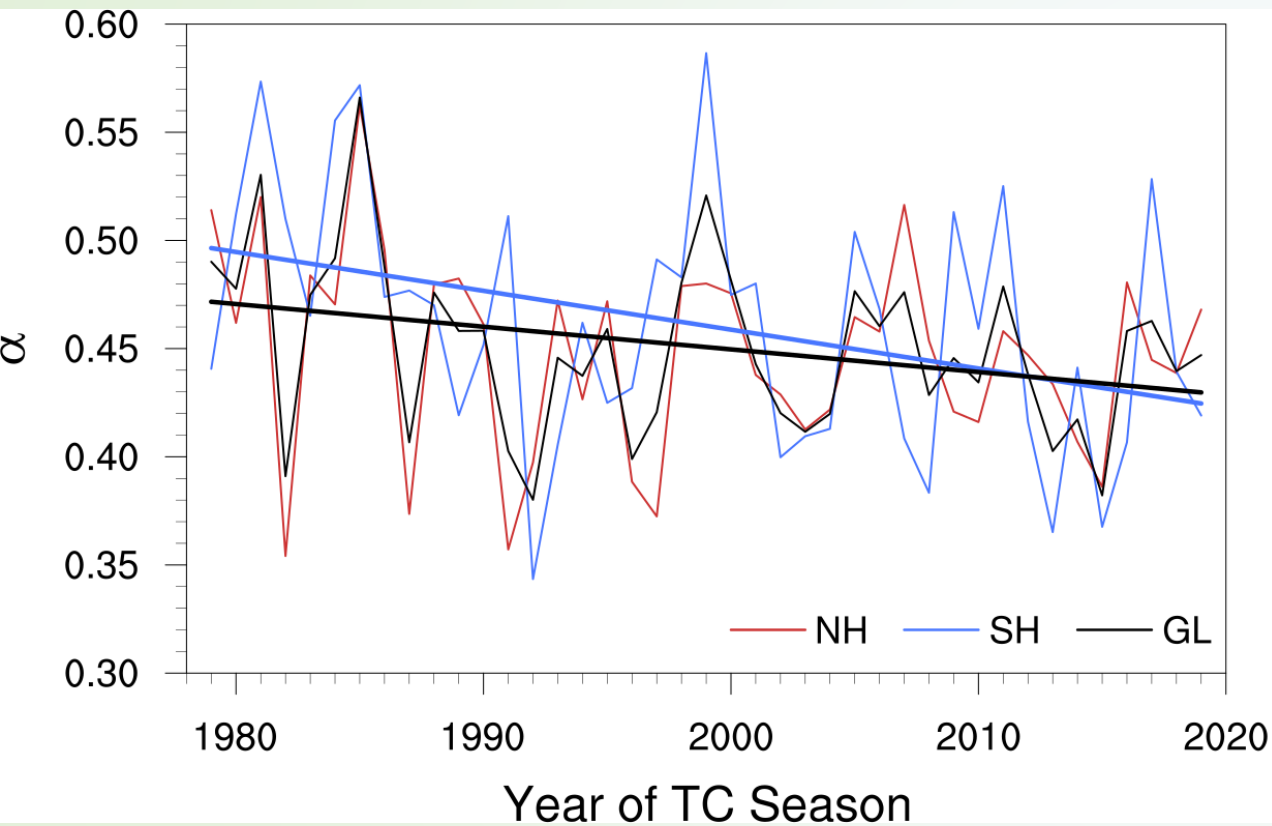
	WNP	ENP	NA	SI	SP	NH	SH	GL
No. of samples	10050	2823	4001	4852	3004	16874	7856	24730
No. of TCs	768	259	638	402	262	1665	664	2329
α								
Mean	0.41	0.48	0.49	0.44	0.47	0.44	0.45	0.44
Standard deviation	0.31	0.34	0.32	0.32	0.32	0.32	0.32	0.32
25 th percentile	0.16	0.20	0.21	0.18	0.20	0.18	0.19	0.18
75 th percentile	0.57	1	0.70	0.60	0.65	0.61	0.61	0.61
T (%)								
O	17.64	14.84	10.07	15.44	12.38	15.38	14.27	15.03
H	45.65	45.84	47.84	47.49	43.01	46.20	45.77	46.07
X	1.55	0.32	0.87	0.95	3.03	1.19	1.74	1.36
C	4.76	9.67	6.02	6.90	6.62	5.88	6.80	6.17
L	30.40	29.33	35.19	29.23	34.95	31.36	31.42	31.37
O (%)								
☉	17.64	14.84	10.07	15.44	12.38	15.38	14.27	15.03
☾	14.42	28.27	14.42	5.15	9.39	16.74	6.77	13.57
☾	1.82	0.46	2.87	1.96	3.03	1.84	2.37	2.01
☾	5.75	1.88	10.30	23.95	12.42	6.18	19.54	10.42
☾	23.66	15.23	20.24	16.43	18.18	21.44	17.1	20.06
☾	0.13	0.18	0.07	0.80	2.90	0.12	1.6	0.59
☾	1.42	0.14	0.80	0.14	0.13	1.06	0.14	0.77
☾	0.25	0.74	0.25	1.2	1.33	0.33	1.25	0.62
☾	0.83	0.07	1.35	0.70	0.50	0.82	0.62	0.76
☾	1.04	1.31	1.02	4.23	3.76	1.08	4.05	2.03
☾	2.64	7.55	3.40	0.78	1.03	3.64	0.88	2.76
☾	13.05	20.30	13.87	5.71	15.78	14.46	9.56	12.9
☾	6.35	3.44	6.42	2.12	1.33	5.88	1.82	4.59
☾	0.65	0.53	2.07	6.92	9.89	0.97	8.06	3.22
☾	10.35	5.07	12.82	14.47	7.96	10.05	11.98	10.66
Q (%)								
1	37.11	59.55	38.39	18.30	38.32	41.17	25.95	36.34
2	13.04	9.67	11.35	6.10	5.63	12.08	5.92	10.12
3	2.87	1.81	6.72	15.17	19.61	3.60	16.87	7.82
4	29.33	14.13	33.47	44.99	24.07	27.78	36.99	30.70

PDF of α and T

- α exhibits trimodal distribution.
- By definition,
Low end is Type O exclusive;
High end is Type L exclusive.



Interannual Variations and Trends

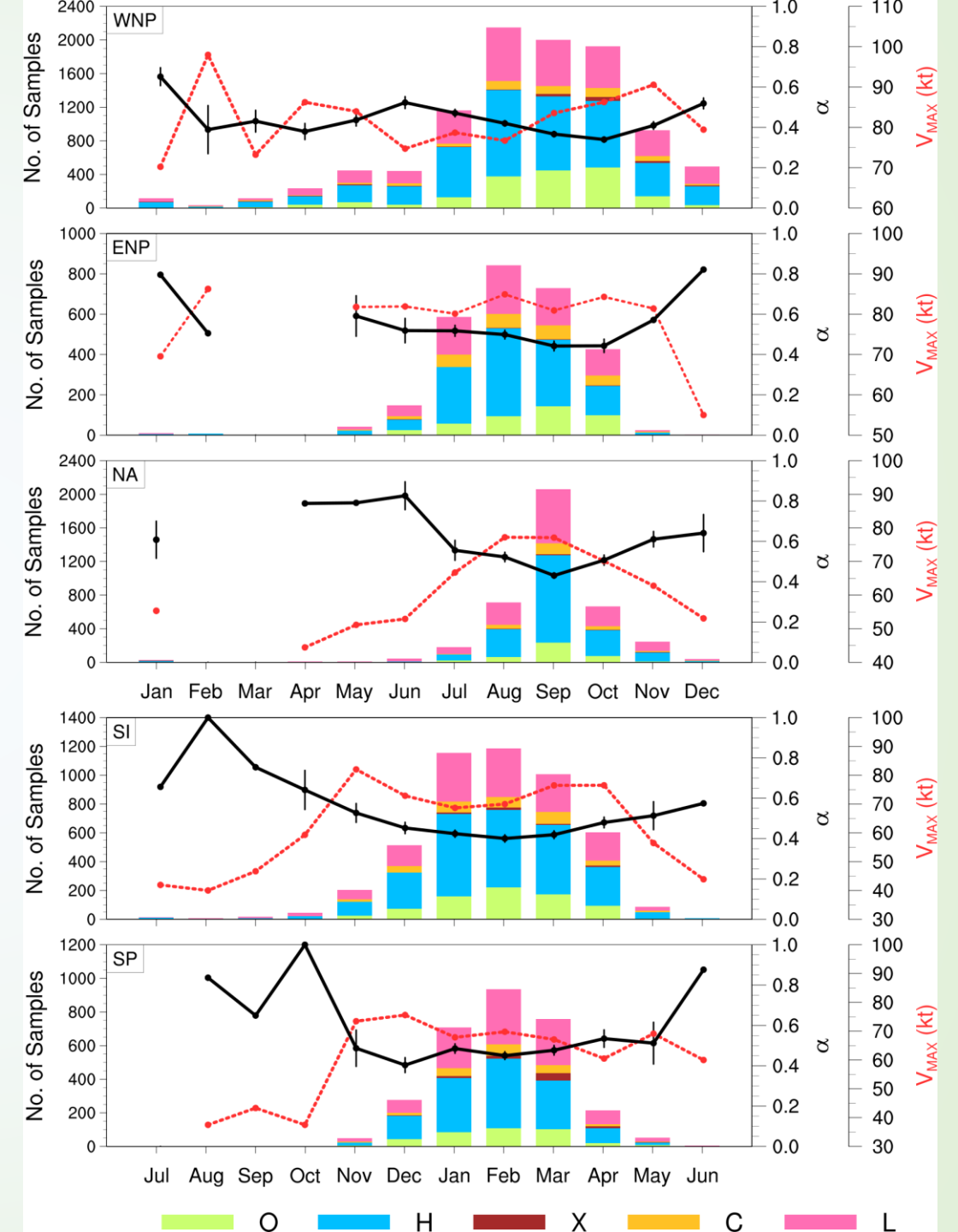


Chan et al. 2023, *Climate Dynamics*

Monthly Variations

- α generally decreases from the early summer, reaches the minimum in fall, and then rebounds, whereas V_{MAX} exhibits inversely.
- It is partly because
 - (1) more Type H and Type L TCs are in early and late TC season; and
 - (2) the intensity of TCs is generally stronger in mid-to-late TC season such that more Type O TCs appear in the late summer and early fall.
- Monthly TC translation speed is weakly correlated with the monthly α (not shown).

Chan et al. 2023, *Climate Dynamics*



Intensity and Translation Speed

- About half of the tropical storms are Type L.
- The proportion of Type L TCs decreases significantly with TC intensity, while that of Type O TCs increases considerably. The corresponding mean α decreases with TC intensity.
- The correlation coefficient between α and TC intensity is statistically significant at 0.39.
- Results imply that both the pattern and degree of TC asymmetry are TC intensity dependent.
- Climatologically, weak TCs are more asymmetric, whereas strong TCs are less asymmetric.
- A weaker TC possesses lower inertial stability to resist perturbations from the environment contributing to the size asymmetry, and vice versa.

	Category	n	Type O	Type H	Type X	Type C	Type L	$\bar{\alpha}$
Intensity V_{MAX} (kt)								
$34 \leq V_{\text{MAX}} < 48$	Tropical storm	3847	3.82	39.85	1.74	4.70	49.88	0.67
$48 \leq V_{\text{MAX}} < 64$	Severe tropical storm	5042	8.61	45.82	1.77	6.23	37.58	0.54
$64 \leq V_{\text{MAX}} < 81$	Typhoon	6186	15.87	47.66	1.20	6.66	28.61	0.43
$81 \leq V_{\text{MAX}} < 100$	Severe typhoon	3580	21.90	47.09	1.17	6.76	23.07	0.34
$V_{\text{MAX}} \geq 100$	Super typhoon	6075	22.53	47.98	1.07	6.21	22.21	0.30
Translation speed M (km h ⁻¹)								
$M < 8$	Very slow	2719	28.28	33.65	1.03	8.02	29.02	0.40
$8 \leq M < 16$	Slow	7722	22.34	41.18	0.73	8.35	27.40	0.40
$16 \leq M < 24$	Medium	7685	11.61	51.02	1.12	5.31	30.94	0.44
$24 \leq M < 32$	Fast	3671	5.91	54.05	1.61	3.90	34.54	0.50
$M \geq 32$	Very fast	2933	3.85	47.46	3.68	3.82	41.19	0.55

Chan et al. 2023, *Climate Dynamics*

Intensity and Translation Speed

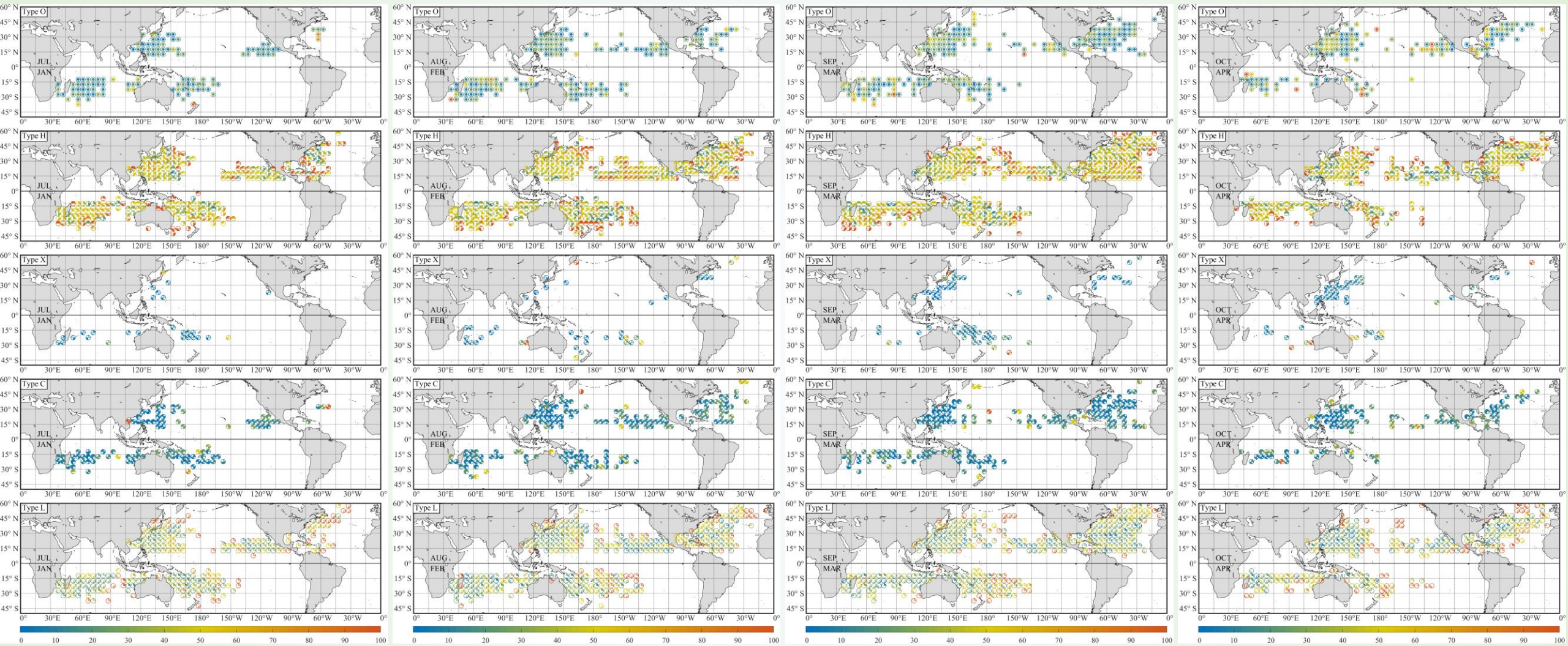
- Among the fast-moving TCs, the Type H and Type L TCs dominate. The sizes of fast-moving TCs are therefore more asymmetric in general.
- Among the slow-moving TCs, the proportions of Type O, Type H, and Type L TCs are comparable.
- The slow-moving TCs are thus not solely prevailed by the less asymmetric TCs. They can be highly asymmetric either.
- This implies that when the movement of TC is slow, the factors other than the TC translation speed contributing to the size asymmetry become effective.

	Category	n	Type O	Type H	Type X	Type C	Type L	$\bar{\alpha}$
Intensity V_{MAX} (kt)								
$34 \leq V_{\text{MAX}} < 48$	Tropical storm	3847	3.82	39.85	1.74	4.70	49.88	0.67
$48 \leq V_{\text{MAX}} < 64$	Severe tropical storm	5042	8.61	45.82	1.77	6.23	37.58	0.54
$64 \leq V_{\text{MAX}} < 81$	Typhoon	6186	15.87	47.66	1.20	6.66	28.61	0.43
$81 \leq V_{\text{MAX}} < 100$	Severe typhoon	3580	21.90	47.09	1.17	6.76	23.07	0.34
$V_{\text{MAX}} \geq 100$	Super typhoon	6075	22.53	47.98	1.07	6.21	22.21	0.30
Translation speed M (km h ⁻¹)								
$M < 8$	Very slow	2719	28.28	33.65	1.03	8.02	29.02	0.40
$8 \leq M < 16$	Slow	7722	22.34	41.18	0.73	8.35	27.40	0.40
$16 \leq M < 24$	Medium	7685	11.61	51.02	1.12	5.31	30.94	0.44
$24 \leq M < 32$	Fast	3671	5.91	54.05	1.61	3.90	34.54	0.50
$M \geq 32$	Very fast	2933	3.85	47.46	3.68	3.82	41.19	0.55

Chan et al. 2023, *Climate Dynamics*

Spatiotemporal Distributions

Chan et al. 2023, *Climate Dynamics*



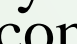


Global climatological spatiotemporal distributions of TOQ in NH July and SH January. In each T , the most corresponding prominent TOQ in each 5° latitude $\times 5^\circ$ longitude grid is shown by the corresponding symbol. The colour of symbol depicts the proportion (unit: %) of the corresponding T within the grid. Note that when there are two or more TOQ sharing the same maximum proportion in the same grid, only the corresponding T symbol is shown.

Spatiotemporal Variations

- In the ENP, \ominus and \odot prevail in early TC season (\ominus and \odot in particular), and more \bullet and \ominus appear at higher latitudes (\bullet and \ominus in particular) from mid to late season gradually. Type X TCs are rare throughout the TC season.
- In the WNP and NA, the main orientation of Type H TCs transits from \ominus at low latitudes to \bullet and \ominus at higher latitudes, while that of Type L TCs transits from \odot to \ominus correspondingly. These could be probably attributed to the TC track or movement, that is, the superposition of the large scale subtropical high-driven steering and the TC circulation itself. The west-northwestward steering at low latitudes and the northward-to-northeastward steering under TC recurvature at higher latitudes could lead to these asymmetries.

Spatiotemporal Variations

- Comparing to those in the NH, the spatiotemporal distributions of size asymmetry patterns are more diverse in the SH, especially in SP. Type X TCs are slightly more in the SH. The main orientations of asymmetry are  and , which are north-south flipped from those in the NH.
- The proportions of Type O TCs are found to increase broadly along the TC season. This suggests that the seasonal increases in Type O TCs are not featured by the small regional scale increases in Type O TCs, but the basin-wide or worldwide increases. This could be related to the large scale seasonal variability. The occurrence of Type O TCs becomes more scattered along the TC season over NA.
- $R34_{MAX}$ generally appears in quadrants 1 and 4 globally. More than 60% of Q are found in these two quadrants. In particular, for Type L, the majority of Q does not change from July to September in some regions (e.g., 15–30° N, 135–150° E) where  is the commonest. These could be related to the intrinsic properties of TC itself, self-rotating earth, or regional environmental factor(s).

KTFCHAN Font

For popularization and accessibility, a dedicated font KTFCHAN in formats of OpenType Font ([OTF](#)), TrueType Font ([TTF](#)), Web Open Font Format version 1 ([WOFF](#)), and Web Open Font Format version 2 ([WOFF2](#)) are developed, published, and **freely** available in Chan et al. (2023).

Chan et al. 2023, *Climate Dynamics*

Order	Symbol	Description	Input character	Unicode name
1		Blank space		Space
2	⦿	SAI: O, OO, OOO	!	Exclamation mark
3	◉	SAI: H, Ha	“	Quotation mark
4	◊	SAI: Ha1	#	Number sign
5	◈	SAI: Ha2	\$	Dollar sign
6	◉	SAI: Hb	%	Percent sign
7	◊	SAI: Hb2	&	Ampersand
8	◈	SAI: Hb3	‘	Apostrophe
9	◉	SAI: Hc	(Left parenthesis
10	◊	SAI: Hc3)	Right parenthesis
11	◈	SAI: Hc4	*	Asterisk
12	◉	SAI: Hd	+	Plus sign
13	◊	SAI: Hd1	,	Comma
14	◈	SAI: Hd4	-	Hyphen-minus
15	◉	SAI: X, Xa	.	Full stop
16	◊	SAI: Xa1	/	Solidus
17	◈	SAI: Xa3	0	Digit zero
18	◉	SAI: Xb	1	Digit one
19	◊	SAI: Xb2	2	Digit two
20	◈	SAI: Xb4	3	Digit three
21	◉	SAI: C, Ca	4	Digit four
22	◊	SAI: Ca1	5	Digit five
23	◈	SAI: Ca2	6	Digit size
24	◉	SAI: Ca3	7	Digit seven
25	◊	SAI: Cb	8	Digit eight
26	◈	SAI: Cb2	9	Digit nine
27	◉	SAI: Cb3	:	Colon
28	◊	SAI: Cb4	;	Semicolon
29	◈	SAI: Cc	<	Less-than sign
30	◉	SAI: Cc1	=	Equal sign
31	◊	SAI: Cc3	>	Greater-than sign
32	◈	SAI: Cc4	?	Question mark
33	◉	SAI: Cd	@	Commercial at
34	◊	SAI: Cd1	A	Latin capital letter A
35	◈	SAI: Cd2	B	Latin capital letter B
36	◉	SAI: Cd4	C	Latin capital letter C
37	◊	SAI: L, La	D	Latin capital letter D
38	◈	SAI: La1	E	Latin capital letter E
39	◉	SAI: Lb	F	Latin capital letter F
40	◊	SAI: Lb2	G	Latin capital letter G
41	◈	SAI: Lc	H	Latin capital letter H
42	◉	SAI: Lc3	I	Latin capital letter I
43	◊	SAI: Ld	J	Latin capital letter J
44	◈	SAI: Ld4	K	Latin capital letter K
45	○	White circle	L	Latin capital letter L
46	●	Black circle	M	Latin capital letter M
47	☯	Northern Hemisphere cyclone	N	Latin capital letter N
48	☯	Southern Hemisphere cyclone	O	Latin capital letter O

Conclusions

- SAI is proposed to specify the degree and pattern of TC size asymmetry synthetically.
- The distribution of the degree of TC size asymmetry is trimodal.
- The size asymmetry of TC is found to be TC intensity, TC movement, time, and space dependent.
- In general, the weak or fast-moving TCs are more asymmetric.
- The interannual variations and long-term trends of α could be a compound of various factors.
- The seasonal variation of α generally decreases from the early summer, reaches the minimum in the fall, and then rebounds.
- The proportions of asymmetric types are not evenly distributed along the TC season, within the basin, and across basins.

References

- Hong, W., Zheng, Y., Chen, B., Su, T. & Ke, X. (2020) Monthly variation and spatial distribution of quadrant tropical cyclone size in the western North Pacific. *Atmospheric Science Letters*, 21, e956.
- Olfateh, M., Callaghan, D. P., Nielsen, P. & Baldock, T. E. (2017) Tropical cyclone wind field asymmetry – development and evaluation of a new parametric model. *Journal of Geophysical Research: Oceans*, 122, 458–469.
- Sun, Z., Zhang, B., Zhang, J. A. & Perrie, W. (2019) Examination of surface wind asymmetry in tropical cyclones over the Northwest Pacific Ocean using SMAP observations. *Remote Sensing*, 11, 2604.
- Chan, K. T. F., Zhang, K., & Xu, L. (2023) Tropical cyclone size asymmetry index and climatology. *Climate Dynamics*, 61, 5049–5064.